COMPARISON OF TRUCK'S WIDE-BASE-SINGLE AND DUAL TIRES ROLLING RESISTANCE

TEERAPAN UTTARANAGARA

A THESIS REPORT SUBMITTED IN PARTIAL FULFILLMENT
OF THE REQUIREMENTS FOR THE DEGREE OF
MASTER OF ENGINEERING IN AUTOMOTIVE ENGINEERING
INTERNATIONAL COLLEGE
KING MONGKUT'S INSTITUTE OF TECHNOLOGY LADKRABANG
ACADEMIC YEAR 2017
KMITL-2017-IC-M-004-007

COMPARISON OF TRUCK'S WIDE-BASE-SINGLE AND DUAL TIRES ROLLING RESISTANCE

TEERAPAN UTTARANAGARA

A THESIS REPORT SUBMITTED IN PARTIAL FULFILLMENT
OF THE REQUIREMENTS FOR THE DEGREE OF
MASTER OF ENGINEERING IN AUTOMOTIVE ENGINEERING
INTERNATIONAL COLLEGE
KING MONGKUT'S INSTITUTE OF TECHNOLOGY LADKRABANG
ACADEMIC YEAR 2017
KMITL-2017-IC-M-004-007

THESIS TITLE	Comparison of Truck's Wide-Base-Single and Dual Tires Rolling Resistance
STUDENT NAME	Mr. Teerapan Uttaranagara
STUDENT ID	56610011
DEGREE	Master of Engineering
PROGRAME	Automotive Engineering
ADVISOR	Asst.Prof.Chinda Charoenphonphanich
CO-ADVISOR	Dr.Sittikorn Lapapong
CO-ADVISOR	Prof.Dr.Masaaki Okuma

ABSTRACT

This research compares and indicates the Rolling Resistance (RR) between Wide-Base-Single (WBS) tire and Dual tires of semi-trailer truck. The RR affect to fuel consumption rate, and more fuel consumption rate in semi-trailer truck of transportation causes to energy problem in the world. The author assumption is focuses on both types of tires are impact on fuel consumption rate from the variation of tread width and shape of tire footprint, which cause to RR difference too. The RR of WBS tire and Dual tires are calculated and predicted by use the Finite Element Method (FEM) with simulation software. From the results, WBS tires should be consuming lower fuel than Dual tires because the low value of Rolling Resistance which indicate the reduction of fuel consumption rate. As an expected results, this research is expected to be used as reference and motivation for changing government regulations of many countries are unsupported which regarding to the using of WBS tire in the future. Therefore, truck fleet operators can offer the WBS tire as the better choice as fuel efficient vehicles. And if in the future need to design the new WBS tire or other types of tires, they can use the knowledge and method of FEM to predict the accurate result of the tires. This methodology can reduces more time and more cost from construct the tire prototype.

ACKNOWLEDGEMENT

This thesis could succeed with many assistance from many people. First, thank you very much to advisors who advised me to reach the target. I am thank you to Asst. Prof. Dr. Chinda Charoenphonphanich, Prof. Dr. Masaaki Okuma, and Dr. Sittikorn Lapapong, who provided me the many helpful, opportunity, motivation, knowledge and experience.

Thank you to TAIST-Tokyo Tech program and National Science and Technology Development Agency (NSTDA), who provided the opportunity and scholarship for study program to me. And thank you King Mongkut's Institute of Technology Ladkrabang for facility of library, the laboratory and the study host.

I am thank you so much to Research and Researchers for Industries (RRI) and Michelin Siam Co., Ltd for the research budget and many supports.

I am thank you very much to Mr. Jittrin Nimitpermpoon who is the senior of me, who provided the many advices, motivation and teach me many knowledges.

I am also thank you to tire and rubber testing teams of Rubber Technology Research Centre for many suggestions and service for tire and rubber testing.

Finally, I am thank you to my family, my dear friends too, who support me to finish this thesis. Without help from these people, I could never have done it.

Teerapan Uttaranagara

TABLE OF CONTENTS

Chapter **Page**

TABLE OF CONTENTS

(Continued)

Chapter **Page**

TABLE OF CONTENTS

(Continued)

Chapter **Page**

TABLE OF CONTENTS

(Continued)

Chapter **Page**

LIST OF TABLES

Table **Page**

LIST OF FIGURES

Figure **Page**

LIST OF FIGURES

(Continued)

Figure **Page**

LIST OF FIGURES

(Continued)

Figure **Page**

LIST OF SYMBOLS

$\varepsilon_{bending}$	The ratio about the tread block deformation and its initial dimensions
h	The tread block thickness
R_f	The radius of the initial curvature
R_i	Radius of the final curvature
$\varepsilon_{compression}$	The compression strain
σ	Pressure exerted
M_{10}	Modulus measured at 10 % stretching
F	Aspect ratio equal to S/S’
$\frac{d}{h}$	The shear strain
N	Load in vertical
OD	Overall diameter of tire
CL	Contact length of tire
b	Radius of tire when deformed
F_{pl}	The parasitic losses related to tire/drum
F_t	The tire spindle force
r_L	Effective radius of tire
R	The test drum radius
RR_{25}	The Rolling Resistance at 25 °C
t_{amb}	The ambient temperature

K	The constant of Rolling Resistance temperature correction (equal to 0.006 for class C3 tires)
R_1	The radius of drum 1
R_2	The radius of drum 2
r_T	One-half of the nominal tire diameter
F_{r01}	The Rolling Resistance value measured on drum 1
F_{r02}	The Rolling Resistance value measured on drum 2
U	Strain energy
I_1	The first deviatoric strain invariants
I_2	The second deviatoric strain invariants
I_3	The third deviatoric strain invariants
λ_1	The deviatoric stretches at axis 1
λ_2	The deviatoric stretches at axis 2
λ_3	The deviatoric stretches at axis 3
C_{10}, C_{20}, C_{30}	Temperature-dependent material parameters
$g_t(t)$	The dimensionless relaxation modulus
τ_i^G	Relaxation time
$N, \bar{g}_i^P$	The material constants
t	Time period
η	Scalar variable
$\mathbf{F}$	The deformation gradient tensor or some other appropriate strain measure

LIST OF DEFINITIONS

RR	Rolling Resistance
RRC	Rolling Resistance Coefficient
WBS	Wide-Base-Single
FEM	Finite Element Method
FEA	Finite Element Analysis
CAD	Computer Aided Design
CAE	Computer Aided Engineering
SSR	Steady State Rolling
SST	Steady State Transport

CHAPTER 1

INTRODUCTION

1.1 Research Background

Nowadays, energy problems are interesting topic in the world. Because of the most energy source came from limited fossil as Figure 1.1 [1]. Energy problems had many effect on transportation. For transportation, trucks have been necessary using more energy. If we can increase the efficiency of trucks for reduce the fuel consumption, Energy problems in country will decrease too.

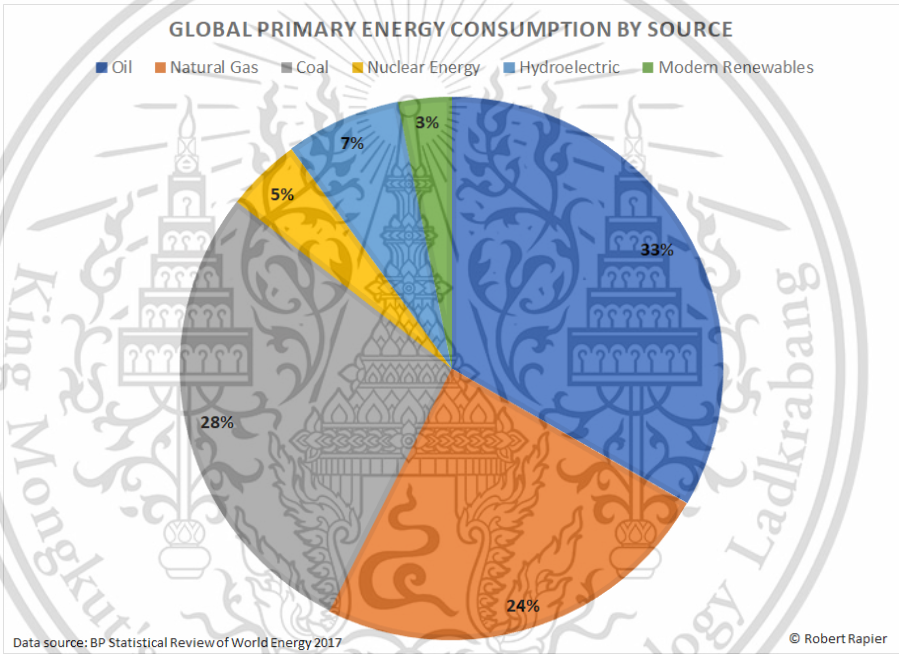

Figure 1.1 Energy Consumption in the world in year 2016.

Source: RAPIER, R. (2017, November 07). Renewable Gains Offset Coal's Decline In 2016. Retrieved from Financial Sense: https://www.financialsense.com/robert-rapier/renewable-gains-offset-coals-decline-in-2016

Many countries especially in North America, they countries have many transportations by trucks. So, researches and developments about the reduction of fuel consumption rate and increasing efficiency of trucks have widely used. Thailand has many transportations by trucks too. But Thailand still hasn't researchers in this field. Because of these, we lost many opportunities especially fuel consumption that effect

on transportation cost. Moreover, high transportation cost have been troubling the economic development of the country too. Fuel consumption of vehicle could performs in three resistance main causes [2] these were Aerodynamic Drag, Mechanical Loss, and Rolling Resistance (RR). Aerodynamic Drag would lose approximately 40% at 60 mph, Mechanical Loss approximately 25% and RR approximately 35%.

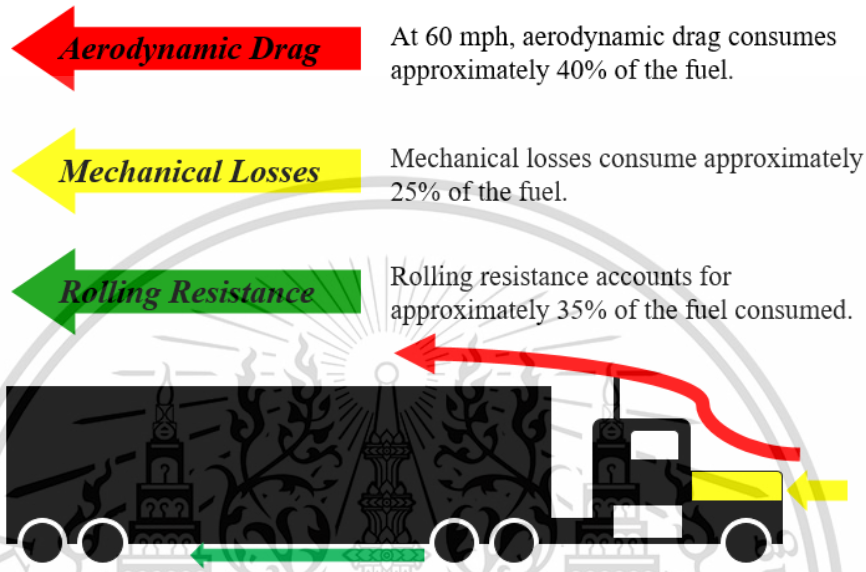

Figure 1.2 Three resistance main causes of the truck.

Many researches from collecting the data, the Wide-Base-Single (WBS) tire using instead of Dual tires using could reduce the RR, fuel consumption rate and increase efficiency of truck significantly. Most problems came from transportations by trucks. Trucks have been using Dual tires to carry more loads, but Dual tires have high RR. Thus it used more fuel consumption and effect to transportation cost. Not only cost, but also became to causes of greenhouse gas global warming too. When used the WBS tire, it could reduce the fuel consumption approximately 3% to 6%, it would be to result in fuel savings per year per truck of 3,962 $ dollar [3] and Thailand had many transportations by trucks, there were 1,187,731 trucks in Thailand [4] in year 2016. Figure 1.2 presents the fuel consumption in year 2016, this figure show the diesel consumption was the most [5]. Which the truck used diesel to transportation.

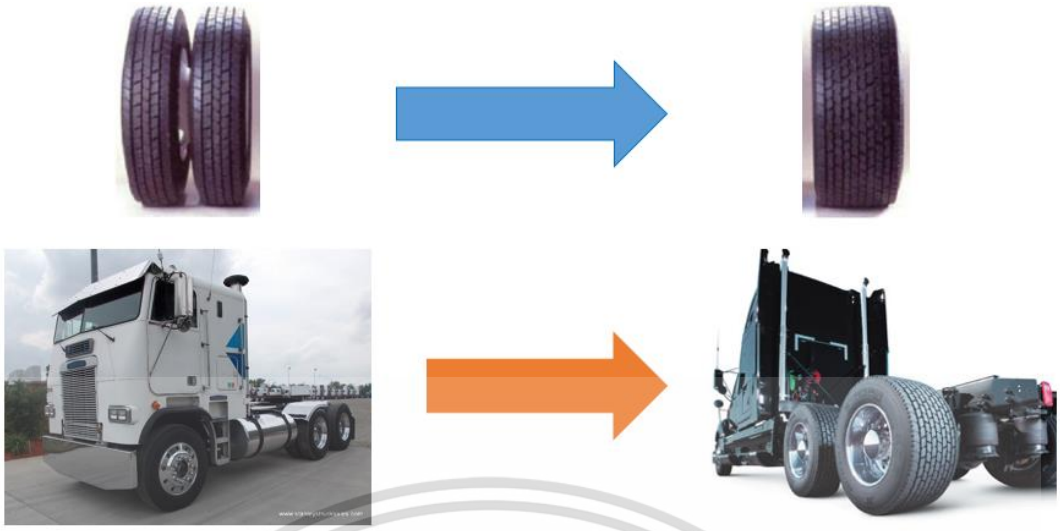

Figure 1.3 Dual tires and Wide-Base-Single tire.

Source: http://nacfe.org/wp-content/uploads/2010/12/NACFE-ER-1002-Wide-Base-Tires-Dec-2010.pdf.

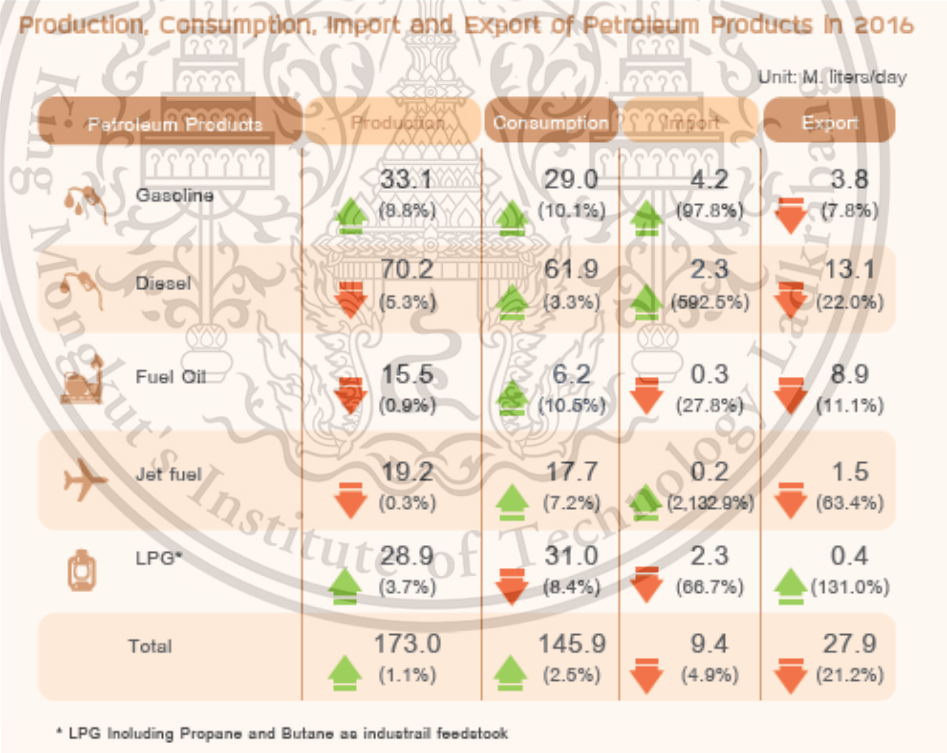

Figure 1.4 Fuel Consumption in Thailand as of 2016.

Source: EPPO. (2017). ENERGY STATISTICS OF THAILAND. Bangkok: EPPO.

(คัน : Unit)

ประเภทรถ Type of Vehicle	ทั่วประเทศ Whole Kingdom	กรุงเทพฯ Bangkok	ส่วนภูมิภาค Regional
ข. รวมรถตามกฎหมายว่าด้วยการขนส่งทางบก Total Vehicle under Land Transport Act	1,187,731	178,712	1,009,019
รวมรถโดยสาร Bus : Total	**153,454**	**42,921**	**110,533**
แยกเป็น - ประจำทาง Fixed Route Bus	85,311	24,421	60,890
- ไม่ประจำทาง Non Fixed Route Bus	56,158	15,444	40,714
- ส่วนบุคคล Private Bus	11,985	3,056	8,929
รวมรถบรรทุก Truck : Total	**1,033,403**	**135,791**	**897,612**
แยกเป็น - ไม่ประจำทาง Non Fixed Route Truck	261,415	71,837	189,578
- ส่วนบุคคล Private Truck	771,988	63,954	708,034
โดยรถขนาดเล็ก Small Rural Bus	**874**	**-**	**874**

Figure 1.5 Number of Vehicle Registered in Thailand as of 28 February 2016.

Source: https://data.go.th/DatasetDetail.aspx?id=21372366-e78b-4d4a-b040-8a702ecedd5f

In the future, if will needs to designs or remodels the new WBS tire. It can uses the simulation to predict the results of the new WBS tire model, not only the RR result but it can predicts other results too. The simulation can reduces the time and the cost to construct the WBS tire prototype. Because of this, the simulation is important methodology to saving the time and the cost to design, remodel and construct the prototype of tire.

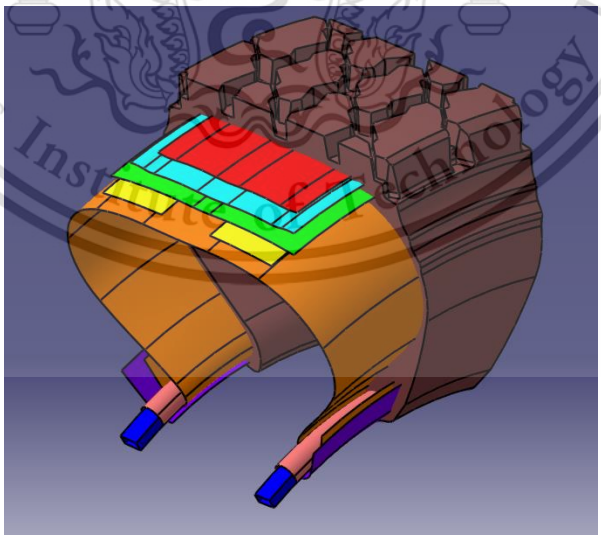

Figure 1.6 CAD tire model (Finite Element tire model).

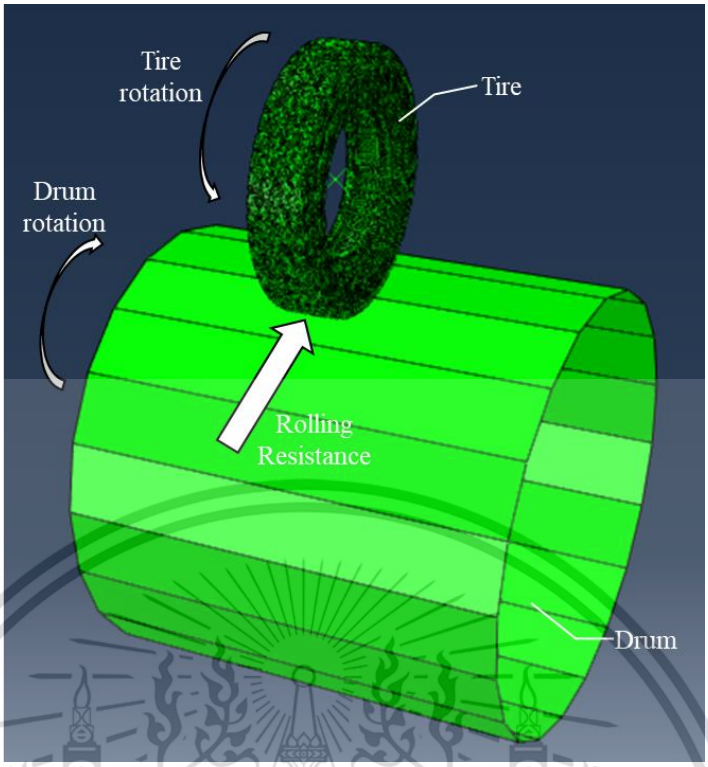

Figure 1.7 Rolling Resistance simulation by Finite Element Method.

1.2 Thesis Outline

In this Chapter 1, will presents about the reasons and motivation to research the WBS tire to reduce the RR and it leads to reduce the fuel consumption too. The reason uses the Finite Element Method (FEM) to predict the result and uses this method to remodel or design the new model was explained too.

Chapter 2 will presents literature reviews relative with RR, Finite Element Analysis (FEA) and WBS tire. The RR from other researches are research on passenger car tire, slick tire, truck tire and WBS tire too, each research uses several methods to obtain the results such as testing, FEA. The tire FEA researches from literatures are research on the tire behavior such as breaking, traction, cornering, rolling, RR, etc. The WBS tire literatures are present the benefit when WBS tire used instead of Dual tires, it is the fuel consumption reduction.

Chapter 3 will presents background knowledges to use in this research, there are RR occurrence sources, RR measurement, tire material properties, material properties obtained methodology, FEA modeling and FEM.

Chapter 4 is the research methodology of this research. It will presents the FEA modeling or Computer Aid Design (CAD) modeling for FEM. It is modeling from 11R22.5 truck tire cross-section and WBS tire model too. After modeling, simulate the 11R22.5 truck tire model by FEM to obtain RR results and validate with the results from UN-ECE R117 testing method. Next, simulate the WBS tire model to obtain RR. Finally, compare WBS tire RR results with Dual tires.

Chapter 5 is results and discussion. It will presents RR results from the research methodology and discussing about the results to find the conclusion of this research.

Chapter 6 will presents the conclusion from results and discussion in Chapter 5. This Chapter summarize the tire which has the lower RR means it has the lower fuel consumption too.

CHAPTER 2

LITERATURE REVIEW

Chapter 2 is a review of the literature on relevant to this investigation. Which there are theories related on tires.

2.1 Executive Report – Wide Base Tires

NACFE & Driving Innovation [2] presented the report about Wide-Base-Single (WBS) tire, they said "WBS tire can reduce the fuel consumption by 3% to 6%, depending on the choice of where to install the tires both head of truck or trailer". In addition to the weight loss too.

This literature was the research by testing in North America and did not used the simulation to investigate. Because of this, they would paid the cost too much and take a lot of time too.

2.2 Factors Affecting Truck Fuel Economy

Goodyear commercial tire systems [6] presented academic papers on the subject factors that affect fuel efficiency of trucks, they said "factors that affect fuel economy, there are plenty such as speed of car, air resistance, load, wheel alignment, tire pressure, driving style, model of trailers, air temperature, climate, landscape, road surface, characteristics of road, Rolling Resistance (RR), form of tire maintenance and many other variables, which tire has contributed significantly to fuel economy of the truck, because the truck has many wheels that make the tires have many effects on the rate of fuel consumption and for heavy trucks a 10% change in RR can contribute 2% to 3% to fuel economy.

This research investigated many factors affect to truck tire by testing and simulation but wasn't the WBS tire investigation.

2.3 Effect of Tires on Class-8 Heavy Truck Fuel Efficiency

Oscar FranZese, et al [7] studied effects of tire to fuel efficiency of truck. Comparison of the truck used all WBS tires with and the truck used some WBS tire and the truck used all Dual tires, found that the truck used all WBS tire and some WBS tire have better fuel efficiency than the truck used all Dual tires.

This literature investigated the WBS tire and Dual tires by fuel efficiency experiment not RR simulation and they must paid many cost to experiment.

2.4 Investigating the Effect of Velocity, Inflation Pressure, and Vertical Load on Rolling Resistance of a Radial Ply Tire

Hamid Taghavifar., et al [8] was utilized to investigate the effect of velocity, tire inflation pressure, and vertical load on RR of wheel. A 9.5L-14, 6 radial ply tire was used as the tester wheel on clay-loam soil and was installed on a carriage traversing the length of soil bin. Three inflation pressures of 100, 200, and 300 kPa as well as three levels of velocity (i.e. 0.7, 1.4, and 2 m/s) and five levels of vertical load applied on wheel (i.e. 1, 2, 3, 4, and 5 kN) were examined. As results, the RR of wheel was increasingly influenced by inflation pressure and vertical load than velocities being investigated in this study. The RR would be quite constant relation with low velocities (0.7, 1.4, and 2 m/s). Basically, operational speeds of tractors in the farm cannot exceed to high levels, Hence these velocities were investigated in a soil bin indicating no considerable effect on RR. Based on obtained results of this study, increasing of inflation pressure suggests reverse relation with RR particularly at higher values of vertical load. Vertical load applied on wheel had considerable impact on RR and its increase results in polynomial with order two increasing of RR.

This Literature investigated the important various effect of tire that impact to RR by UN-ECE R117 standard. But they investigated on the soil bin not based on drum testing and did not used the simulation including WBS tire wasn’t investigated too.

2.5 Engineering Design of Tyres for Energy Saving Tyres

Dr. Pairote Jittham., et al [9] investigated and designed to reduce the RR that depend on depth, pattern of tread and structure of radial pick up and solid tire. From the results, they found the pattern of tread is greatly effect to RR of radial pick up tire, but it rarely affect to solid tire. The area and depth of tread are greatly effect to both tires, if the tread had high depth, the RR would increase too. And structure affect to solid tire only, if solid tire had many layer of structure, the RR would increase too.

For this literature, they used the Finite Element Method (FEM) to simulate the solid and radial pick-up tire based on Drum testing. But the WBS tire wasn't investigated.

2.6 Mechanical Testing of Rubber for Structural Finite Element Analysis

Dr. Pairote Jittham [10] investigated the material properties and testing method of Hyperelastic property, because it was important for the simulation by Finite Element Analysis (FEA) with LS-Dyna software. The testing methods for the Hyperelastic property were uniaxial tension or uniaxial compression, biaxial extension, planar shear or simple shear and volumetric. If defined material properties to incompressible, the volumetric wasn't testing.

This literature review presented about how to found the material properties of rubber to use in tire simulation by FEM, but wasn't the WBS tire or RR research.

2.7 Finite Element Analysis of Tire Thermomechanical Coupling Rolling Resistance

Guolin Wang., et al [11] predicted the RR of 12R20 truck tire and influence factors on RR. They compared the simulation with the rubber wheel specimens were made from tread rubber, the RR testing by RRS II model RR testing machine. They ran by 30 minute at load 30 kg, rolling speed 400 and 1200 RPM. The surface temperature and energy loss of the rubber wheels were measured. The maximum error between simulation and testing was 6.68%. After that, they simulated the 12R20 truck tire RR by FEA with influence factors such as inflation pressure, vertical loads and speeds.

Results presented if speed and inflation pressure increasing, the RR would decreasing. But, if load increasing, the RR would increasing too.

This research used the wheel specimen made from truck tire rubber to experiment, but the wheel specimen had the rubber material only and in truck tire structure there was reinforcement too. And they did not investigated WBS tire and Dual tires.

2.8 Numerical Estimation of Rolling Resistance and Temperature Distribution of 3-D Periodic Patterned Tire

J.R. Cho, et al [12] compared the RR of periodic patterned tire simulation with experiment, in this research they simulated the periodic patterned tire instead of full pattern tire with ABAQUS program, because of reduced the simulation time. If used the full model pattern tire, it used a lot of time to obtain the results. After conclusion, they compared the RR simulate results with experiment and found the relative error was approximately 12.82%.

From periodic methodology, it could save more time and relative error was acceptable too. This literature, they researched the passenger car tire. The WBS tire wasn't investigated herein.

2.9 Finite Element Analysis and Experimental Investigation of Tyre Characteristic for Developing Strain - Based Intelligent Tyre System

Xiaoguang Yang [13] investigated relationships between the tire strain feature and the tire operating conditions based on FEA and experiments for the development of the strain-based intelligent tire system. Which could estimate the tire operating characteristics for optimizing vehicle dynamics control and improve the vehicle safety too. In this research used the 175/505R13 tire to study. The material properties of rubber and reinforcement in the tire were investigated. The rubber material properties in this case used the Yeoh model of Hyperelastic material. Models of Hyperelastic material had many models such as Mooney-Rivlin, Polynomial, Yeoh, Ogden, Arruda-Boyce, etc. Each models had different usability, precision, suitable of simulation. The Yeoh

model could be obtained the material properties data from uniaxial tension only. Not only had the Hyperelastic property, the rubber had Viscoelastic material property too. The Prony series of Viscoelastic was adopted for this study. The Finite Element model used to simulation used the novel image based method to capture the tire geometry feature from the tire product cut cross-section. They were created in the commercial Finite Element program ABAQUS.

Yang's research investigated about slick tire of student formula car and did not investigated RR too.

2.10 Importance of Capturing Non-linear Viscoelastic Material Behavior in Tire Rolling Simulations

Biswanath Nandi., et al [14] provided a theoretical background of the linear and non-linear Viscoelastic models available in ABAQUS. It also described a methodology to calibrate parameters of the Parallel Rheological Framework model (PRF) model in ABAQUS starting from material test data. This research also briefly described a simulation methodology to predicted temperature distribution in a rolling tire due to Viscoelastic energy dissipation in the rubber material. In the conclusion, the step-by-step procedure used Isight to calibrate the PRF model parameters starting with stress relaxation test data was provided to help the analysts. The linearized PRF model parameters were a good starting point for the Isight optimization process.

This literature presented about importance of Viscoelastic material property in tire rolling simulation. The Viscoelastic was the important property of energy dissipation in tire, but this literature did not investigated the WBS tire.

2.11 Conclusion

After review all literatures, the WBS tire using instead of Dual tire using could reduce RR and fuel consumption significantly.

From 2.1 and 2.2 of literature reviews, these were presented the WBS tire using instead of dual tires could decreased the RR approximately 10-20% and fuel saving approximately 3-6%.

The tire simulation in literatures described the RR came from energy dissipation from material properties of tire. And they guideline about FEM or FEA to use in tire simulation too.

The load, velocity and inflation pressure affect to RR of tires. And before simulate tire with FEM, which must collect the material properties data of tire from material testing.

2.12 Research Objectives and Scope of Work

After concluded the literatures, research objectives will established. The author seen the many researches used the FEM to simulate the characteristic of tire. The periodic method used in FEM is suitable with WBS tire and Dual tires RR simulation. In the J.R. Cho research [12], they used the periodic method and have relative error approximately 12.82%.

The destination of this research is to demonstrate the result when WBS tire using instead of Dual tires and how the dimension of tires are effect on RR.

After investigated the theory, literatures and establish objectives, the scope of work will the next topic. The first of research will obtain the RR testing results of truck tire to uses in validation with simulation results. Before simulate the truck tire RR, the material properties are required. The material properties of tire will be obtained from material testing. Material specimens are receive by extract from the tire. After obtain the material properties, the simulation will process to obtain the RR results. If the result validation of testing and simulation are acceptable, the next process is the WBS tire simulation and obtain the RR results. Finally, conclude and demonstrate the results of WBS tire and Dual tires.

2.12.1 Research Objectives

1) Indicate the Rolling Resistance of the Wide-Base-Single tire instead of the dual tire from UN-ECE R117 standard experimented results validate with simulation results and the error must haven't over than 20%
2) Demonstrate how the width and footprint of the Wide-Base-Single tire and the Dual tire affect to Rolling Resistance.

2.12.2 Scope of Work

1) Bring the truck tire to RR testing with UN-ECE R117 standard and obtain the results.
2) Extract the raw material from the truck tire.
3) Bring raw materials to material properties testing and obtain the results
4) Draw the CAD model of truck tire to uses in simulation.
5) The truck tire Static simulation by inflation pressure and load variation with same input value of RR testing.
6) Steady State Rolling (SSR) simulation of truck tire to obtain the results with Steady State Transport (SST) function and calculate with simulate results to obtain the RR results.
7) Validate results of RR simulation with testing.
8) If results are unacceptable, return to improve the model and simulation. But if the results are acceptable, draw the CAD model of WBS tire.
9) Simulate the WBS tire model with same methods as 5) - 6)
10) Conclude the WBS tire results with Dual tires results

CHAPTER 3

BACKGROUND KNOWLEDGE

The Chapter 3 presents the knowledge relation and using in this research. The majority of Rolling Resistance (RR) occurrence is the Hysteresis loss from material properties of the rubber. The Hysteresis loss of the rubber leads to more energy loss in the tire when rolling or deformed.

3.1 Where Does Rolling Resistance Come From?

When the tire is rolling, tire is deformed by load and flattening out in the contact patch. The repeated deformation cause energy loss as RR. The RR comes from three main causes [15]: Deformation (Internal friction of the tire material), Aerodynamic (Wind drag) and Microslippage (Friction between tire and road). The majority of RR from energy loss is dissipated as heat created by interfriction of tire material approximately 80-95%, other causes from Aerodynamic drag approximately 0-15% and Friction between tire and road less than 5%. These causes will explain in subtitle 3.1.1 - 3.1.3.

There are at least 8 physical mechanisms responsible for three main causes of RR [16], there are sidewall deformation, contact patch scrubbing, lateral tire slip, energy loss on bump, deflection of the tread element, deflection of the road surface, aerodynamic drag, longitudinal tire slip. And addition, there are mechanisms influenced by real usability factors from the world [16], there are load, tread wear, material, road surface, equilibrium time, inflation pressure, weather, speed, alignment. These mechanisms have an influence on more than one of physical origins. Increasing the load in tire will increase RR because when tire has high load, the deformation will increase from internal friction. While some factors are difficult to control such as weather, road surface, equilibrium time etc.

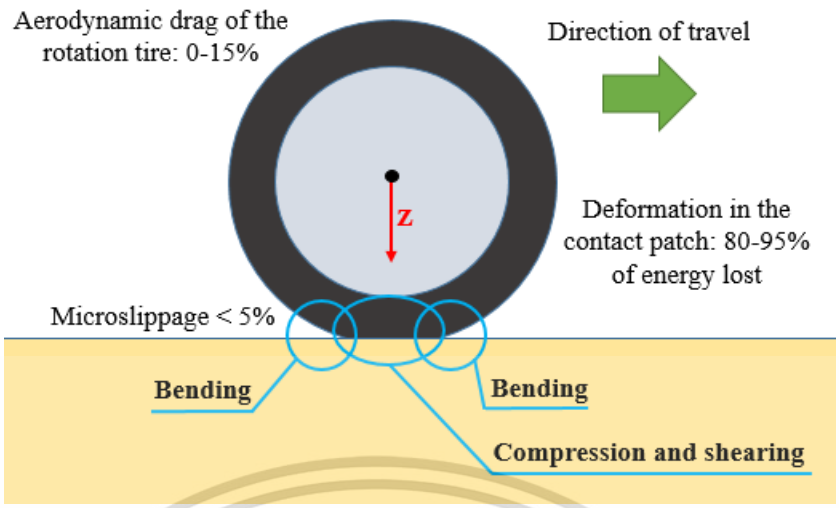

Figure 3.1 The main three causes of Rolling Resistance.

3.1.1 Aerodynamic

When the tire is rolling, it disturbs the air approximately them. Air movement resists the tire movement or rotation. This resistance by air movement is causes of RR. The bigger of tire surface area is increases of RR too. Because the RR also increases with the square of the rotational speed. The Aerodynamic drag of a rotating tire account approximately 0-15% of total RR.

3.1.2 Microslippage

The loaded tire when contact with ground, it occurs the contact patch. When the tire is rolling, the contact patch is constantly subject to Microslippage which occurs between the tread of tire and the road surface. In addition to between the tread of tire and the road surface, Microslippage can occurs between the tire and the wheel too. Which Microslippage will causes of energy dissipation and contributes to RR. However, this factor isn't contributes to RR not so much if a truck is driven in a straight line without accelerating and braking. Because of this, Microslippage account for less than 5% of total RR.

3.1.3 Deformation

The tire is a complex object, because the tire is a composite object made from elastomers, metal, fabric reinforcement materials. Elastomers or rubbers of tire are Hyperelastic and Viscoelastic materials. These materials are factors of high RR occurrence. They therefore dissipate energy to heat form whenever they are being deformed. Deformation contributes the energy dissipation accounts for approximately 90% of total RR. This means, deformation is majority of RR. Which amount of energy dissipated by a given rubber compound depends on the strain to which the tire complete a full revolution.

Tire can separates into 3 main areas, these are Crown, Sidewall and Bead. Crown can be likened to a composite with tread, belt and inner liner. From the Figure 3.2, the energy dissipation is distributed as follow: Crown 70%, Sidewall 15% and Bead 15%. From results, the Crown deformation is the main source of energy loss. Because of this, it will not going into details on Sidewall and Bead area deformation. This will focus on the Crown area. When tire flattening in contact patch, its causes three main kinds of deformation: Bending, Compression and Shearing.

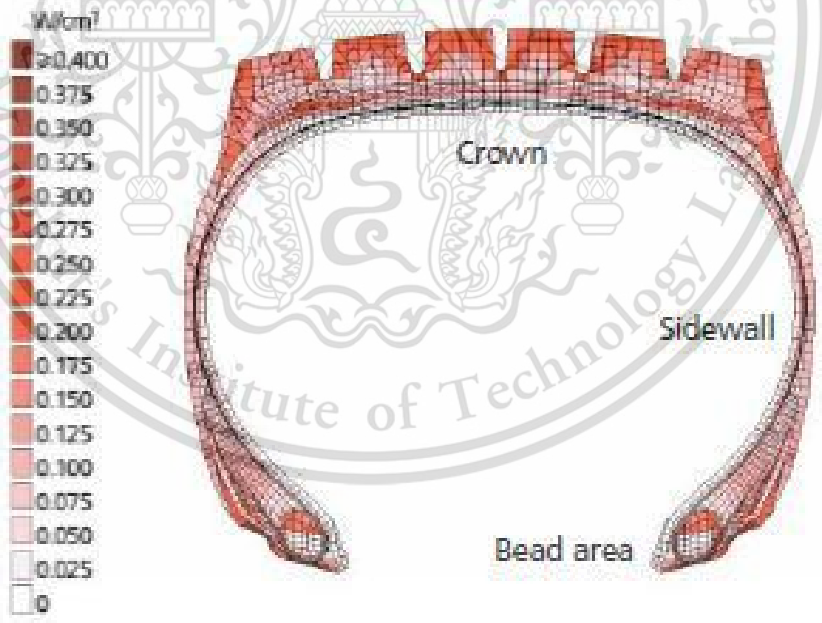

Figure 3.2 The energy dissipation of truck tire.

Source: Michelin. (2003). The tyre Rolling resistance and fuel saving, 2003. Clermont-Ferrand: Société de Technologie Michelin 23, rue Breschet, 63000.

3.1.3.1 Bending

When the truck is being driven, the Crown hugs with the road surface, flattening in contact patch. The tire flattens throughout the length and width of tread. This is longitudinal bending and transversal bending as Figure 3.3

When the Crown reaches the contact patch, its circumferential curvature is modified. The Crown first bend, then flattens and finally return to its initial shape. When the Crown bends, the outside layer is stretched and inside layer compressed as Figure 3.3.

The bending strain ($\varepsilon_{bending}$) is the ratio about the tread block deformation and its initial dimensions. The maximum strain of the tread block subjected to bending equals:

$$\varepsilon_{bending} = h \cdot \left(\frac{1}{R_f} - \frac{1}{R_i} \right) \quad (3.1)$$

Where: h is the tread block thickness

R_f is the radius of the initial curvature

R_i is radius of the final curvature

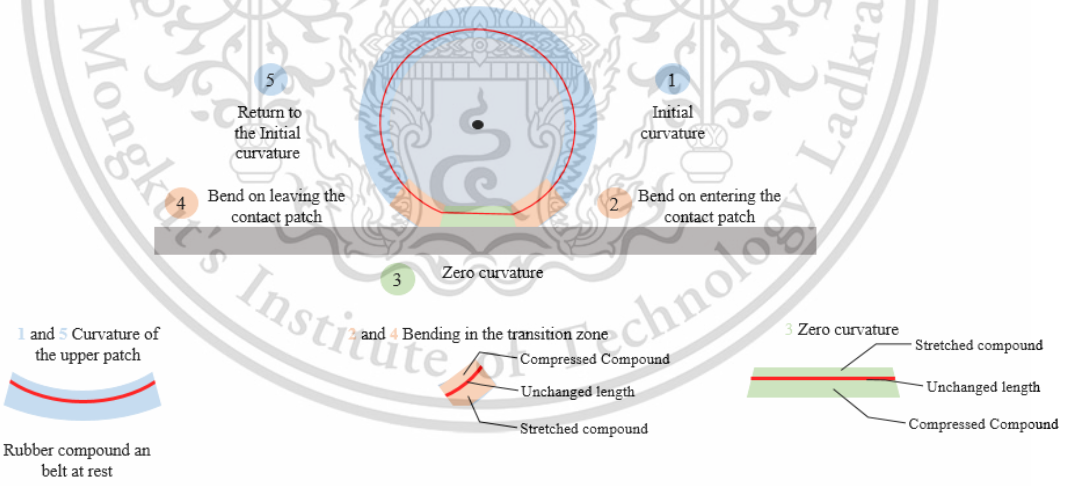

Figure 3.3 Longitudinal bending.

The longitudinal bending strain in the crown is approximately 4 % for truck tire.

3.1.3.2 Compression

When the tire under the vehicle's load, the tread block will compressed in a contact patch.

From the equation (2), the calculation can calculates the compression $\varepsilon_{compression}$ strain of truck tire approximately 14%:

$$\varepsilon_{compression}=0.33\times(1-e^{\left(\frac{\sigma}{M_{10}\cdot F}\right)}) \quad (3.2)$$

Where: σ is pressure exerted

M_{10} is the modulus measured at 10 % stretching

F is the aspect ratio equal to S/S'

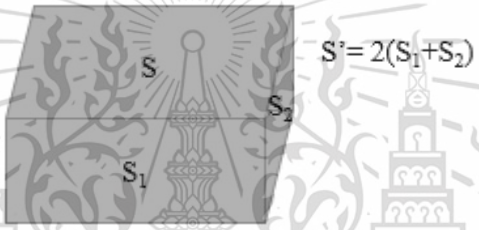

Figure 3.4 The calculation of S/S'.

3.1.3.3 Shearing

When the tread of tire in the contact patch is subjected not only to compression but it to shearing too.

In Figure 3.5, the tire is circumstance and when tread block enters to contact patch, the tread doesn't contact the ground vertically but at an angle instead. In the absence of slippage between the ground surface and the tread, the angle of tread is determined by the relative position between blue dot (point of impact on ground surface) and green dot (point of attachment to the belt). To maintain with the belt as its get closer to middle of contact patch, the tread block gradually becomes upright. Finally, the shearing force exerted on it before leaving the contact patch makes it appear to lean forwards.

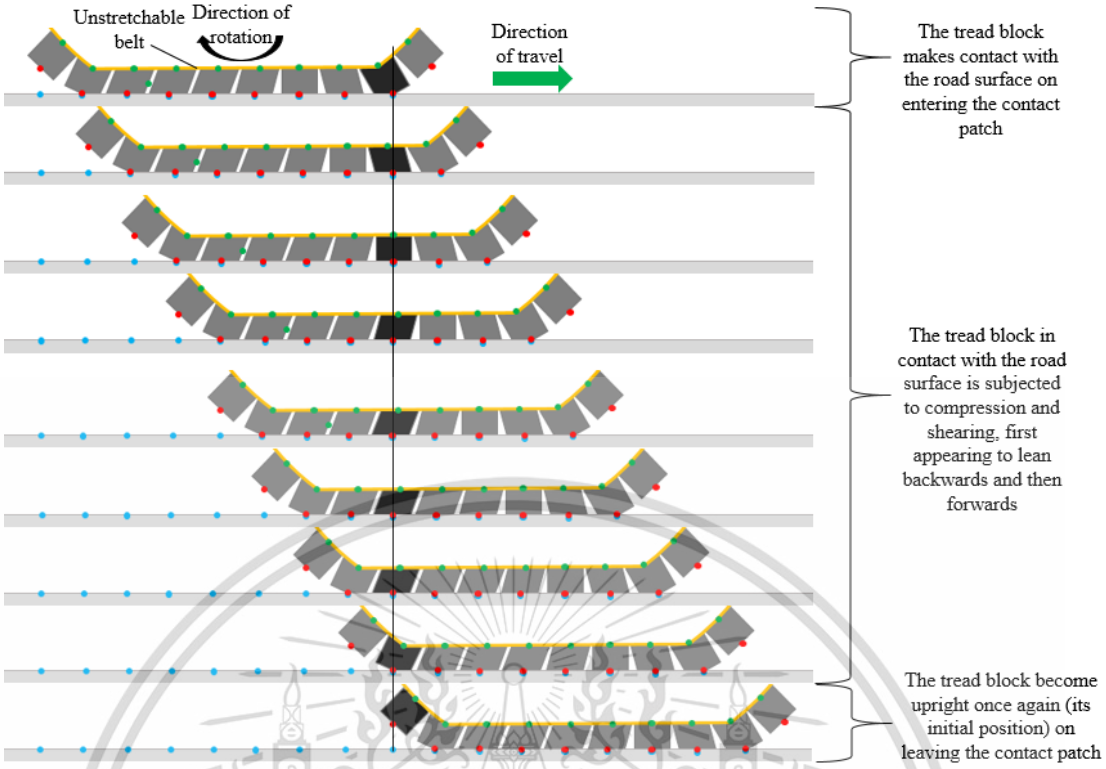

Figure 3.5 Movement of tread block in contact patch.

From the equation (3.3), the calculation can calculates the shear strain (d/h) of truck tire approximately 15%:

$$\frac{d}{h} \approx \tan\alpha_{transition} \approx \sqrt{2 \cdot \frac{\Delta h}{R'_{transition}}} \tag{3.3}$$

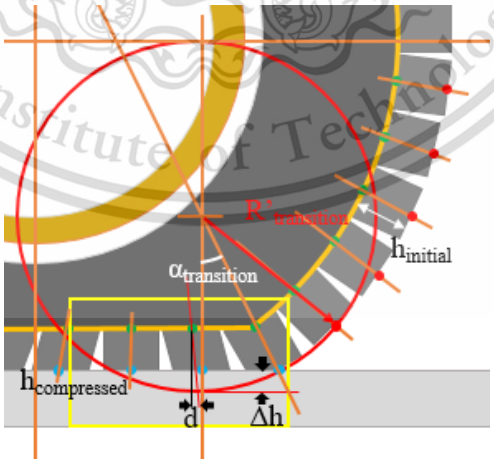

Figure 3.6 Position of d, h, α, Δh and $R'_{transition}$

3.1.3.4 Effect of the Dimension

The Rolling Resistance Coefficient (RRC) is equal to:

$$RRC=\frac{RR}{N} \tag{3.4}$$

Where: N is load in vertical

By definition, a RRC is a value without units. In this case, RR and N both expressed in Newton. It can also be expressed as a percentage or as per millimeter.

The RRC of tire decreases as its outer dimension increasing. Because the bending of the tire on entering and leaving from the contact patch is less severe with a bigger diameter. Increasing the tire diameter by 1 cm can reduces the RR by approximately 1%.

In the Wide tire, the outer diameter is less than Narrow tire. From Figure 3.7, the Narrow tire has high deformation than Wide tire [17] because from Pythagoras theory as equation (3.5):

$$(\frac{OD}{2})^2=(\frac{CL}{2})^2+b^2 \tag{3.5}$$

$$b=\sqrt{(\frac{OD}{2})^2-(\frac{CL}{2})^2} \tag{3.6}$$

$$deflection=\frac{OD}{2}-\sqrt{(\frac{OD}{2})^2-(\frac{CL}{2})^2} \tag{3.7}$$

Where: OD is overall diameter

CL is contact length

b is radius of tire when deformed

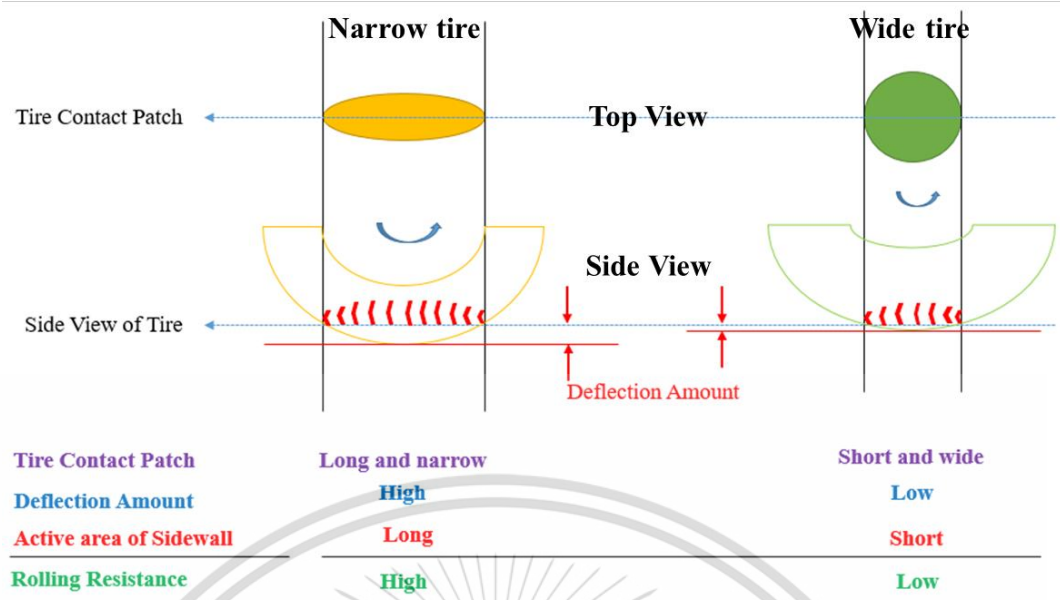

Figure 3.7 The Rolling Resistance comparison of Narrow tire and Wide tire.

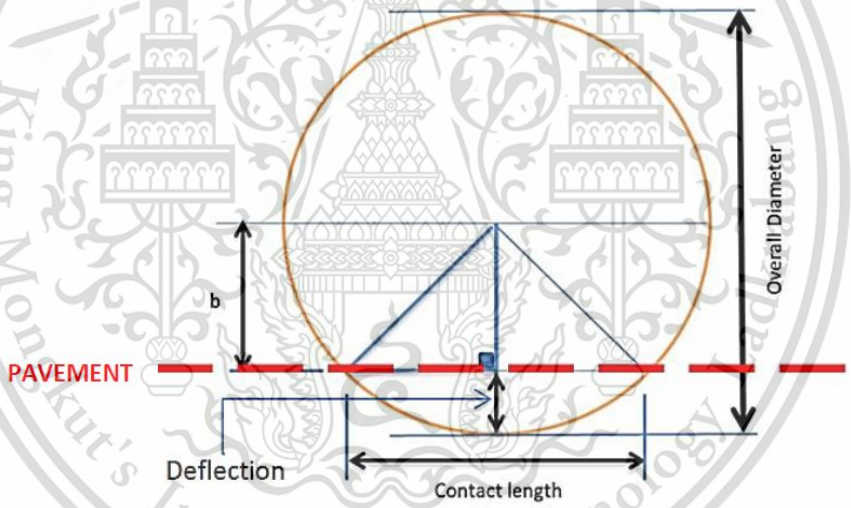

Figure 3.8 The tire deflection diagram.

From equation (3.7), when the contact length is decreasing, the outer diameter will increasing, it leads to deformation will decreasing.

3.1.4 Measurement of Tire Rolling Resistance

3.1.4.1 Measurement of Force in the Contact Patch

The recording of horizontal force is the reaction forces on the ground with tread are greater at the back of the contact patch than the front. Because of these, forces are directed backwards, thus opposing the tire's forward movement. This horizontal resultant is the RR force.

The recording of vertical forces is the ground reaction forces with the rubber compound are greater at the front of contact patch than at the back. Because of these, vertical resultant is offset towards the front of the contact patch.

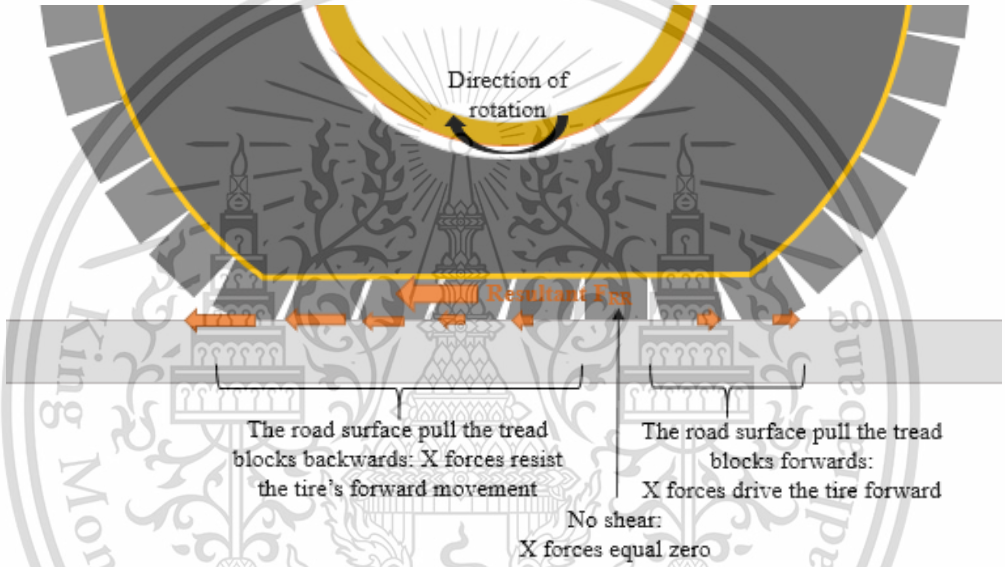

Figure 3.9 The horizontal forces of tire diagram.

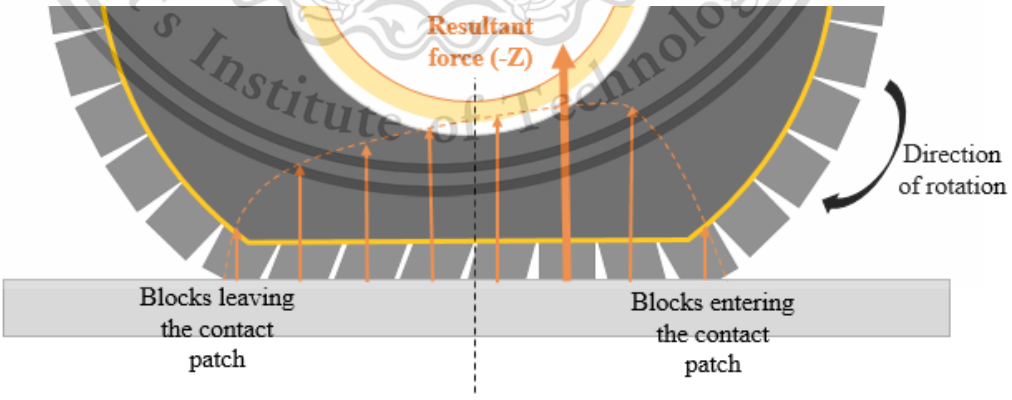

Figure 3.10 The vertical forces of tire diagram.

3.1.4.2 Measurement of Rolling Resistance on Testing.

From UN-ECE R117 standard testing [18], this testing uses the large test drum by an actuating cylinder aligned with the center of the drum as Figure 3.11. A motor coupled to the drum makes it rotating, thus making the tire rotating. The tire's RR has a braking effect on the drum's rotation which is then measured.

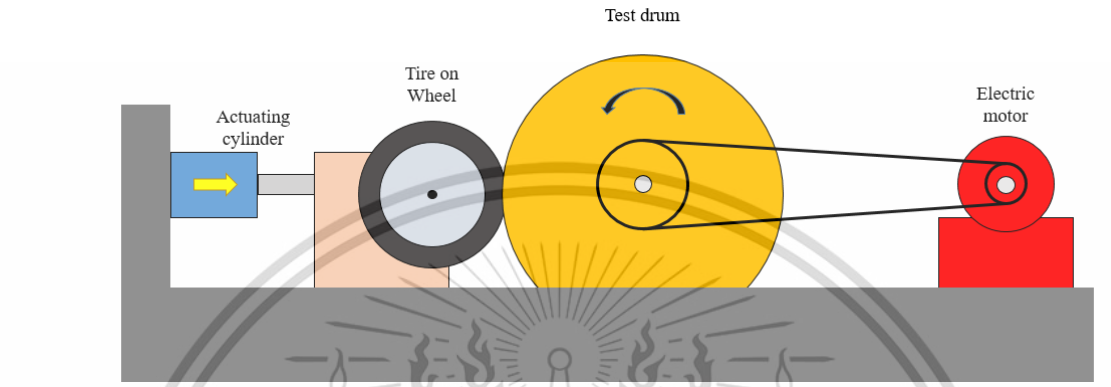

Figure 3.11 Diagram of Rolling Resistance drum tester.

This standard has 4 methods to measure the RR: force method, torque method, deceleration method and power method. In this case uses the force method to testing, the reaction force is measured or converted at the tire spindle on longitudinal axis. In test condition, the truck tire (Class C3) test speed will be obtained at the drum, speeds specified in Table 3.1, the speed for class C3 is 80 km/hr. The test loads and inflation pressures follow as Table 3.2, the load is 85% of maximum tire vertical load and the inflation pressure depend on marked on sidewall at maximum pressure. In test procedure, before testing the inflated C3 tire shall be placed in the thermal environment of the test location for a minimum of 6 hours. After placed in the thermal environment, the inflation pressure shall be adjusted to the test pressure, and verified 10 minutes after the adjustment was made. Next procedure, the warm-up durations shall be as specified in Table 3.3, the class C3 and rim size equal to 22.5 inch is the 180 minute. After warm-up, test the parasitic losses related to tire/drum (F_{pl}) with skim test reading and calculates with equation (3.8):

$$F_{pl}=F_t \cdot \left(1+\frac{r_L}{R}\right) \tag{3.8}$$

Where: F_t is the tire spindle force

r_L is effective radius

R is the test drum radius

Table 3.1 Test speeds of UN-ECE R117.

Tyre Class	*C1*	*C2 and C3*	*C3*	
Load Index	All	LI ≤ 121	LI > 121	
Speed Symbol	All	All	J 100 km/h and lower or tyres not marked with speed symbol	K 110 km/h and higher
Speed	80	80	60	80

Source: E/ECE/324/Rev.2/Add.116/Rev.2−E/ECE/TRANS/505/Rev.2/Add.116/Rev.2

Table 3.2 Test loads and inflation pressures of UN-ECE R117.

Tyre Class	*C1* [a]		*C2, C3*
	Standard Load	*Reinforced or Extra Load*	
Load- % of maximum load capacity	80	80	85[b] (% of single load)
Inflationpressure kPa	210	250	Corresponding to maximum load capacity for single application[c]

Note: The inflation pressure shall be capped with the accuracy specified in paragraph 4 of Appendix 1 to this annex.

(a) For those passenger car tyres belonging to categories which are not shown in ISO 4000-1:2010, the inflation pressure shall be the inflation pressure recommended by the tyre manufacturer, corresponding to the maximum tyre load capacity, reduced by 30 kPa.

(b) As a percentage of single load, or 85 per cent of maximum load capacity for single application specified in applicable tyre standards manuals if not marked on tyre.

(c) Inflation pressure marked on sidewall, or if not marked on sidewall, as specified in applicable tyre standards manuals corresponding to maximum load capacity for single application.

Source: E/ECE/324/Rev.2/Add.116/Rev.2−E/ECE/TRANS/505/Rev.2/Add.116/Rev.2

Table 3.3 Warm up durations of UN-ECE R117.

Tyre Class	*C1*	*C2 and C3 LI ≤ 121*	*C3 LI > 121*	
Nominal Rim Diameter	All	All	< 22.5	≥ 22.5
Warm up duration	30 min.	50 min.	150 min.	180 min.

Source: E/ECE/324/Rev.2/Add.116/Rev.2−E/ECE/TRANS/505/Rev.2/Add.116/Rev.2

After skim testing, test the RR and calculate by equation (3.9):

$$RR=F_t\cdot\left(1+\frac{r_L}{R}\right)-F_{pl} \tag{3.9}$$

If measurements at temperatures other than 25 °C are unavoidable (only temperatures not less than 20 °C or more than 30 °C are acceptable), then a correction for temperature shall be made using the following equation (3.10):

$$RR_{25}=RR\cdot[1+K(t_{amb}-25)] \tag{3.10}$$

Where: RR_{25} is the RR at 25 °C

t_{amb} is the ambient temperature

K is equal to 0.006 for class C3 tires

Test results are obtained from different drum diameters shall be compared by using the following equation (3.11):

$$F_{r02}=KF_{r01} \tag{3.11}$$

With:

$$K=\sqrt{\frac{(\frac{R_1}{R_2})(R_2+r_T)}{(R_1+r_T)}} \tag{3.12}$$

Where: R_1 is the radius of drum 1

R_2 is the radius of drum 2

r_T is one-half of the nominal tire diameter

F_{r01} is the RR value measured on drum 1

F_{r02} is the RR value measured on drum 2

3.2 MATERIAL PROPERTIES

3.2.1 Material of Rubber

In the tire, rubber is the most complex material, the properties of which change with time, effected by the environment and deteriorate on contact with heat, oils, chemicals, sunlight, and the weather [19]. Rubber is incompressible or nearly incompressible material. It shows the nonlinear behavior under large strain. From this behavior, it can explain in Hyperelasticity and Viscoelasticity.

3.2.1.1 Hyperelastic Material Property

The Hyperelastic material property of rubber provides highly nonlinear and incompressible material behavior such as a spring is subjected to a force. The models of Hyperelastic can divides into two methodologies: Phenomenological model and Physical Based model. Phenomenological model is the model reference with testing data. The coefficient is obtained from curve fitting and predicts behavior by Constitutive model. Advantages of this model is accuracy in testing data phase but disadvantages aren't obtained coefficient data from one testing and it must testing in various conditions. Physical Based model can predicts the behavior in less or not testing data phase.

Material models are feature by different forms of strain energy functions. The regularly strain energy functions are explain in term of the strain invariants which are functions of stretch ratio. For isotropic, compressible materials the strain energy (U) is a function of:

$$U=U(\bar{I}_1,\bar{I}_2,\bar{I}_3) \quad (3.13)$$

Where: I_1 is the first deviatoric strain invariants

I_2 is the second deviatoric strain invariants

I_3 is the third deviatoric strain invariants

With:

$$\bar{I}_1=\lambda_1^2+\lambda_2^2+\lambda_3^2 \quad (3.14)$$

$$\bar{I}_2=\lambda_1^2\lambda_2^2+\lambda_2^2\lambda_3^2+\lambda_1^2\lambda_3^2 \quad (3.15)$$

$$\bar{I}_3=\lambda_1^2\lambda_2^2\lambda_3^2 \quad (3.16)$$

Where: λ_1 is the deviatoric stretches at axis 1

λ_2 is the deviatoric stretches at axis 2

λ_3 is the deviatoric stretches at axis 3

For incompressible and isothermal material, equation (3.16) is equal to 1.

The most popular tire material property model is the Mooney-Rivlin of Phenomenological model. But Mooney-Rivlin isn't capable of predicting large strain behavior of rubber material [20]. The Yeoh model is the Phenomenological model too, and it has advantages follows [13]: 1. It can cover a much wider range of deformation than other models, 2. It can be obtained the data from uni-axial tension only, 3. It can predict the shear modulus varying with increasing deformation. Yeoh strain energy function in terms of the first deviatoric strain invariant is described as equation (3.17):

$$U=C_{10}(\bar{I}_1-3)+C_{20}(\bar{I}_1-3)^2+C_{30}(\bar{I}_1-3)^3 \quad (3.17)$$

Where: C_{10}, C_{20}, C_{30} are temperature-dependent material parameters

These parameters can be obtained from material testing data as uni-axial tension, bi-axial tension, planar shear and volumetric. But Yeoh model can uses the uni-axial tension only.

3.2.1.2 Viscoelastic Material Property

The viscoelasticity of rubber has a significant influence on the traction, steering response and RR [20]. The Viscoelastic material behavior is like a damping in mechanism [21].

The viscoelastic models are depend on time and frequency such as stress relaxation and creep. The viscoelastic material responds in the time domain is adopted here, which is defined by a Prony series expansion of the dimensionless relaxation modulus ($g_t(t)$) as equation (3.18):

$$g_t(t)=1-\sum_{i=1}^{N} \bar{g}_i^P \left(1-e^{-t/\tau_i^G}\right) \quad (3.13)$$

Where: τ_i^G is relaxation time

$N, \bar{g}_i^P$ are the material constants

t is time period

The Viscoelastic material property should be considered together with the Hyperelastic model to define large-deformation, nonlinear, Viscoelastic behavior for the Transient Static analysis, Transient Implicit Dynamics analysis, Explicit Dynamic analysis and Steady State Transport analysis, etc.

3.2.1.3 Mullins Effect and Hysteresis Losses

The real behavior of filled rubber or compound rubber under cyclic loading is quite complex [22]. When the rubber or elastomer deformed with load from its virgin state, unloaded, and reloaded, the stress required on reloading is less than that on the initial loading for stretches up to the maximum stretch achieved during the initial loading as Figure 3.12.

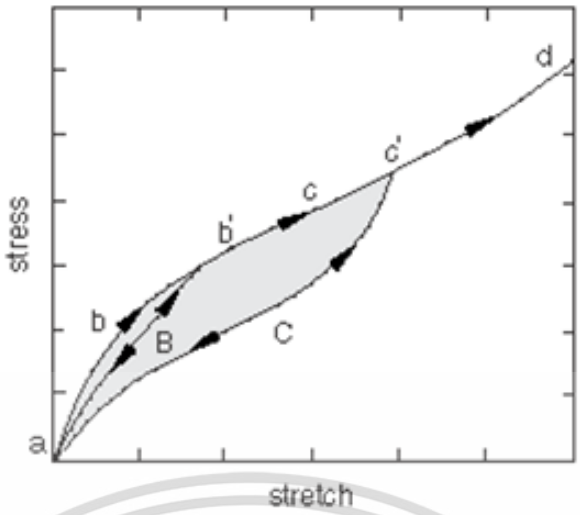

Figure 3.12 Stress-Stretch graph of Mullins effect and Hysteresis loop.

Source: Ogden, R. W., and D. G. Roxburgh, "A Pseudo-Elastic Model for the Mullins Effect in Filled Rubber," Proceedings of the Royal Society of London, Series A, vol. 455 2861–2877, 1999.

The Mullins effect represents the energy dissipation in term of Hysteresis loop. The Hysteresis losses show in the stress-strain or stress-stretch graph of one revolution. In Figure 3.12, the area in ellipse shows the Hysteresis losses, it called Hysteresis loop. If it has high strain or deflection, the area in ellipse will increasing and it causes of chance to high Hysteresis losses occurrence. Hysteresis losses are major cause of RR from energy dissipation.

$$\frac{\partial U}{\partial \eta}(\mathbf{F}, \eta) = 0 \tag{3.14}$$

Where: U is the stored elastic energy potential

η is a scalar variable

F is the deformation gradient tensor

or some other appropriate strain measure

The basic framework for model in equation (3.14), Hyperelastic materials are described in terms of a strain energy potential function, U, which defines the strain energy stored in the material per unit reference volume. The quantity F is the

deformation gradient tensor or some other appropriate strain measure. To account for Mullins effect, Ogden and Roxburgh [22] proposed a material description that is based on an energy function of the form U (F,η) form, where η is a scalar variable. This scalar variable controls the material properties in the sense that it enables the material response to be governed by an energy function on unloading and subsequent submaximal reloading different froms that on the initial loading path from a virgin state.

3.2.2 Material of Reinforcement

The tire is the composite object not only has a rubber, but it has the reinforcement made from metal and fabric too. The reinforcement in the tire is the orthotropic cord rubber composite material that mainly controls the performance of pneumatic tires. It shows the high modulus and low elongation of elastic behavior. From the large strain of rubber material and damping effect from Viscoelastic material property, the reinforcement is reinforce to control the deformation and return to original form of tire.

CHAPTER 4

RESEARCH METHODOLOGY

After investigated the Rolling Resistance (RR), tires and Finite Element Method (FEM), the first methodology of this research was to find the truck tire in size of 11R22.5 to RR experiment with UN-ECE R117 to validate with simulation before compare the Wide-Base-Single (WBS) tire and Dual tires RR and RRC results by simulation. The reason to use the 11R22.5 size in this research because of this size widely used in Dual tires and R22.5 is the rim size of the WBS tire too.

4.1 UN-ECE R117 Truck Tire Testing

After collected the knowledges and information, the Michelin XZY3 11R22.5 148/145K 16PR, Manufacturing date of 2817 truck tire as Figure 4.1 is adopted for RR testing and validation. The truck tire specification presents as Table 4.1. This specification follows the information from Sidewall of tire and brand label.

Figure 4.1 XZY3 Truck tire 11R22.5 used to testing and validation.

The RR results of this truck tire were obtained from testing on the drum tester as Figure 4.2 with UN-ECE R117 standard, the specification of drum tester showed as Table 4.2 and the working system of drum tester presented as Figure 4.3

Table 4.1 Truck tire specification

Sample Name	MICHELIN, XZY3
Tire Size	11R22.5 148/145K 16PR.
Type	Radial, Tubeless
Max Load (single)	3150 kg
Max Load (dual)	2900 kg
Max Inflation Pressure	115 psi
Speed Symbol	K
Max Speed	110 km/hr

Table 4.2 Drum tester specification

Brand	KAYTON
Model	DTM-350PC
No.	KT00737-2
Registration number	SC RDCTRI 51-02-12
Speed and load usage	Speed 35-350 $^{km}/_{hr}$
	Load 2.5-29 kN

Figure 4.2 Rolling Resistance drum tester.

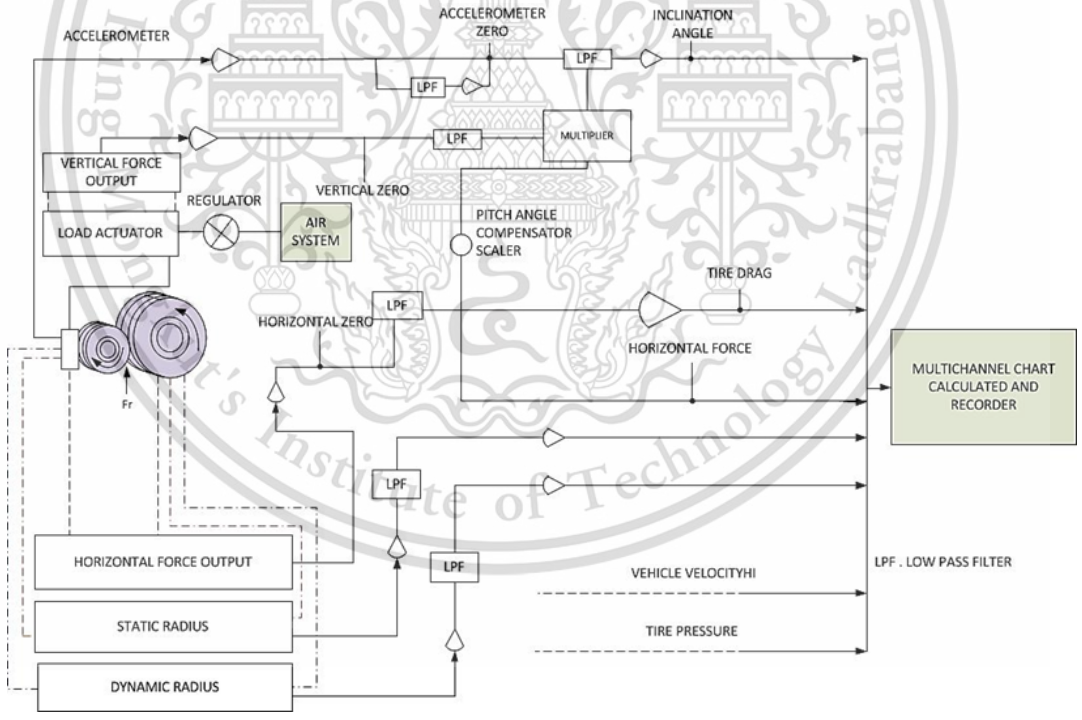

Figure 4.3 Drum tester working system.

In the UN-ECE R117 standard, the 11R22.5 truck tire classifies to C3 class. Before testing, the inflated truck tire placed in the test location 6 hours at temperature

25±5 ºC. After placed in the thermal environment at the test location, then warm-up the truck tire for 180 minutes with the speed and loading of 100 N. The tire was assembled to testing rim and inflated to 110, 115, 120 and 125 psi, and then conditioned at testing temperature for 6 hours. The inflation pressure was re-adjusted prior to testing. The following test conditions were used.

- Test speed: 60, 80, 100, and 110 km/hr
- Test inflation pressure: 110, 115, 120 and 125 psi
- Test load: 2,465 (24.18), 2,677.5 (26.27), 2,900 (28.45) and 3,150 (30.90) kg (kN)
- Test time per step: 210 minutes
- Test temperature: 25±5 ºC

The RR testing has 4 method to measures and calculates the RR, in this research uses the force method. The reaction force will measured or converted at the tire spindle and it separated in two main conditions, there are: 1. Skim test 2. Condition test (the insight of UN-ECE R-117 standard testing of this research is attach in APPENDIX A).

4.1.1 Skim Test

The skim test is the test condition with Parasitic Losses of tire. This condition test to measures the RR from other effects of tire such as bearing, aerodynamic of drum, aerodynamic of rim, aerodynamic of tire, frictions, gravity, etc. The following test conditions were used:

- Test speed : 60, 80, 100, and 110 km/hr
- Test inflation pressure : 110, 115, 120 and 125 psi
- Test load : 500 N
- Test time per step : 180 minutes
- Test temperature : 25±5 ºC

4.1.2 Condition Test

This condition test is the RR measurement from all effect. The test is setting with ten testing conditions. In this condition test measures the RR from all effects such as other effect of tire and effect from tire. After RR measured from condition test, it must calculate to terminate the RR from skim test. The RR testing conditions are separated below:

1. Load 3150 kg, Speed 80 km/hr and Inflation Pressure 115 psi
2. Load 2900 kg, Speed 80 km/hr, and Inflation Pressure 115 psi
3. Load 2677.5 kg, Speed 80 km/hr, and Inflation Pressure 115 psi (according to the standard)
4. Load 2465 kg, Speed 80 km/hr, and Inflation Pressure 115 psi
5. Load 2677.5 kg, Speed 110 km/hr, and Inflation Pressure 115 psi
6. Load 2677.5 kg, Speed 100 km/hr, and Inflation Pressure 115 psi
7. Load 2677.5 kg, Speed 60 km/hr, and Inflation Pressure 115 psi
8. Load 2677.5 kg, Speed 80 km/hr, and Inflation Pressure 125 psi
9. Load 2677.5 kg, Speed 80 km/hr, and Inflation Pressure 120 psi
10. Load 2677.5 kg, Speed 80 km/hr, and Inflation Pressure 110 psi

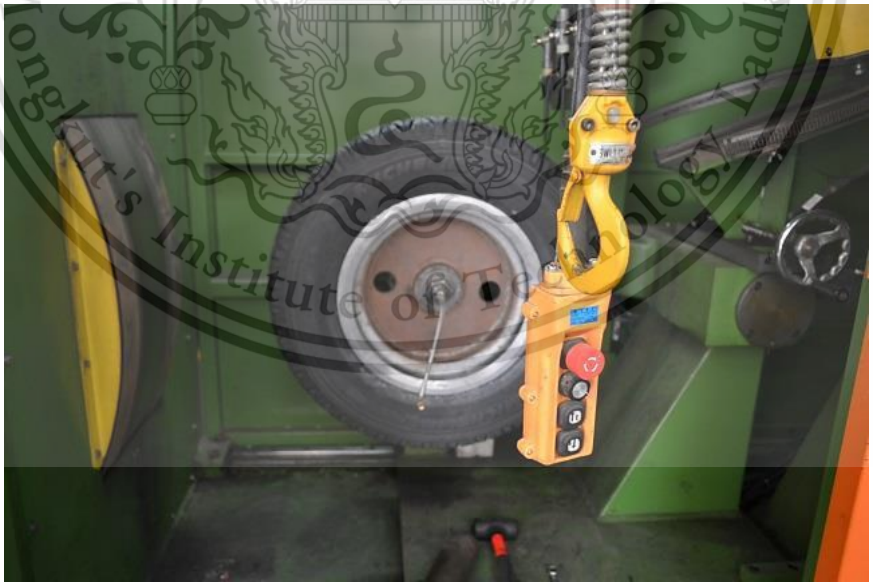

Figure 4.4 The tire installed with the Rolling Resistance drum tester.

Figure 4.5 The controller of Rolling Resistance drum tester.

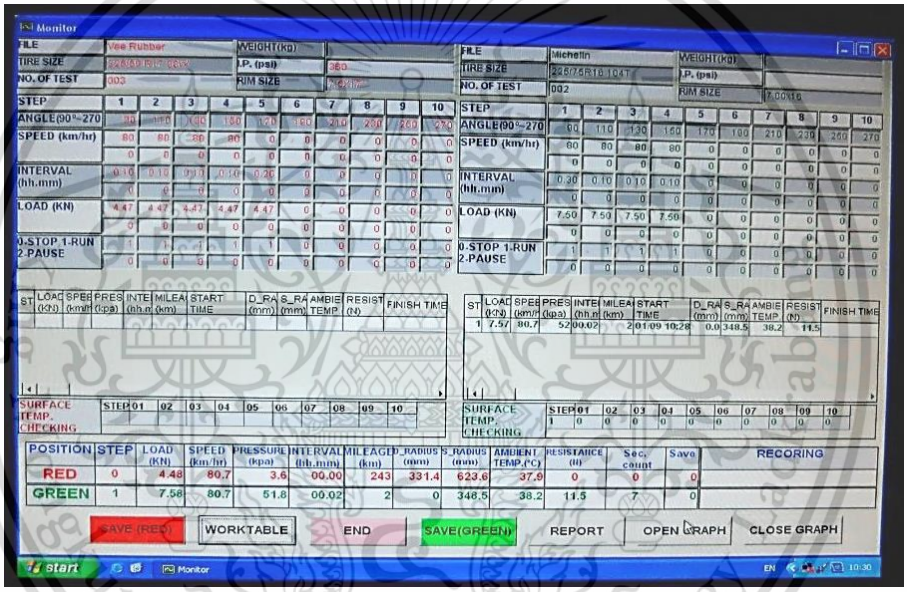

Figure 4.6 The monitor of Rolling Resistance drum tester.

4.1.3 Rolling Resistance Calculation

After test and obtained the tire spindle force results from both skim test and condition test, it must calculates the absolute RR from equations (3.8) - (3.12). The RR of skim test must calculates with equation (3.8). The RR of condition test must calculates with equation (3.9). The ambient temperature of RR test isn't 25 ^{o}C must calculates with equation (3.10) to correction. Not only temperature correction, the drum

diameter must corrected with equations (3.11) and (3.12) too. Because the drum tester diameter is 1,707.6 mm but in the standard requirement is 2,000 mm.

4.2 Truck Tire Material Property Testing

The truck tire simulation with FEM must has the material properties constants to input in the model. The truck tire material properties constants can be obtained from raw materials of truck tire by material properties testing.

The truck tire has many sections of material. The author separates the sections into two majority, there are the rubber section and reinforcement section. In the rubber section can separates into six minor sections, there are Tread, Undertread, Sidewall, Apex, Toeguard and Inner liner. The author assumes Undertread to tread property because of limitation when extract material from tire and its material property is similar to tread. In reinforcement section can separates into 3 minor sections, there are steel belt, steel ply and bead bundle.

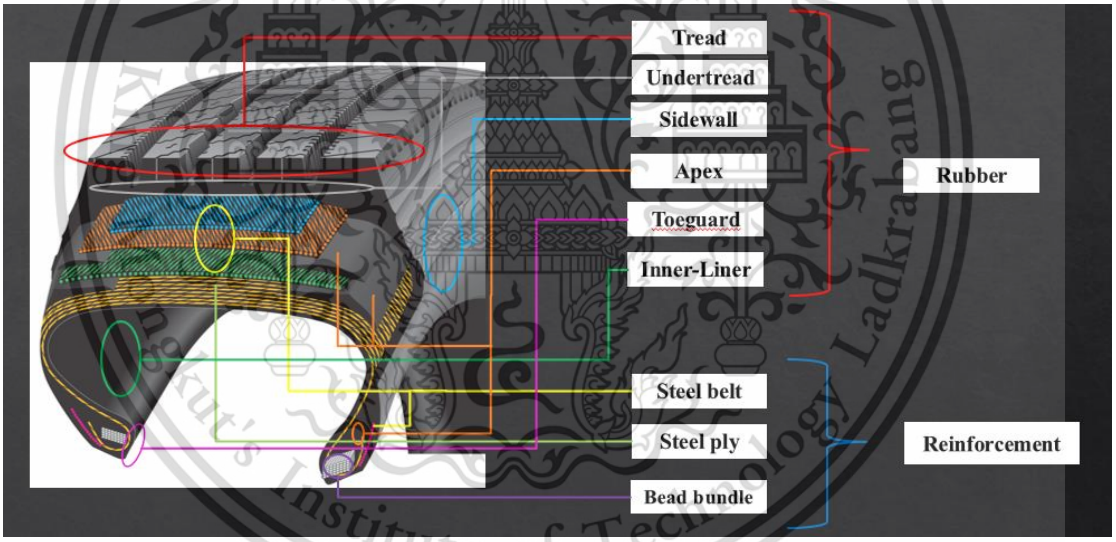

Figure 4.7 The truck tire material sections.

Next process is to extract the rubber sections from the truck tire. First cut the tire to cross section with water jet cutting method as Figure 4.8. After that, extract the rubber sections from the truck tire into raw rubber material as Figure 4.9.

Figure 4.8 Truck tire cross section cutting.

Figure 4.9 Raw rubber materials from truck tire.

After receiving raw materials of rubber sections, bring raw materials to resizing into dumbbell specimen size before pressing to dumbbell specimen with slide machine. Then presses rubber materials into dumbbell specimen as Figure 4.10. And the dimension of dumbbell specimen is following with ASTM D412-80 standard [23] as Figure 4.11.

Figure 4.10 Dumbbell specimens from rubber materials.

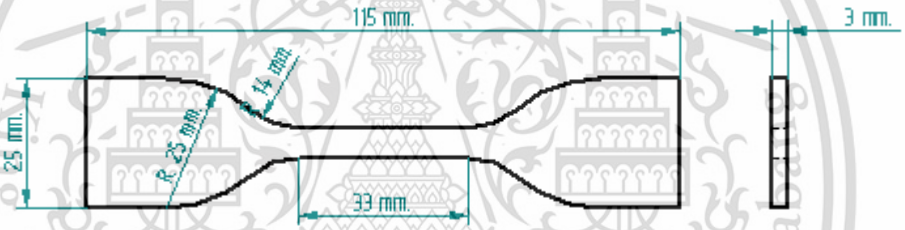

Figure 4.11 Dimension of dumbbell specimen following with ASTM D412-80.

Source: Wipoo Piwat, C. D. (2004). Hyperelastic Material Testing for Finite Element Modeling. The Conference of Mechanical Engineering Network of Thailand. Khonkaen: Khon Kaen University.

4.2.1 Hyperelastic Material Property of Rubbers Testing

After receiving the dumbbell specimen, the first material testing is the Hyperelastic material testing by tensile test. The Hyperelasticity has many models but the author select the Yeoh model because it can cover a much wider range of deformation than other models, and it can predict the shear modulus varying with increasing deformation. The constants in model can be obtained from uniaxial tension, biaxial extension and planar shear testing shows in the graph as Figure 4.12 but in Yeoh model can be obtained the data from uniaxial tension testing only.

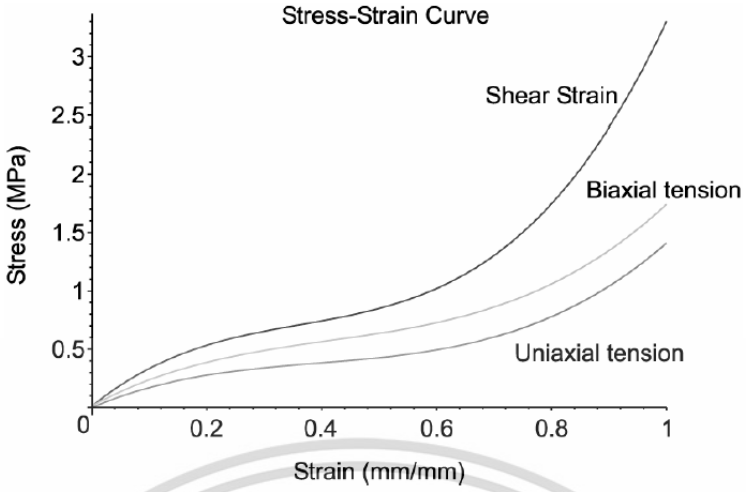

Figure 4.12 Hyperelastic material property testing graph.
Source: Jittham, P. (2009). Mechanical Testing of Rubber for Structural Finite Element Analysis. Nakhon Nayok: MTEC.

Bring specimens to uniaxial tensile test with ASTM D412-80 standard testing as Figure 4.13. This testing pulls the specimen until the specimen fractured. After testing, obtained the raw data as Figure 4.14 – Figure 4.18 (The other data of tensile test will attach in Appendix B).

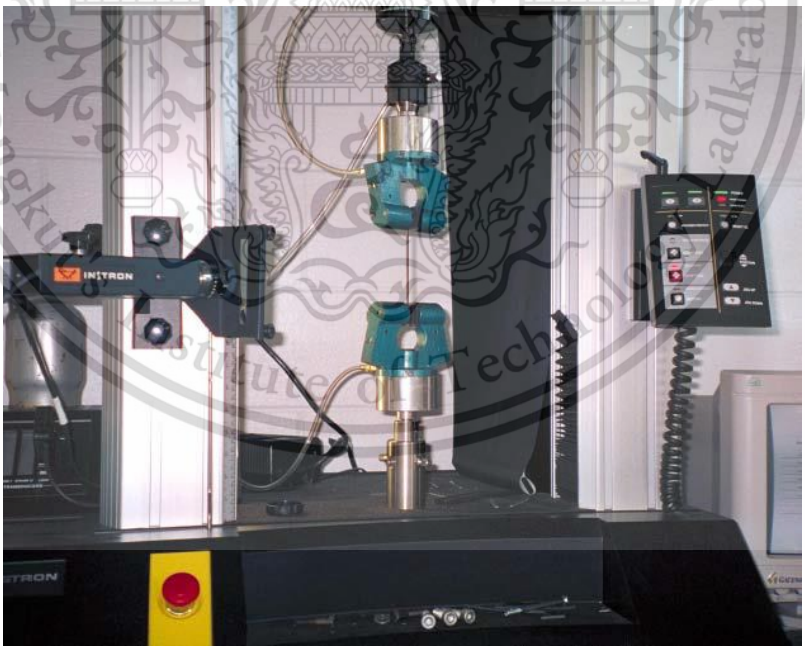

Figure 4.13 Uniaxial tensile material testing.
Source: Jittham, P. (2009). Mechanical Testing of Rubber for Structural Finite Element Analysis. Nakhon Nayok: MTEC.

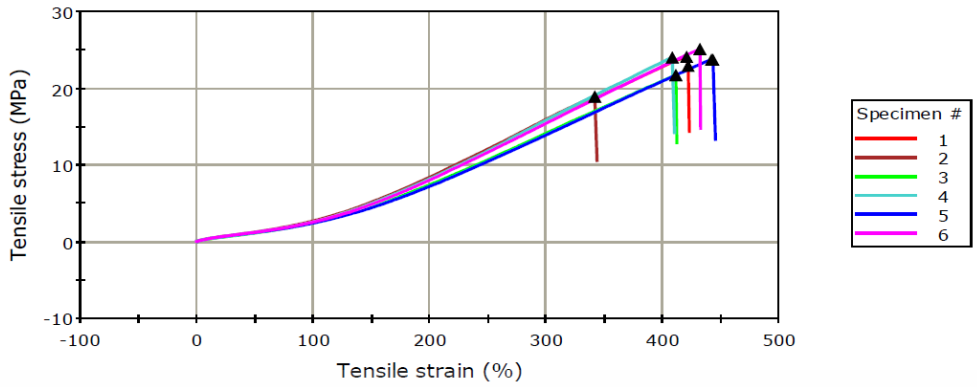

Figure 4.14 Apex uniaxial tensile material testing graph.

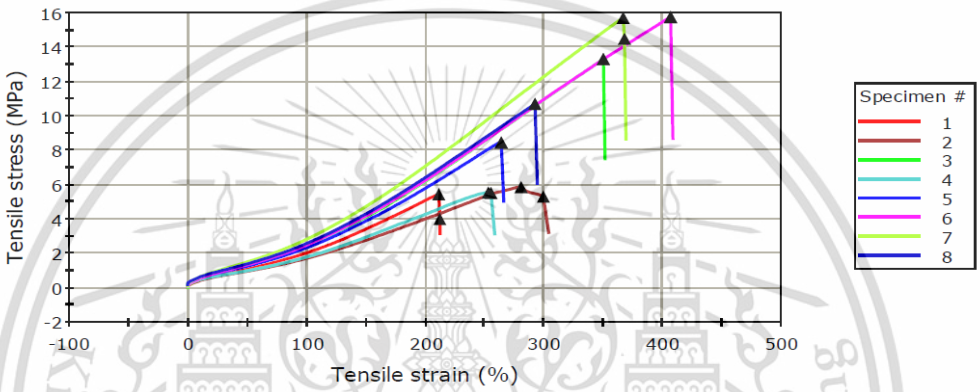

Figure 4.15 Inner liner uniaxial tensile material testing graph.

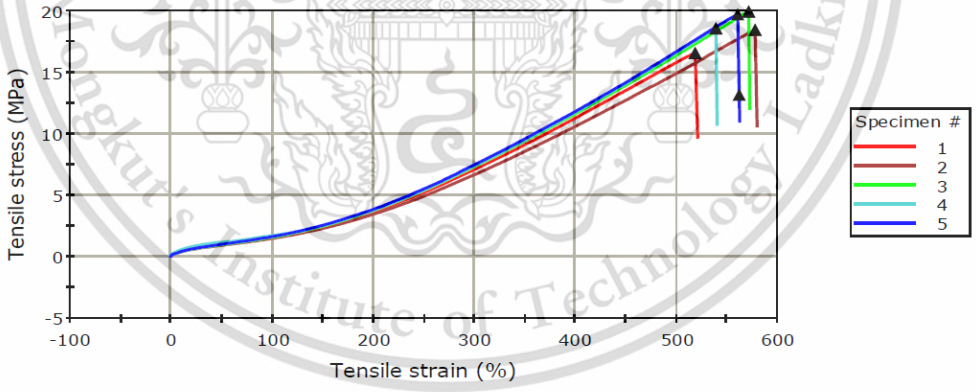

Figure 4.16 Sidewall uniaxial tensile material testing graph.

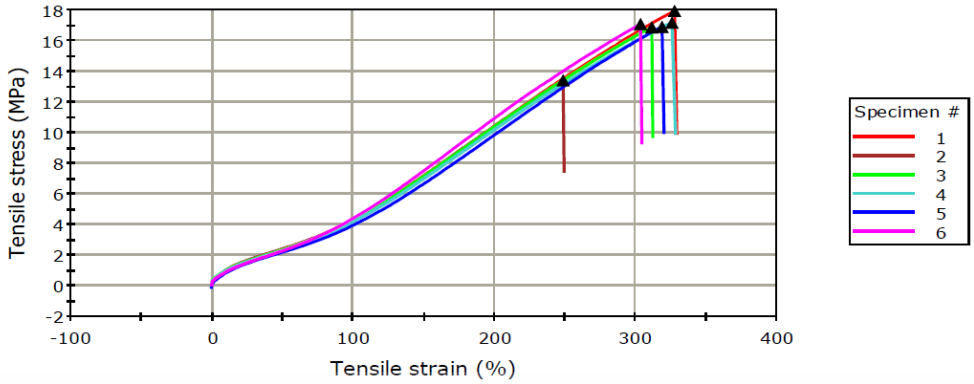

Figure 4.17 Toeguard uniaxial tensile material testing graph.

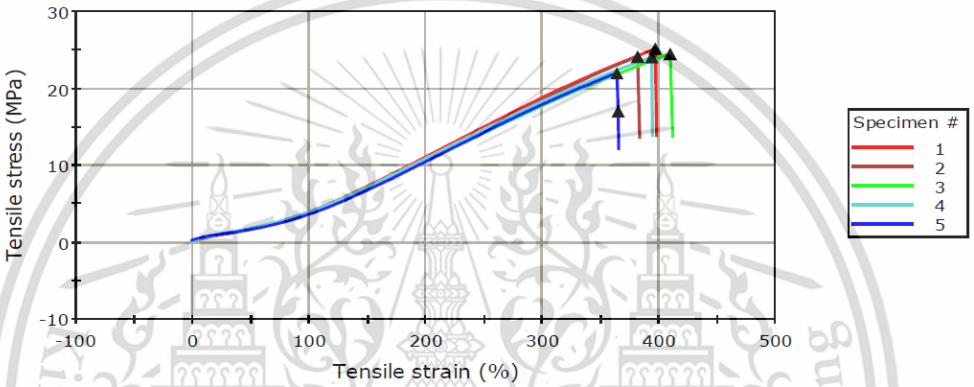

Figure 4.18 Tread uniaxial tensile material testing graph.

After obtained the raw data, evaluates the data to find the mean of data and next process is to find the Hyperelastic material constants C_{10}, C_{20} and C_{30} to input in FEM model by curve fitting with Yeoh model in ABAQUS/CAE software. The curve fitting graphs present as Figure 4.19 – Figure 4.23.

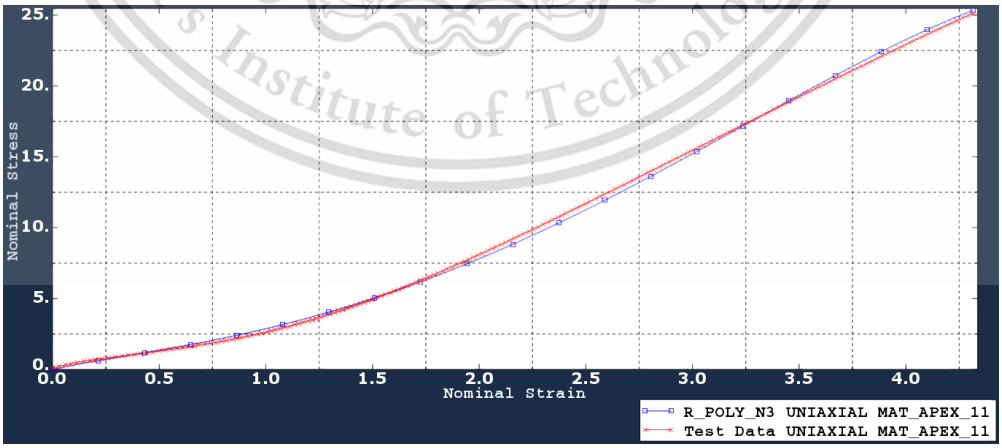

Figure 4.19 The Yeoh model curve fitting graph with testing data of Apex.

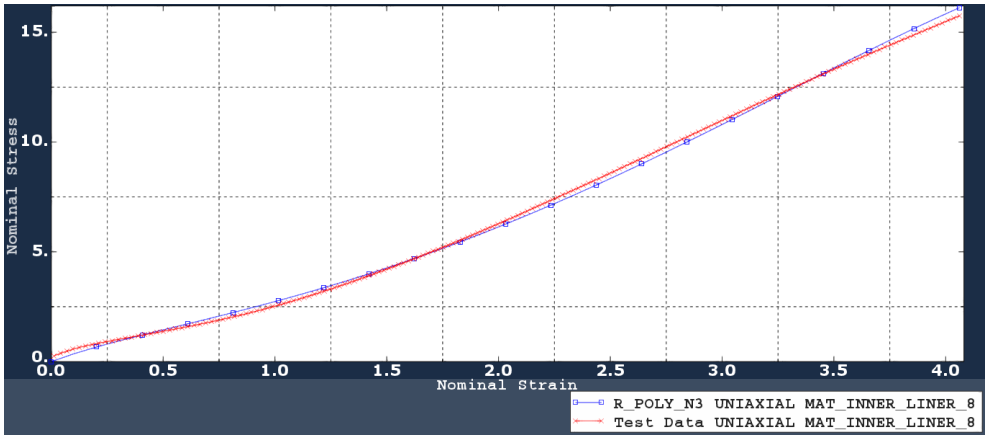

Figure 4.20 The Yeoh model curve fitting graph with testing data of Inner liner.

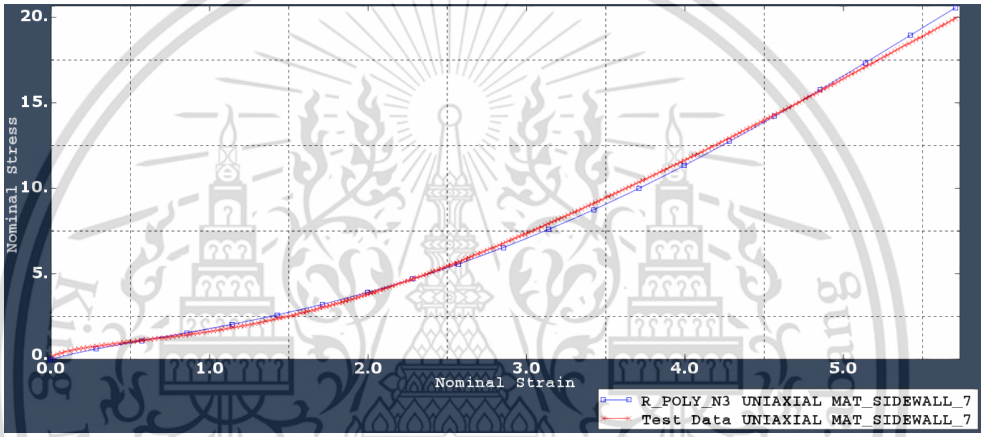

Figure 4.21 The Yeoh model curve fitting graph with testing data of Sidewall.

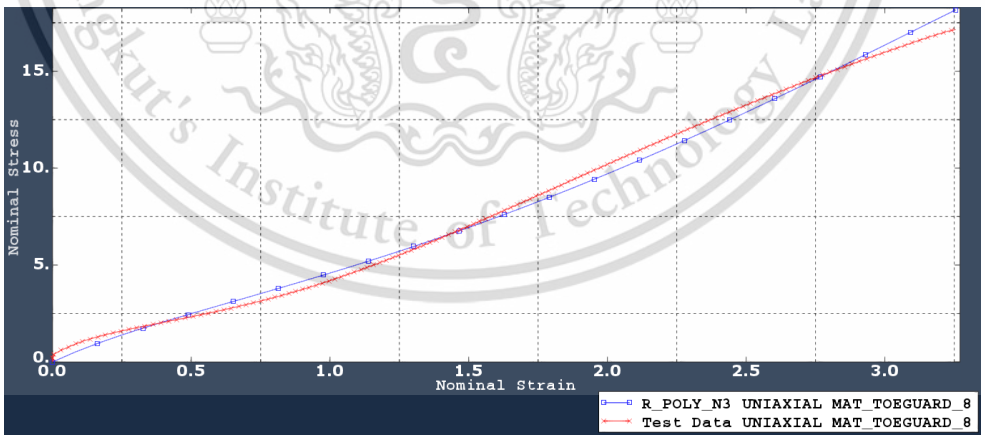

Figure 4.22 The Yeoh model curve fitting graph with testing data of Toeguard.

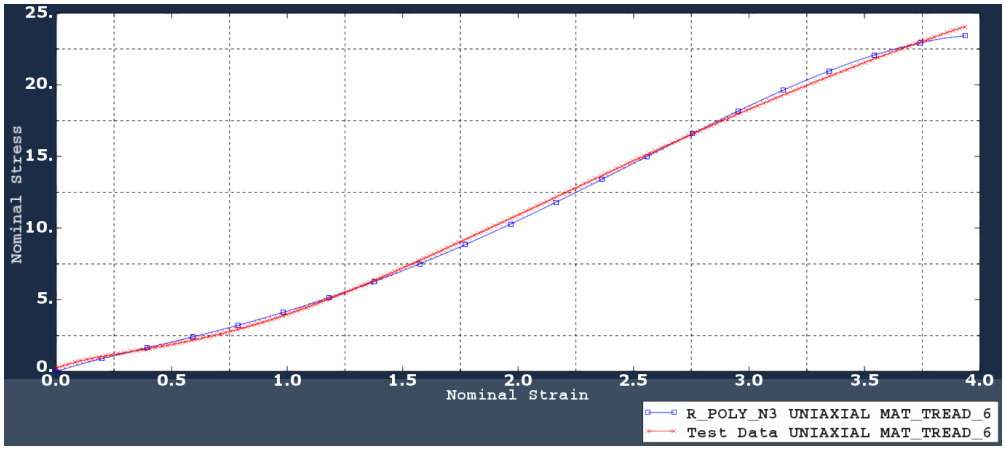

Figure 4.23 The Yeoh model curve fitting graph with testing data of Tread.

From curve fitting, the Hyperelastic material properties constants of Yeoh model will be obtained. The Yeoh strain energy potentials constants of Hyperelastic material constants presents as Table 4.3

Table 4.3 Hyperelastic material constants

Rubber Material	**Yeoh strain energy potentials constants**		
Component	**C_{10} (N/mm^2)**	**C_{20} (N/mm^2)**	**C_{30} (N/mm^2)**
Apex	0.961841	-1.32133	1.56397
Inner liner	0.901528	-0.255138	0.0764628
Sidewall	0.724445	-0.233794	0.060803
Toeguard	2.98704	-19.8756	81.0418
Tread	1.15041	-0.283684	0.102128

4.2.2 Mullins Effect Material Property Testing

Mullins effect material property testing with ASTM D412-80 dumbbell by uniaxial tension like Hyperelastic testing, but in Mullins effect testing is the Hysteresis loop test. The methods of this testing as: 1. Define the stretch of testing (the author defines with 5 range are 20, 40, 60, 80 and 100 mm) 2. Uniaxial tension for each specimens of rubbers with each stretches in 5 loop testing (loaded-unloaded) with same

range of stretch 3. Plotting and obtained the raw data as Figure 4.24 – 4.28 (the data will presented in stretch at range 100 mm, at rest will presents in Appendix C)

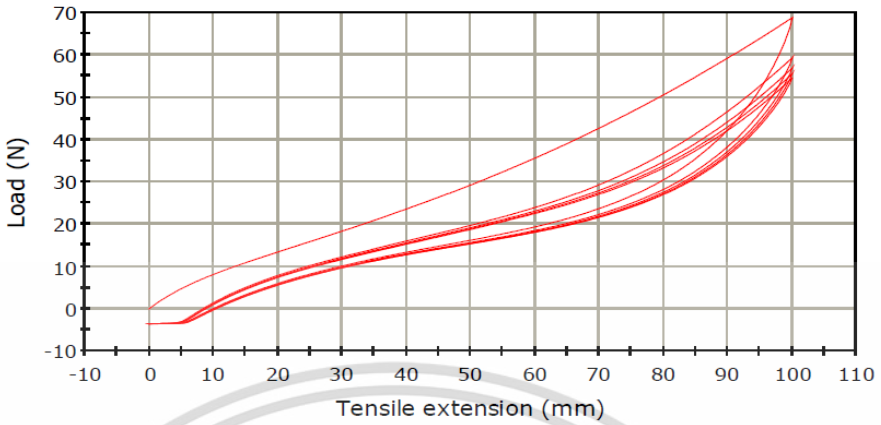

Figure 4.24 Hysteresis loop testing of Apex 100 mm

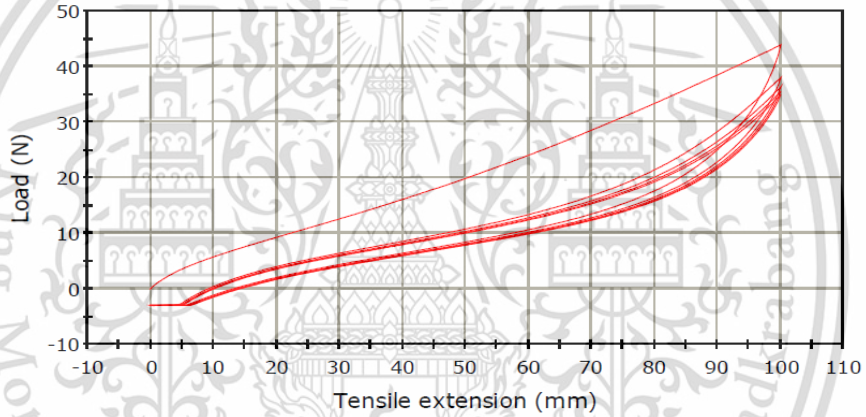

Figure 4.25 Hysteresis loop testing of Inner liner 100 mm

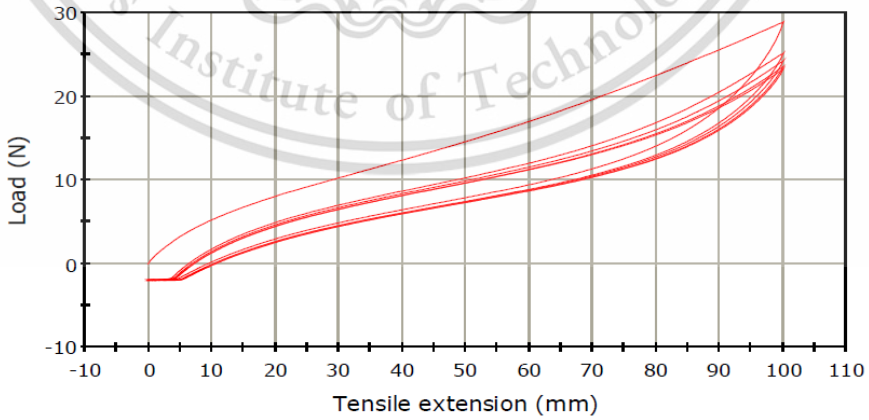

Figure 4.26 Hysteresis loop testing of Sidewall 100 mm

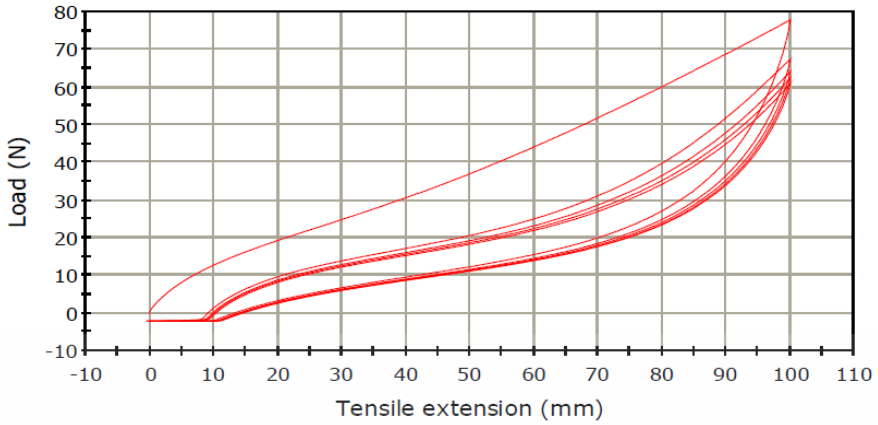

Figure 4.27 Hysteresis loop testing of Toeguard 100 mm

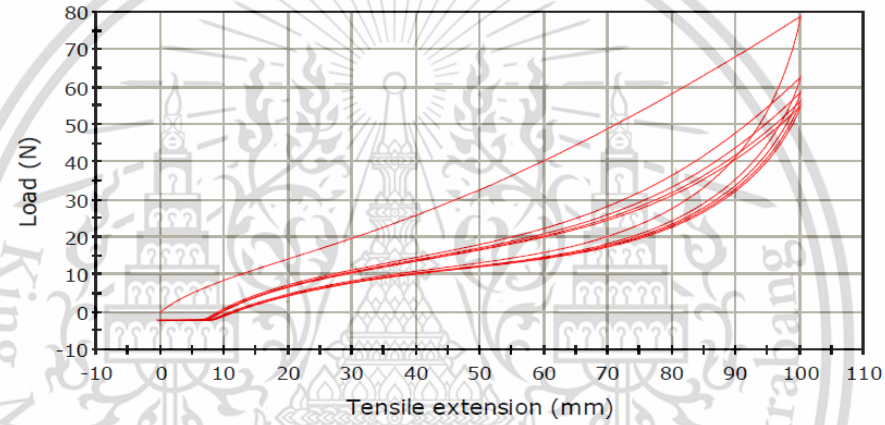

Figure 4.28 Hysteresis loop testing of Tread 100 mm

4.2.3 Reinforcements of Truck Tire

Not only the rubber in the truck tire, the truck tire had reinforcements made from elastic material such as steel, rayon, fabric too. The reinforcements of truck tire such as belt and carcass or pile, the most are made from the steel material. The steel material properties have the standard properties, the author uses the properties refer from Yang's research [13]. The difference of each reinforcements in the tire are the size of cords, position of cords and No. of cords. The material properties of reinforcement defines as Elastic material property and the Table 4.4 will shows the material properties, position and size of reinforcement.

Table 4.4 Reinforcement detail

Component	Young's Modulus (MPa)	Poisson ratio	Area per Bar (mm^2)	Spacing (mm)	Orientation angle (°)	Position (mm)
Steel belt 1	200000	0.3	1.131	2.7	110	0
Steel belt 2					110	0
Steel belt 3					70	0
Steel belt 4					20	0
Steel belt [bead cushion] (Left)					70	0
Steel belt [bead cushion] (right)					110	0
Steel ply					0	0
Bead wire			Depend on CAD	Depend on CAD	Depend on CAD	Depend on CAD
Bead protector (left)	4180		0.1385	0.75	30	0
Bead protector (right)					150	0

4.3 XZY3 11R22.5 Truck Tire CAD Model Generating

After collected the material properties and other data, the truck tire in model XZY3 11R22.5 will proceed to generating. The CAD model will generates following the truck tire cross section. The cross section of tire cuts by water jet cutting method as Figure 4.29.

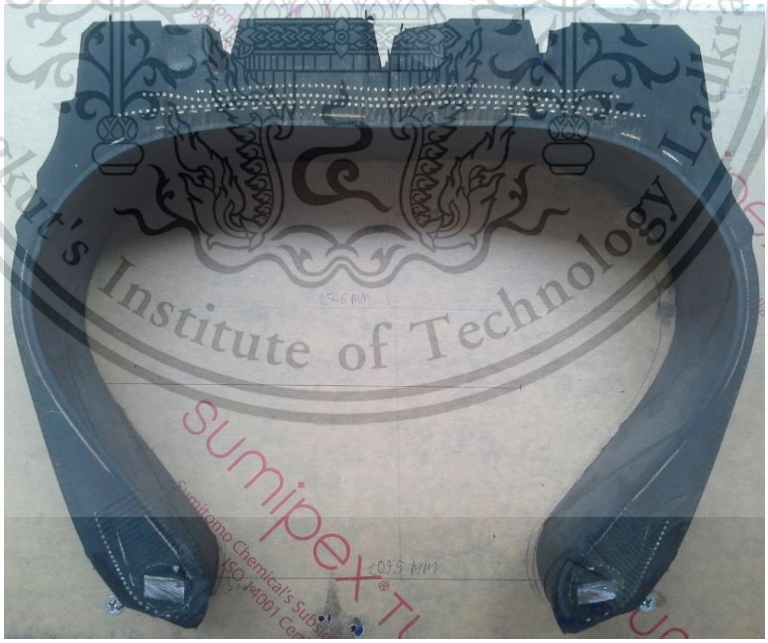

Figure 4.29 XZY3 cross section.

Then pins the cross section of tire to the position of install with the truck tire rim and photographs the cross section to draw the CAD with CATIA V5 software as Figure 4.30. The periodic model of truck tire will shows as Figure 4.31 and the full 3D model will shows as Figure 4.32.

Figure 4.30 XZY3 CAD drawing with CATIA V5.

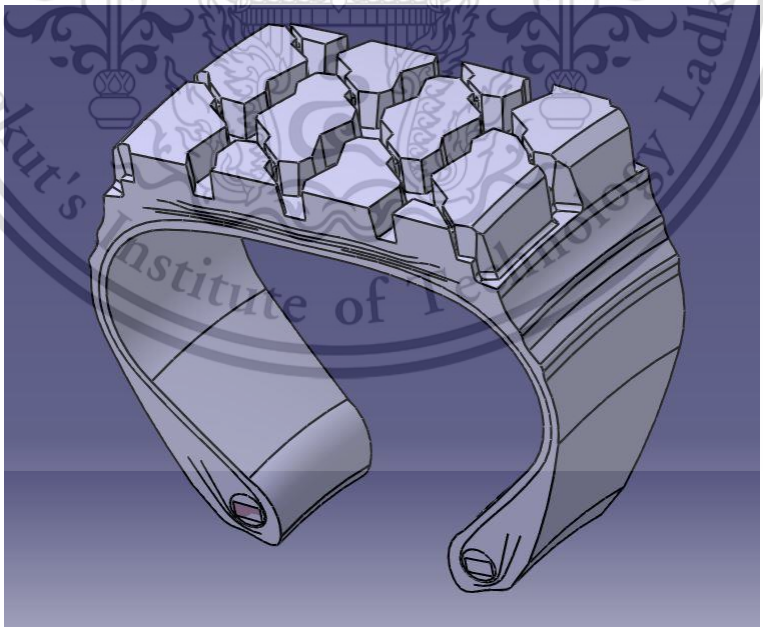

Figure 4.31 XZY3 CAD model (Periodic).

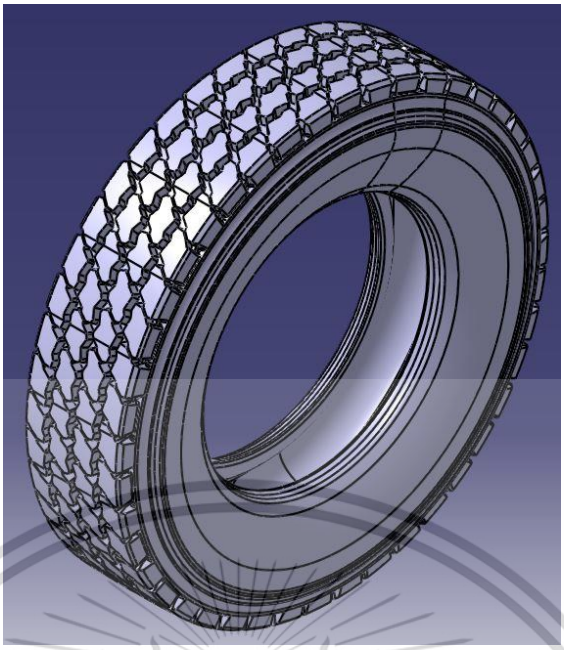

Figure 4.32 XZY3 CAD model (Full 3D).

4.4 The Truck Tire Simulation (FEM)

The simulation with FEM defines the material properties and rebar layers of reinforcements. The definition of material properties following with topic 4.2.1 and 4.2.3. The rebar layer function in ABAQUS software provides the support for modelling cord as rebar element which is embedded in rubber solid element as shown in Figure 4.33.

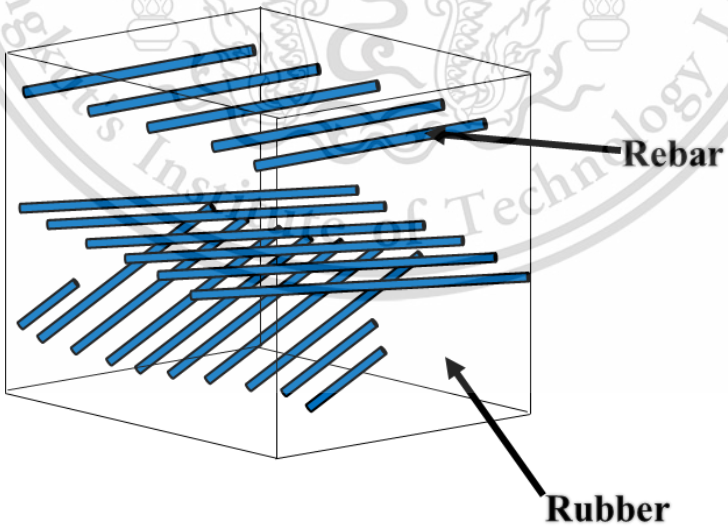

Figure 4.33 Cord rubber composite model by rebar element.

The rebar layers can defines with orientation angle, spacing, thickness, location and material properties which are independent of rubber material properties definition. Values of rebar layers to input in the function are following with Table 4.4.

The sections of tire to define the material properties, orientation angle, spacing, thickness and location of rubber and reinforcement will present as Figure 4.33

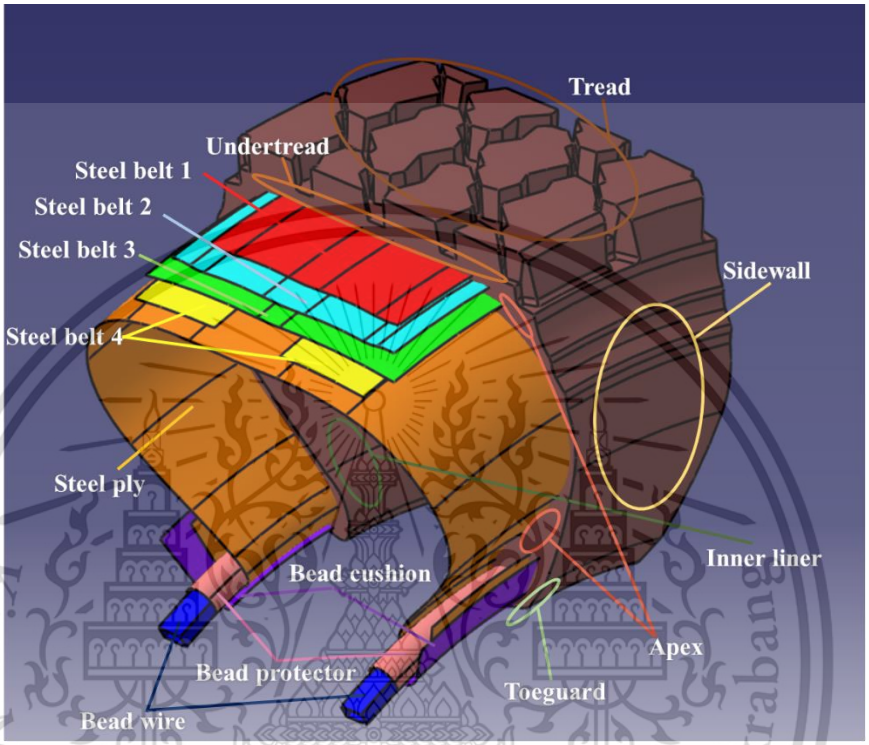

Figure 4.34 Truck tire Finite Element Model sections of definition.

The FEM must be meshing the CAD model into elements model. The solid and surface parts are different element type. The solid parts are Tread, Undertread, Sidewall, Inner liner, Apex, Toeguard and Bead wire. The surface parts are Steel belts, Steel ply, Bead cushion and Bead protector.

The solid parts will be meshing into C3D4H type, this element type is the Continuum (solid) element, Stress/Displacement element, 4-node Linear Tetrahedron and Hybrid with Linear Pressure element. The surface parts will be meshing into SFM3D4R type, this type is the General Surface element, Three-Dimensional and 4-node Surface element with Reduced Integration element. The meshing model will presents as Figure 4.35.

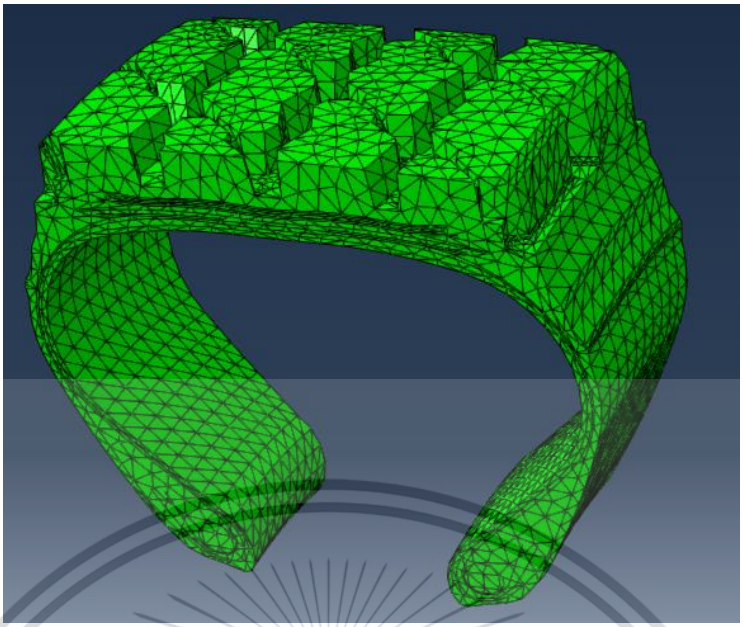

Figure 4.35 Truck tire model meshing into Finite Element Model.

4.4.1 Truck Tire Static Simulation

After defining material properties, orientation angle, spacing, thickness, location, contact interaction and meshing element. Next step is to begin the first simulation, there is the inflation pressure step. This step inputs the pressure into Inner liner surface of the truck tire model as Figure 4.36. The inflation pressure is 115 psi (0.79 MPa) following with the UN-ECE R117 standard of truck tire.

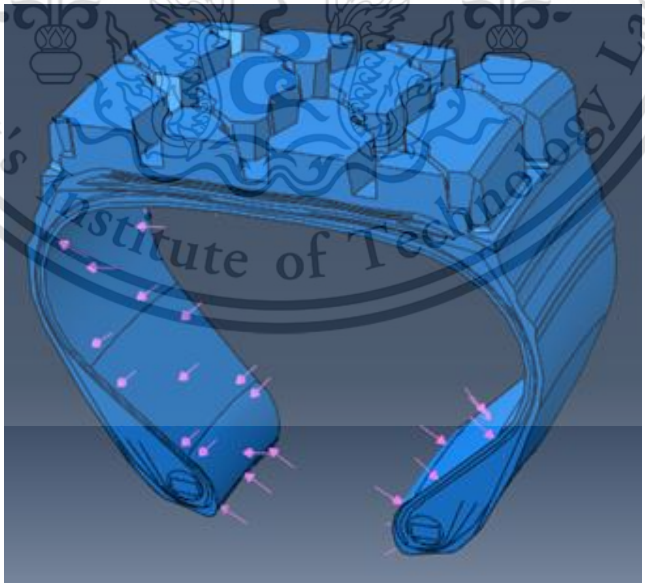

Figure 4.36 Inflation Pressure simulation step of truck tire.

Second step generates the periodic sector of truck tire model to full 3D model with inflation pressure and generates the rigid drum contact with the tire model as Figure 4.37

Figure 4.37 Generating of full 3D tire model and a rigid drum (truck tire).

Third step inputs the concentrate load into the reference node of rim as Figure 4.38. The load value uses in this simulation job is the 2,677.5 kg (26,270 N) following with the UN-ECE R117 standard.

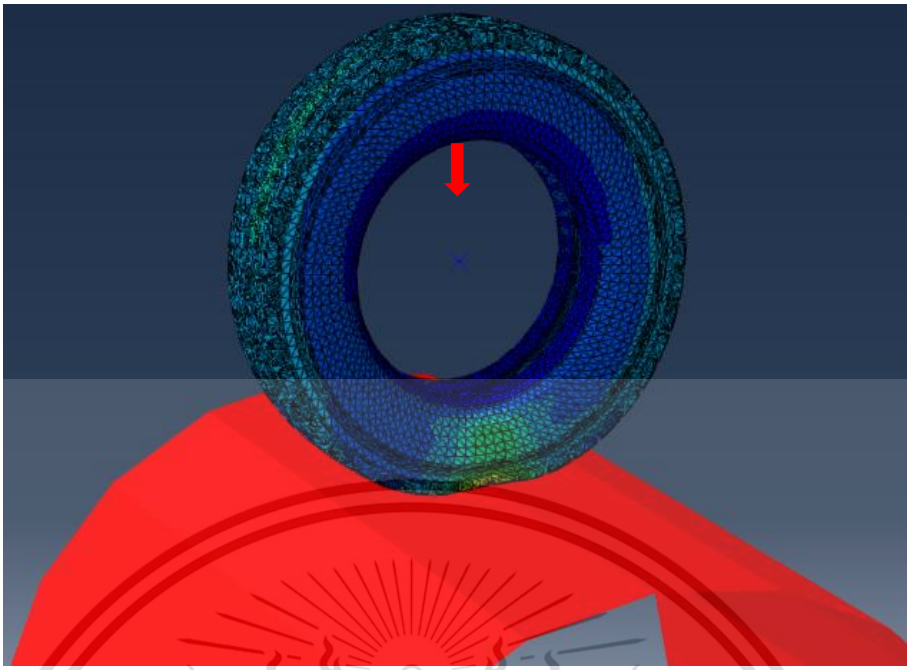

Figure 4.38 Truck tire loading simulation step.

The results of Static simulation will present in Chapter 5. After Static simulation case, next is the dynamic simulation with Steady State Transport (SST) function of ABAQUS/Standard.

4.4.2 Truck Tire Steady State Rolling Simulation

The SST function of ABAQUS/Standard uses to Steady State Rolling (SSR) simulation. From SSR simulation as Figure 4.39, the material is allowed to move through the tire mesh simulated rolling, while the mesh is kept in constant contact with the road surface without rolling about the axis. The Finite Element mesh describes the tire in the frame of reference remains stationary. But in the transient dynamic rolling is based on the Lagrangian approach, namely both the material and mesh translate and rotate as the tire rolling shown as Figure 4.40

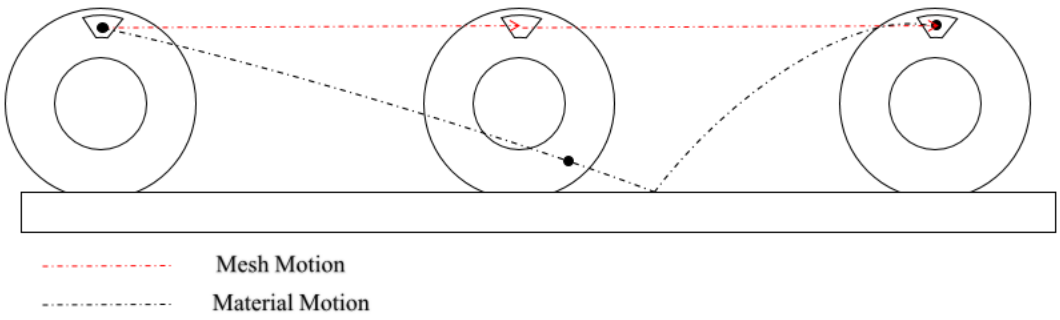

Figure 4.39 Lagrangian/Eulerian Approach for Tire Steady State Rolling Simulation

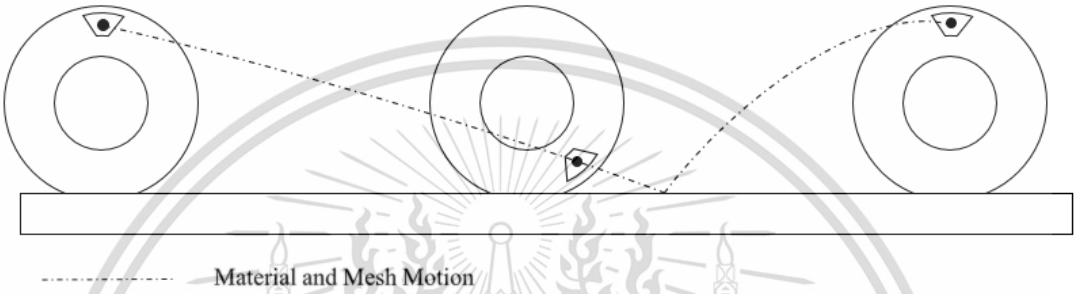

Figure 4.40 Lagrangian Approach for Tire Transient Rolling Simulation

This SST function will suitable with UN-ECE R117 simulation case because UN-ECE R117 standard testing will records the tire spindle force data from steady state and SST function is the function of steady state function too.

From subtitle 4.4.1 Static simulation, then uses the Result Transfer function of ABAQUS to transfers the loading result from Static simulation to SSR simulation. The velocity used in SSR simulation is 80 km/hr (22.22 m/s or 0.02 mm/s). The SSR step drives the rigid drum tester and the material reference frame of the truck tire model with the same angular velocity in SST function as Figure 4.41.

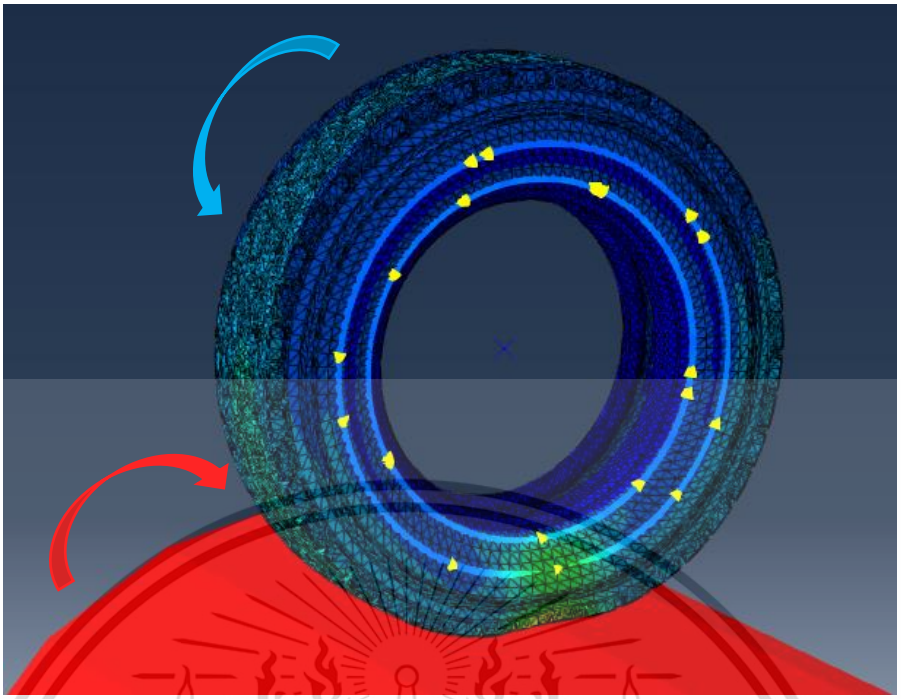

Figure 4.41 Rolling tire with Steady State Transport function of truck tire.

After complete simulation, monitors the longitudinal reaction force at the reference point of truck tire rim and calculates into the RR. Next process is to validate the simulation results with testing results.

When the UN-ECE R117 standard validation will acceptable, simulating the truck tire again following with subtitle 4.4.1 and 4.4.2 with different loads (2,465 kg, 2,900 kg and 3150 kg), inflation pressures (110 psi, 120 psi and 125 psi) and speeds (60 km/hr, 100 km/hr, and 110 km/hr). The RR simulate results will shows in Chapter 5. Input values use in RR simulation will show as Table 4.5.

Table 4.5 Input values of Rolling Resistance simulation

Variable	Value	Unit
Longitudinal Velocity of drum	60, 80, 100, 110	km/hr
Longitudinal Velocity of tire	60, 80, 100, 110	km/hr
Vertical Load	2465, 2677.5, 2900, 3150	kg
Inflation Pressure	110, 115, 120, 125	psi
Friction Coefficient	0.303	
Slip Tolerance (Elastic Slip ratio)	0.02	

The velocity (speed), load and inflation pressure are following by drum testing from subtitle 4.1. The friction coefficient uses in this research simulation refer from Hamilton research [24], there is the coefficient of hard rubber and steel similar to tread rubber and steel drum tester. Slip tolerance or elastic slip is 0.02 as suggested in the ABAQUS user manual in order to account for the relative sliding of contact surfaces.

4.5 Wide-Base-Single Tire CAD Model Generating

Validation of RR simulate results with testing results have be acceptable, the next methodology is the WBS tire model generating. The WBS model used in simulation to investigate the RR occurrence compared with Dual tires.

The real X One XZY3 WBS tire model has the position, orientation angle and number of steel belt difference from XZY Narrow tire model as Figure 4.42 [25][26].

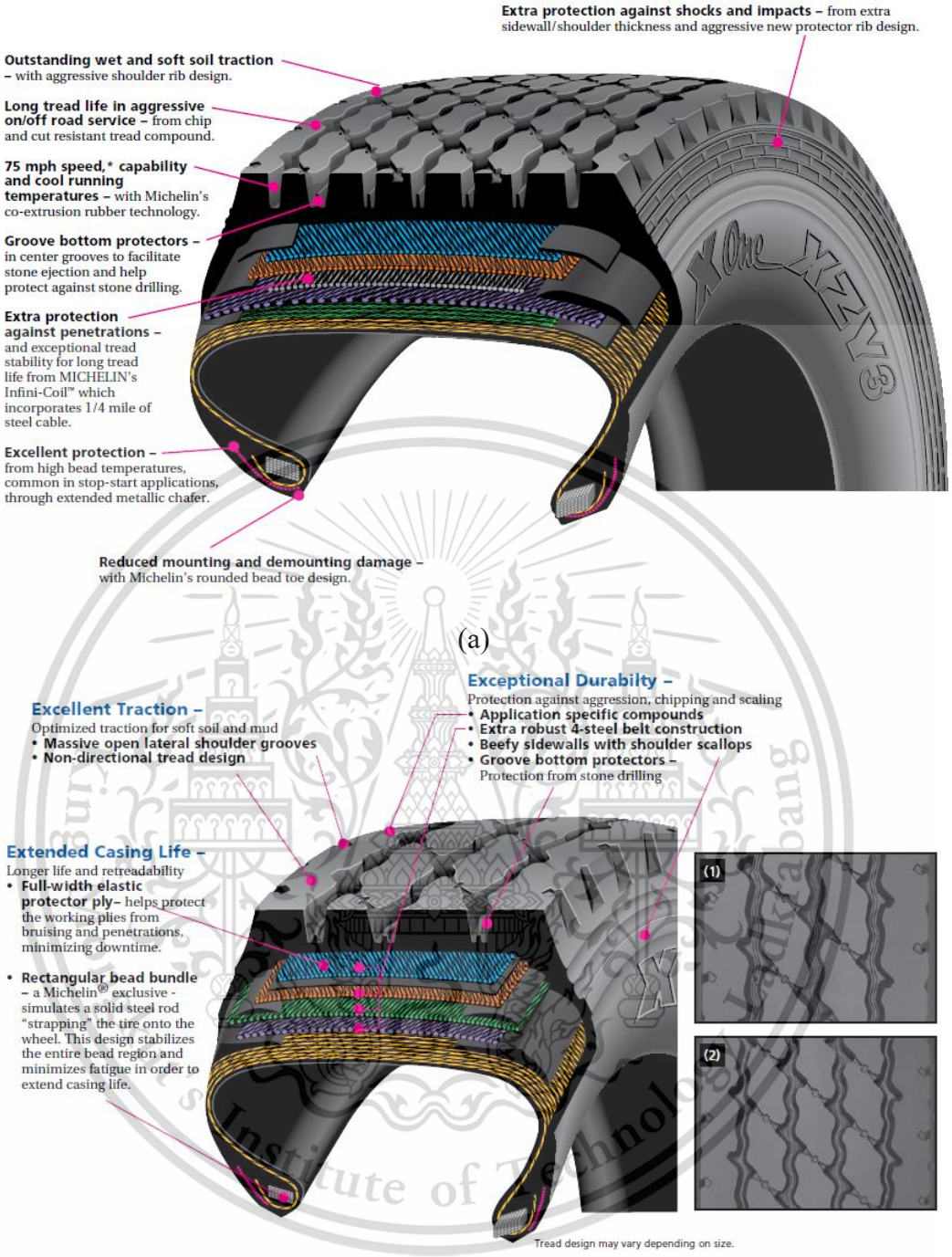

Figure 4.42 (a) X One XZY3 cross section (b) XZY 3 cross section

Source: -Michelin North America, I. (2016). MICHELIN® XZY® 3 TIRE. North America: Michelin North America, Inc.
-Michelin North America, I. (2013). MICHELIN® X ONE® XZY3®3 TIRE. North America: Michelin North America, Inc.

In this research need to investigating about dimension of width affect to RR. Because of this, the author will extends the width from XZY3 truck tire CAD model into WBS tire CAD model only, the number of steel belt, orientation angle and position are same with XZY3 11R22.5 tire model as Figure 4.43 (periodic) and full 3D model as Figure 4.44. The size of WBS tire following with X One XZY3 dimension, there is 455/55 R22.5 [26].

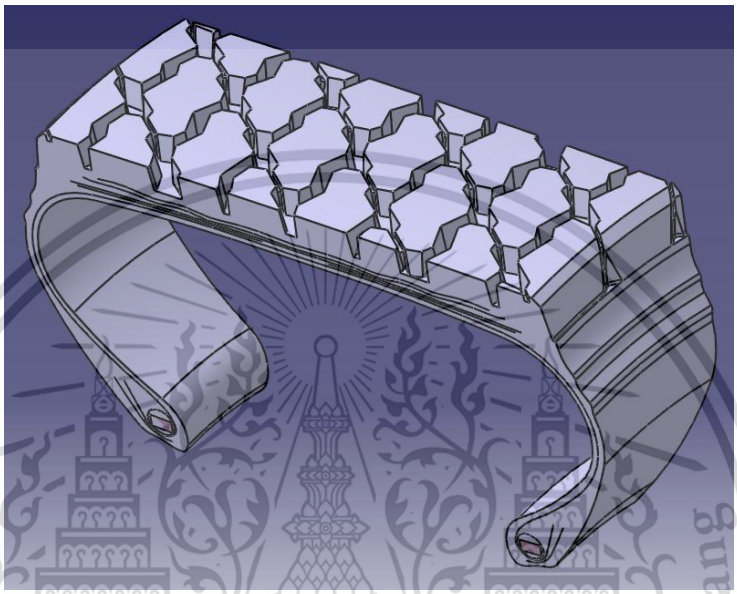

Figure 4.43 WBS XZY3 CAD model (Periodic).

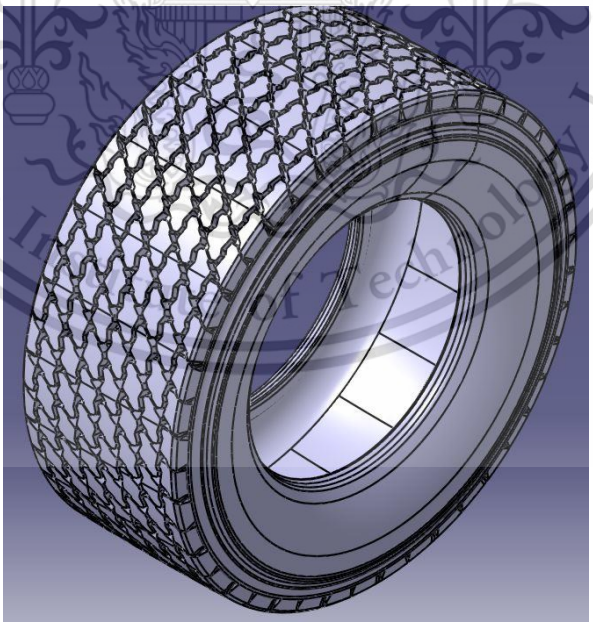

Figure 4.44 WBS XZY3 CAD model (Full 3D).

4.6 The WBS Tire Simulation (Finite Element Method)

The WBS tire simulation has the methodology same with subtitle 4.4 (The truck tire simulation (Finite Element Method)). The material properties, orientation angle, spacing, thickness, location and separated sections are same with Narrow truck tire as Figure 4.45.

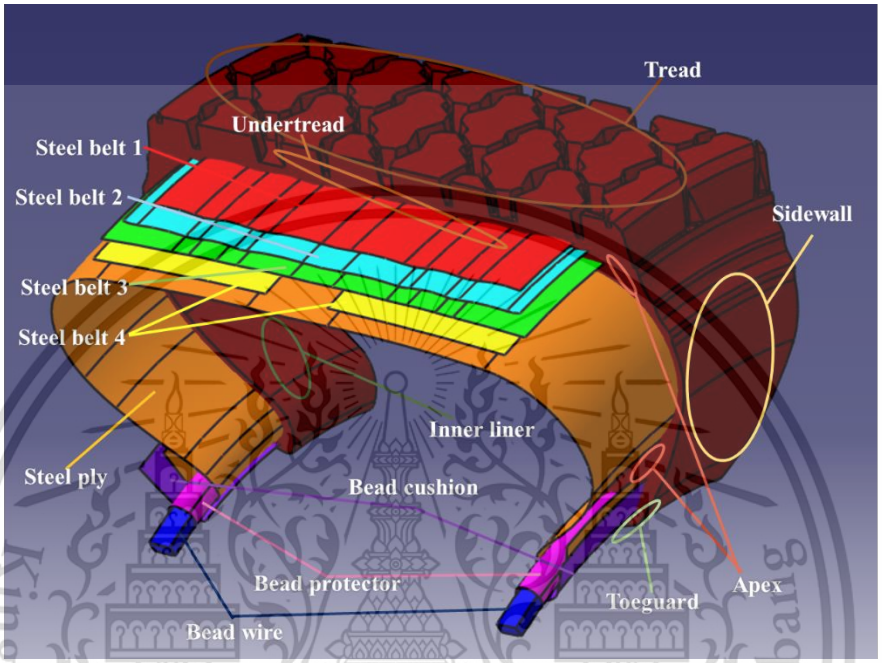

Figure 4.45 WBS tire Finite Element Model sections of definition.

The material properties of WBS tire model define in simulation as Table 4.3 and the rebar layer input detail as Table 4.4 same with Narrow truck tire.

The meshing element of WBS tire model will be same with Narrow tire too. The solid parts will be meshing into C3D4H type, and the surface parts will be meshing into SFM3D4R type as Figure 4.46.

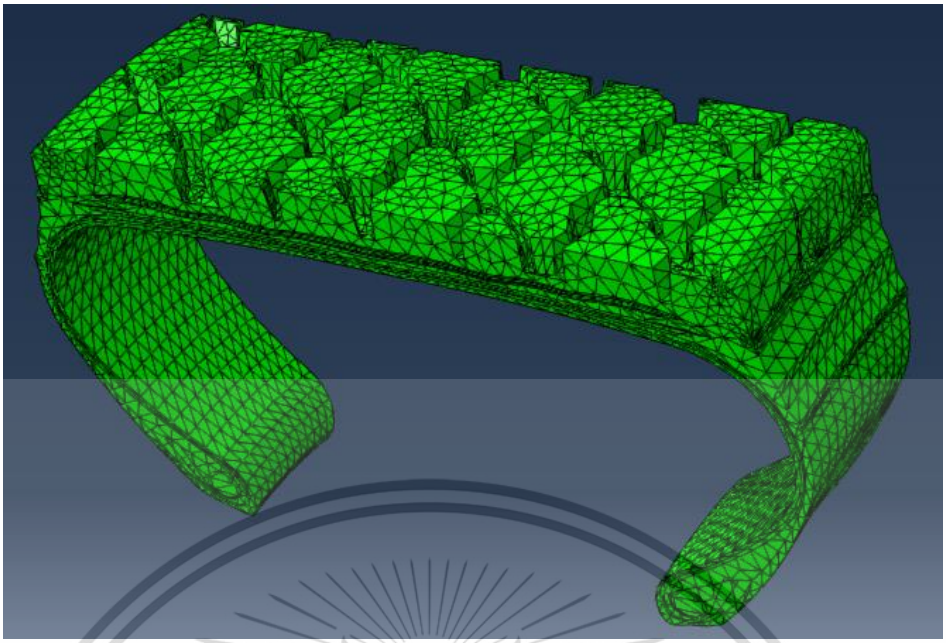

Figure 4.46 WBS tire model meshing into Finite Element Model.

4.6.1 Wide-Base-Single Tire Static Simulation

The Static simulation of WBS tire is same with Narrow tire too, but the different than Narrow tire is the inflation pressure. Because the structure of WBS tire is difference from Narrow tire. The author uses the data specification from specs sheet of X One XZY3 tire [26] but the specification in the specs sheet will be suitable with the North America. The suitable specification with Thailand specify on brand label, if compare with specs sheet of XZY3 11R22.5 tire [26] and specification on sidewall, the inflation pressure used in North America is 120 psi but specification on brand label from Thailand is 115 psi. Because of this reason, the author will minus the inflation pressure of X One XZY3 in specs sheet from 130 psi to 125 psi (0.86 MPa). Because the weather of Thailand is hotter than North America, the tire should be more inflation from the weather. From this reason the inflation pressure requirement in Thailand will be less than North America.

The inflation pressure used in WBS tire inflation pressure step is 125 psi (0.86 MPa) and assigns to Inner liner surface as Figure 4.47.

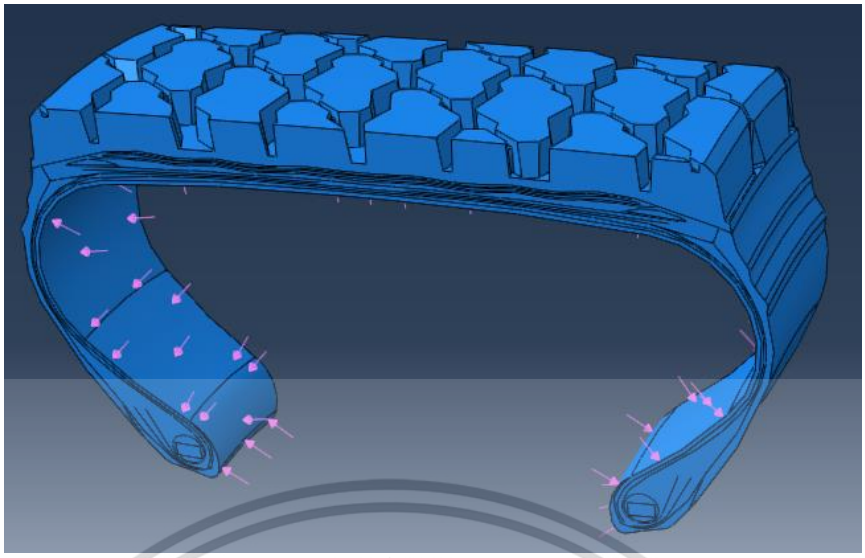

Figure 4.47 Inflation Pressure simulation step of WBS tire.

Second step will be same with Narrow tire, there are generates the periodic sector of WBS tire model to full 3D model with inflation pressure and generates the rigid drum contact with the tire model as Figure 4.48

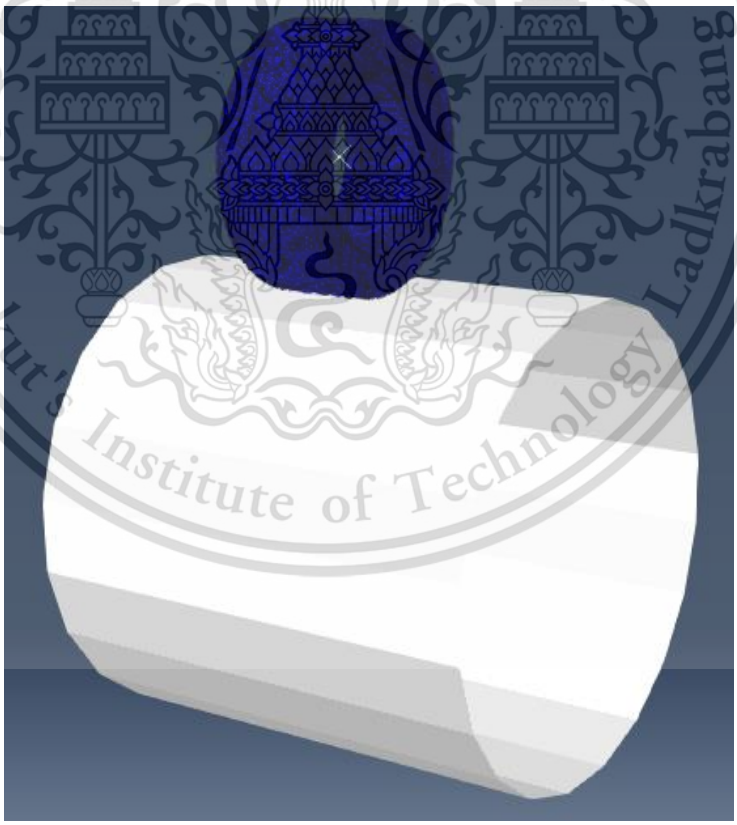

Figure 4.48 Generating of full 3D tire model and a rigid drum (WBS tire).

Third step will be same with Narrow tire there is input the load into the node of rim as Figure 4.49. The load values used in this simulation job are 5,800 kg (maximum load of WBS tire), 5300 kg (maximum load of Dual tires), 4,930 kg (85% of maximum Dual tires load followed the UN-ECE R117 standard) and 4,505 kg (85% of maximum WBS tire load followed the UN-ECE R117 standard) [25][26].

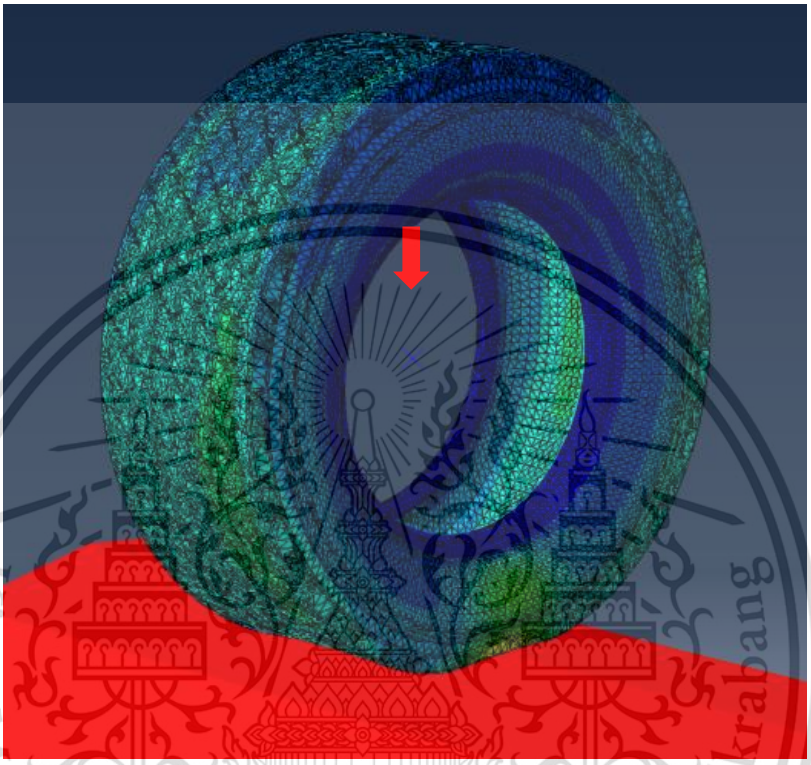

Figure 4.49 WBS tire loading simulation step.

The results of WBS tire Static simulation will present in Chapter 5 too. Next step is the SSR simulation same with Narrow tire.

4.6.2 Wide-Base-Single Tire Steady State Rolling Simulation

The SSR simulation of WBS tire uses the SST function to drive the rigid drum tester and the material reference frame of the truck tire model with the same angular velocity with Narrow tire too. The velocity defines in the model as 80 km/hr (22.22 m/s or 0.02 mm/s) following with UN-ECE R117 standard. The SSR simulation of WBS tire will be same with Narrow tire as Figure 4.50

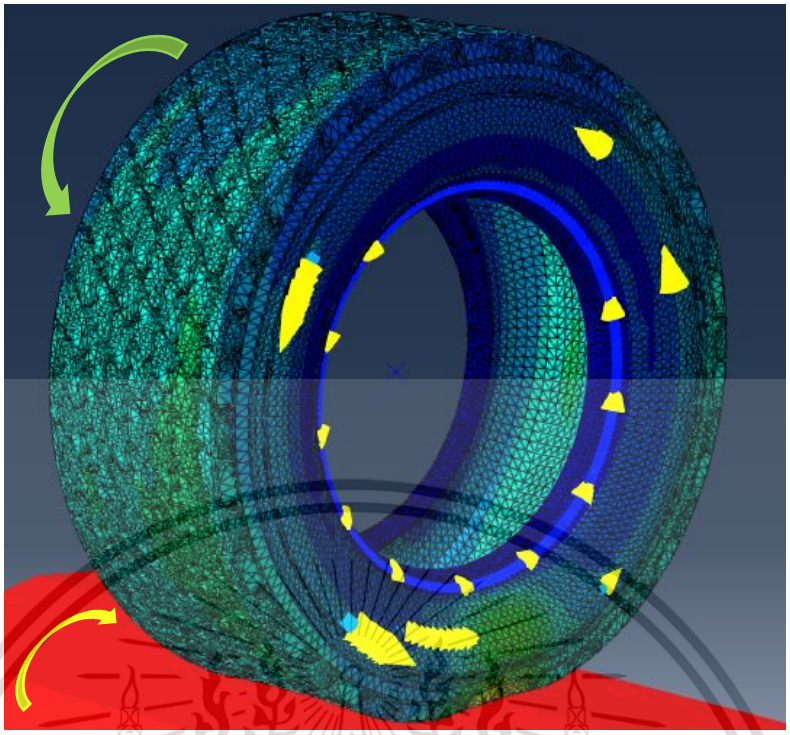

Figure 4.50 Rolling tire with Steady State Transport function of WBS tire.

After SSR simulation, recording the longitudinal reaction force at the reference point of the tire rim and calculating into RR. The RR results of WBS tire compared with Dual tires will present in Chapter 5.

CHAPTER 5

RESULTS AND DISCUSSIONS

5.1 Rolling Resistance UN-ECE R117 Standard Test Results of XZY3 11R22.5 Truck Tire

After warm up the truck tire for 180 minutes at surrounding temperature of 25±5 ^{o}C, the parasitic losses and recording data were measured. All-important data for parasitic losses calculation are present as Table 5.1 – 5.2.

Table 5.1 Data of parasitic losses: inflation pressure of 115 psi

Measurement	Speed (km/hr)			
	60	80	100	110
Rim size test (in)	22.5 X 8.25			
Speed (km/hr)	60.3	80.3	100.2	110.2
Load (N)	500			
Interval (minutes)	180	180	180	180
Ambient temperature (^{o}C)	28.1	28.0	28.0	28.3
Static radius (mm)	525.6	527.5	530.0	532.4
Dynamic radius (mm)	530.2	531.8	534.5	536.1
Test drum Radius (mm)	853.8			
Tire Spindle Force (N)	60	64	69	73

Table 5.2 Data of parasitic losses: speed of 80 km/hr

Measurement	Inflation pressure (psi)			
	110	115	120	125
Rim size test (in)	22.5 X 8.25			
Speed (km/hr)	80.3	80.3	80.4	80.4
Load (N)	500			
Interval (minutes)	180	180	180	180
Ambient temperature (°C)	28.0	28.0	28.2	28.0
Static radius (mm)	527.3	527.5	530.4	531.2
Dynamic radius (mm)	530.3	531.8	535.4	535.4
Test drum Radius (mm)	853.8			
Tire Spindle Force (N)	65	64	64	63

The all-important data for Rolling Resistance (RR) calculation from testing condition are present in Table 5.3 - 5.5.

Table 5.3 Data of RR test: 2,677.5 kg (26.27 kN) load and inflation pressure of 115 psi

Measurement	Speed (km/hr)			
	60	80	100	110
Rim size test (in)	22.5 X 8.25			
Speed (km/hr)	60.1	80.3	100.4	110.2
Load (kN)	26.28	26.28	26.28	26.28
Interval (minutes)	210	210	210	210
Ambient temperature (°C)	28.0	28.3	28.2	28.9
Static radius (mm)	501.7	501.8	504.1	506.1
Dynamic radius (mm)	518.5	518.5	520.6	523.2
Test drum Radius (mm)	853.8			
Tire Spindle Force (N)	157	165	174	190

Table 5.4 Data of RR test: 2,677.5 kg (26.27 kN) load and speed of 80 km/hr

Measurement	Inflation pressure (psi)			
	110	115	120	125
Rim size test (in)	22.5 X 8.25			
Speed (km/hr)	80.3	80.3	80.4	80.4
Load (kN)	26.28	26.28	26.28	26.28
Interval (minutes)	210	210	210	210
Ambient temperature (°C)	28.1	28.3	28.6	28.2
Static radius (mm)	500.7	501.8	504.9	505.6
Dynamic radius (mm)	517.7	518.5	521.0	521.9
Test drum Radius (mm)	853.8			
Tire Spindle Force (N)	166	165	163	162

Table 5.5 Data of RR test: speed of 80 km/hr and inflation pressure of 115 kPa

Measurement	Load kg (kN)			
	2,465 (24.18)	2,677.5(26.27)	2,900 (28.45)	3,150 (30.90)
Rim size test (in)	22.5 X 8.25			
Speed (km/hr)	80.4	80.3	80.4	80.3
Load (kN)	24.19	26.28	28.46	30.91
Interval(minutes)	210	210	210	210
Ambient temperature (°C)	28.3	28.3	28.5	28.6
Static radius (mm)	503.8	501.8	500.6	498.9
Dynamic radius (mm)	518.5	518.5	518.5	518.5
Test drum Radius (mm)	853.8			
Tire Spindle Force (N)	148	165	178	200

After measures all-important data as tire spindle force, the calculation of Rolling Resistance (RR) with equations (3.8) - (3.12) are adopted. The final RR testing results of XZY3 truck tire are presents in the Table 5.6-5.8

Table 5.6 RR results: 2,677.5 kg (26.27 kN) load and inflation pressure of 115 psi

Results	Speed (km/hr)			
	60	80	100	110
Parasitic Losses (F_{pl}) (N)	96.94	103.54	111.83	118.52
Tyre Spindle Force (F_t) (N)	157	165	174	190
Rolling Resistance for force method (F_r) (N)	152.32	158.43	164.29	184.10
Rolling Resistance at 25 °C (F_{r25}) (N)	155.06	161.57	167.44	188.41
Rolling Resistance for drum correction (F_{r02}) (N)	150.68	157.01	162.72	183.09
Rolling Resistance coefficient at 25 °C (C_r) (kg/ton)	5.73	5.97	6.19	6.97

Table 5.7 RR results: 2,677.5 kg (26.27 kN) load and speed of 80 km/hr

Results	Inflation pressure (psi)			
	110	115	120	125
Parasitic Losses (F_{pl}) (N)	105.14	103.54	103.76	102.20
Tyre Spindle Force (F_t) (N)	166	165	163	162
Rolling Resistance for force method (F_r) (N)	158.21	158.43	155.63	155.74
Rolling Resistance at 25 °C (F_{r25}) (N)	161.15	161.57	158.99	158.73
Rolling Resistance for drum correction (F_{r02}) (N)	156.60	157.01	154.51	154.25
Rolling Resistance coefficient at 25 °C (C_r) (kg/ton)	5.96	5.97	5.88	5.87

Table 5.8 RR results: speed of 80 km/hr and inflation pressure of 115 kPa

Results	Load kg (kN)			
	2,465 (24.18)	2,677.5 (26.27)	2,900 (28.45)	3,150 (30.90)
Parasitic Losses (F_{pl}) (N)	103.54	103.54	103.54	103.54
Tyre Spindle Force (F_t) (N)	148	165	178	200
Rolling Resistance for force method (F_r) (N)	131.79	158.43	178.82	213.32
Rolling Resistance at 25 °C (F_{r25}) (N)	134.40	161.57	182.58	217.93
Rolling Resistance for drum correction (F_{r02}) (N)	130.60	157.01	177.42	211.78
Rolling Resistance coefficient at 25 °C (C_r) (kg/ton)	5.40	5.97	6.23	6.85

Speed variation of truck tire testing relate with RR and RRC as Table 5.6. When the speed increasing, the RR and RRC are increasing too.

The inflation pressure various results of RR and RRC as Table 5.7. From the table, it will presents when the tire has high inflation pressures, the RR and RRC are decreasing, the tire stiffness is increasing and it leads to the tire has less deformation when loaded.

The loading results of RR and RRC as Table 5.8 will presented when the tire has high loads, the RR and RRC will increasing and the deformation will increasing too.

5.2 The Simulation Results of XZY3 11R22.5 Truck Tire

From the Chapter 4 subtitle 4.4, the simulation will proceeds from Static simulation to Steady State Rolling (SSR) simulation and will obtains the Static results and SSR results.

5.2.1 Static Results Validation of XZY3 Truck Tire

The first result which is obtained from truck tire simulation is the static simulation. The author will presents about the displacement or deformation of effective radius results to validate with the testing results.

The results of XZY3 11R22.5 truck tire must be acceptable. The validation is the methodology to represent the results can acceptable or unacceptable and the Static results validation of simulation and testing will presents as Figure 5.1-5.3

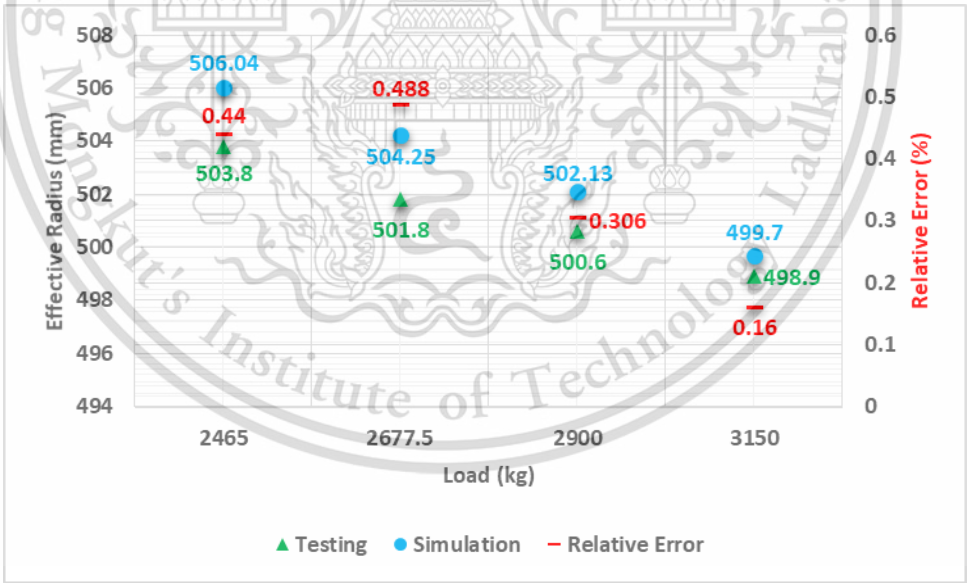

Figure 5.1 Static validation of truck tire (Effective Radius-Load result).

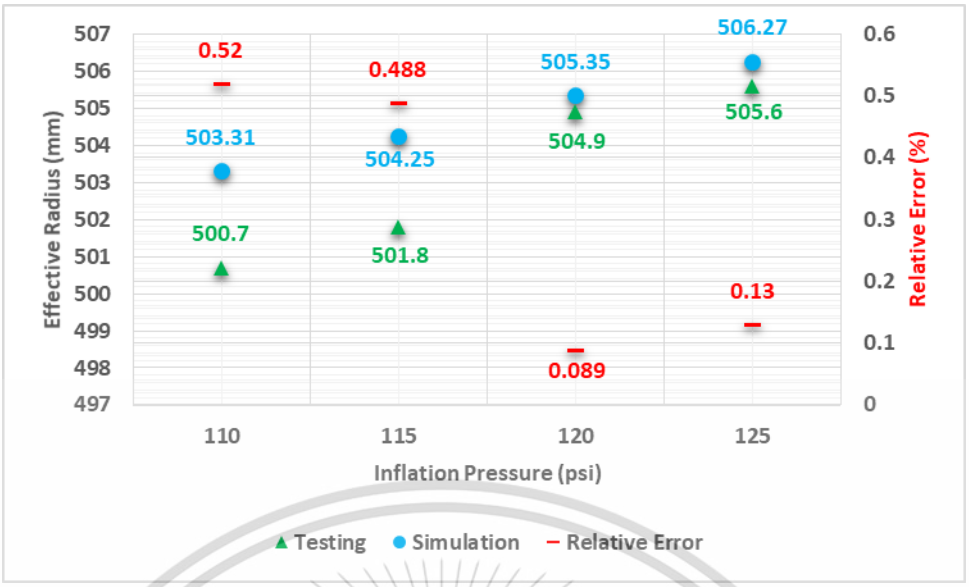

Figure 5.2 Static validation of truck tire (Effective Radius-Inflation Pressure result).

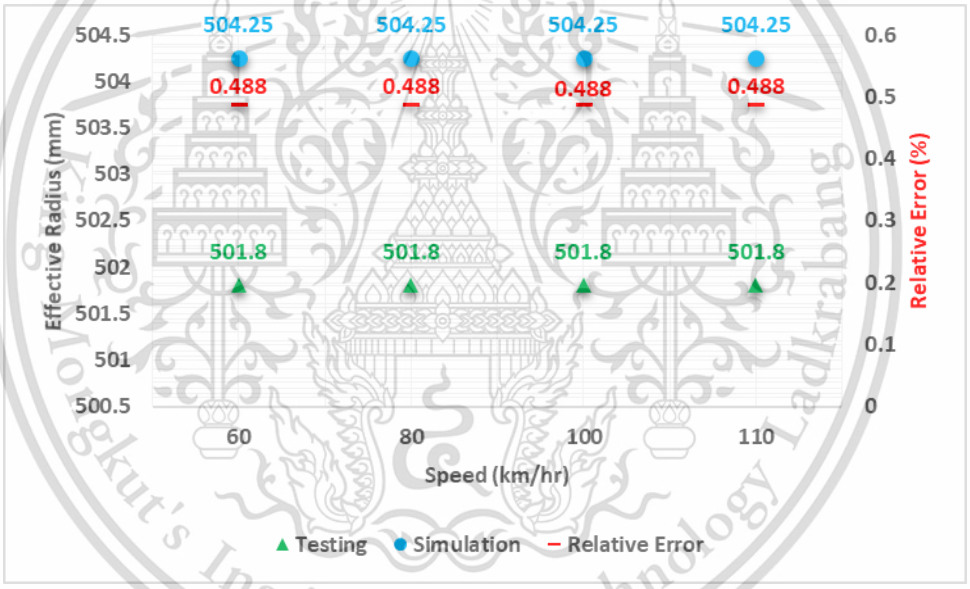

Figure 5.3 Static validation of truck tire (Effective Radius-Speed result).

From the loading various results, which is according to the theory of tire deformation. When the tire has more load, the effective radius of tire will decreasing because of deformation. If the inflation pressure increasing, the effective radius will increasing too from increasing of tire stiffness. But in the speed variation, the Static effective radius result had not been change because the load and inflation pressure aren't change and the speed isn't affect to static effective radius.

The validation of static results are acceptable, each relative errors are less error than 1%. The next validation is the RR and RRC validation and there are present in the next subtitle.

5.2.2 Rolling Resistance and Rolling Resistance Coefficient Results Validation of XZY3 Truck Tire

The second simulation result there is the RR and RRC from SSR simulation. After simulating the tire, next process is monitoring the longitudinal reaction force to RR calculation. The RR will be obtained as Figure 5.4-5.9.

This topic will validates the RR and RRC results of simulation and testing. If results are acceptable, the Wide-Base-Single (WBS) tire simulation will proceed. There are three validations to present, there are: load, inflation pressure and speed validation. Figure 5.4 - 5.9 will present the RR and RRC relate with three variations (load, inflation pressure and speed) and there are relative errors present on each graphs to indicate acceptable or not.

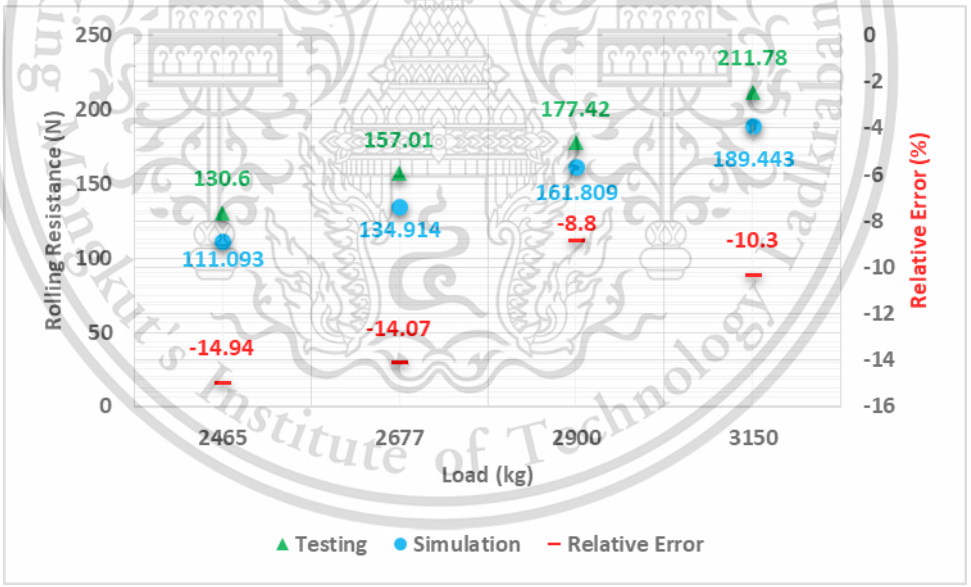

Figure 5.4 Truck tire Rolling Resistance-Load result of validation.

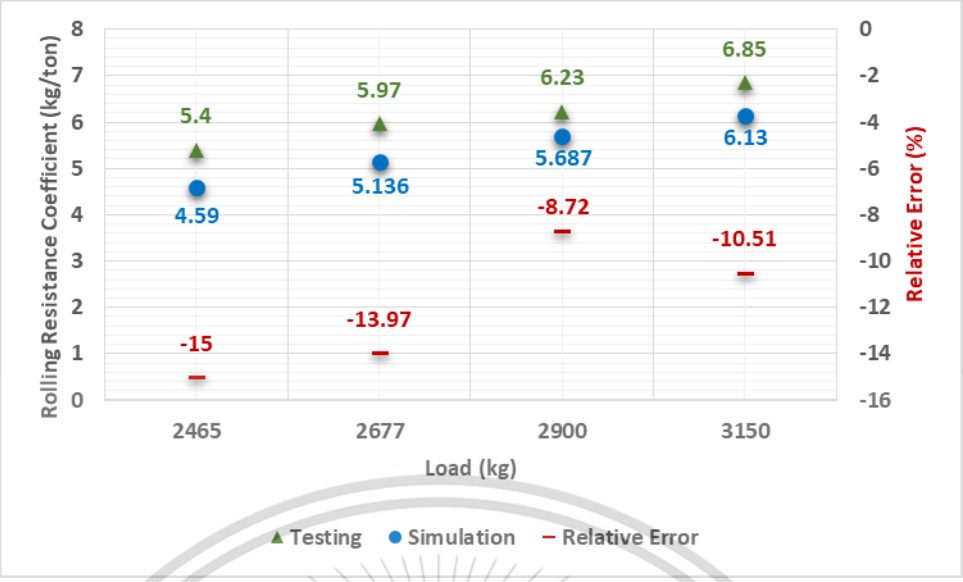

Figure 5.5 Truck tire Rolling Resistance Coefficient-Load result of validation.

In Figure 5.4 and 5.5 are present about the loading results validation of testing and simulation of heavy truck tire. From the effective radius results, there are less relative error and the RR and RRC have relative error approximately -12%. From the objective of this research, the error is acceptable and the trend of results are according to theory of deformation. When the load increasing, the RR and RRC will increasing.

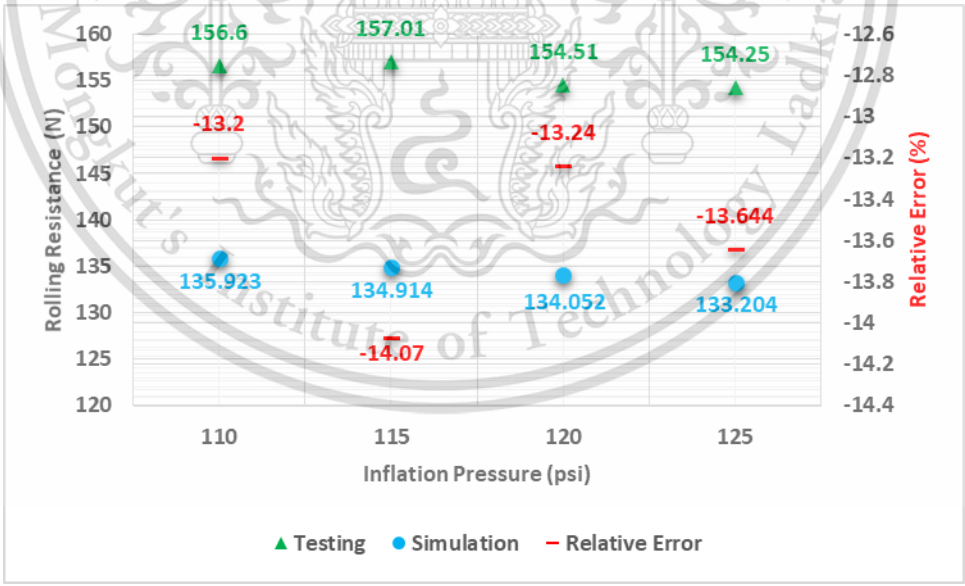

Figure 5.6 Truck tire Rolling Resistance-Inflation Pressure result of validation.

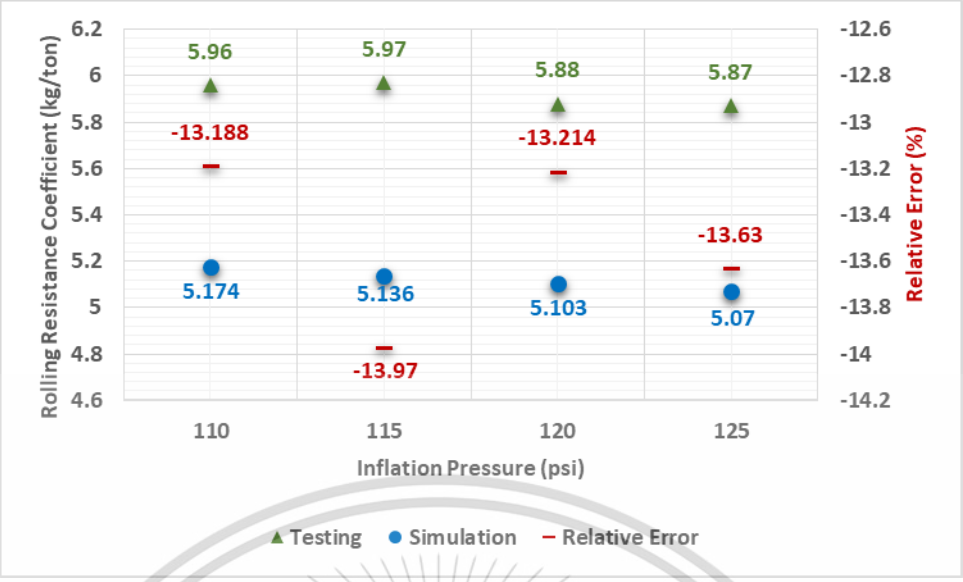

Figure 5.7 Truck tire Rolling Resistance Coefficient-Inflation Pressure result of validation.

Figure 5.6 and 5.7 are present inflation pressure results validation. In the effective radius, relative error have less error same with loading results validation. And relative error are approximately -13%. It is acceptable too. The trend of the results are according to the stiffness theory of tire too. Because when tire has been stiff, the RR and RRC will decreasing.

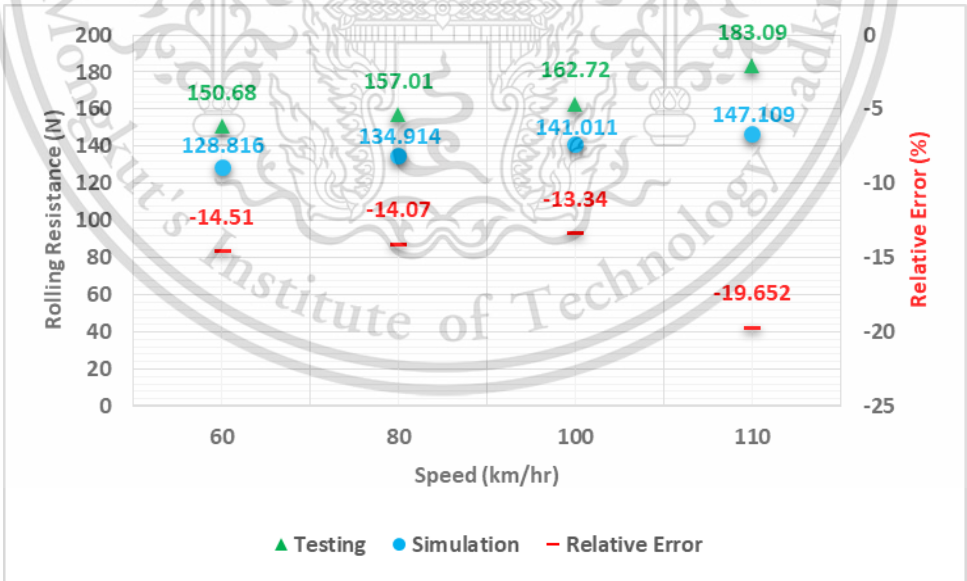

Figure 5.8 Truck tire Rolling Resistance-Speed result of validation.

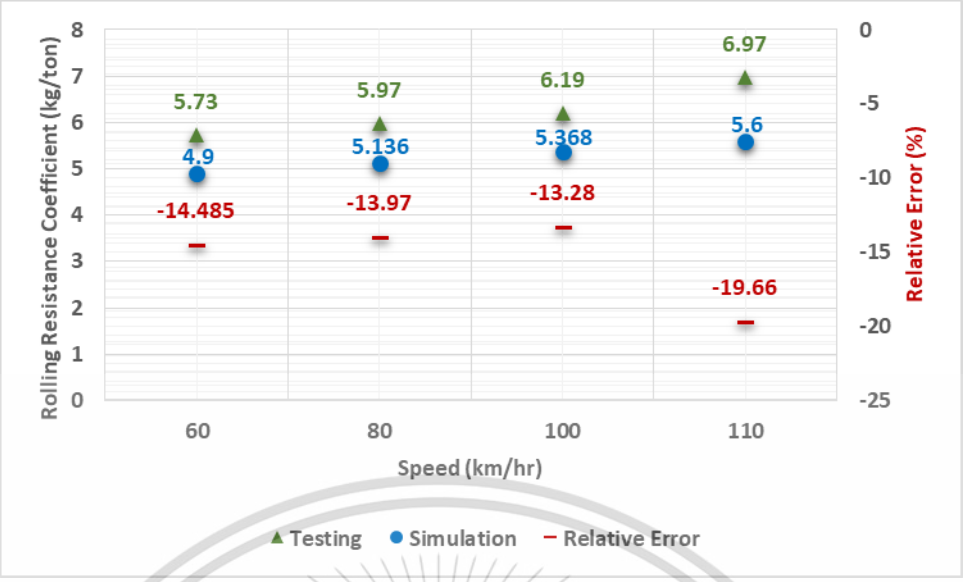

Figure 5.9 Truck tire Rolling Resistance Coefficient-Speed result of validation.

Figure 5.8 and 5.9 are speed results validation. The relative errors of RR are approximately -15%. In this validation is acceptable. And the trending results are following with energy dissipation by slippage and deformation theory. The energy dissipation by slippage and deformation of tire per revolution is increasing, the energy dissipation is leads to the increasing of RR too.

And in the speed at 110 km/hr, there is error over from another conditions because when test the tire in this condition, the tire is inflating at tread too much from overheat when tire rolling at over speed.

The specification of XZY3 11R22.5 specifies the maximum speed is 110 km/hr [26], but this is the North America specification. The North America weather will be cooler than Thailand. Because of this reason, the speed at 110 km/hr aren't suitable with Thailand weather, there is overheat occurrence when drive at speed 110 km/hr.

5.3 The Comparison of WBS Tire and Dual Tires Rolling Resistance

After collecting the important information, data, theory and results of WBS tire and Dual tires. The final of this research is the RR and RRC comparison between WBS tire and Dual tires. The comparison will indicates the fuel consumption of each tires by RR and RRC. If which tire has less RR and RRC, the less RR and RRC of tire will

express the less fuel consumption too. From the Chapter 4, after collecting the RR and RRC results of WBS and Dual tires from simulation by FEM, the comparisons of two type tires will represent as Figure 5.10 - 5.15.

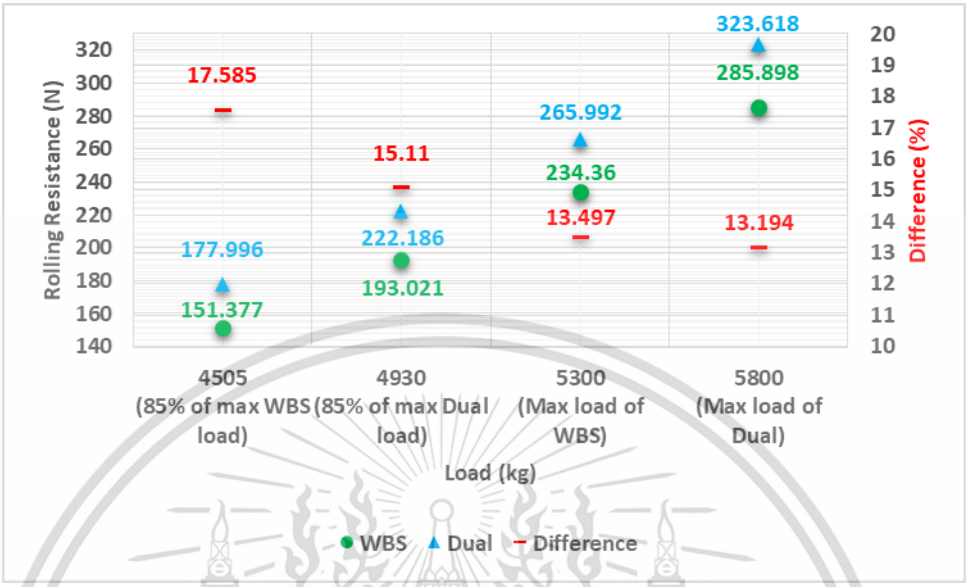

Figure 5.10 The comparison of WBS tire and Dual tires (Rolling Resistance-Load).

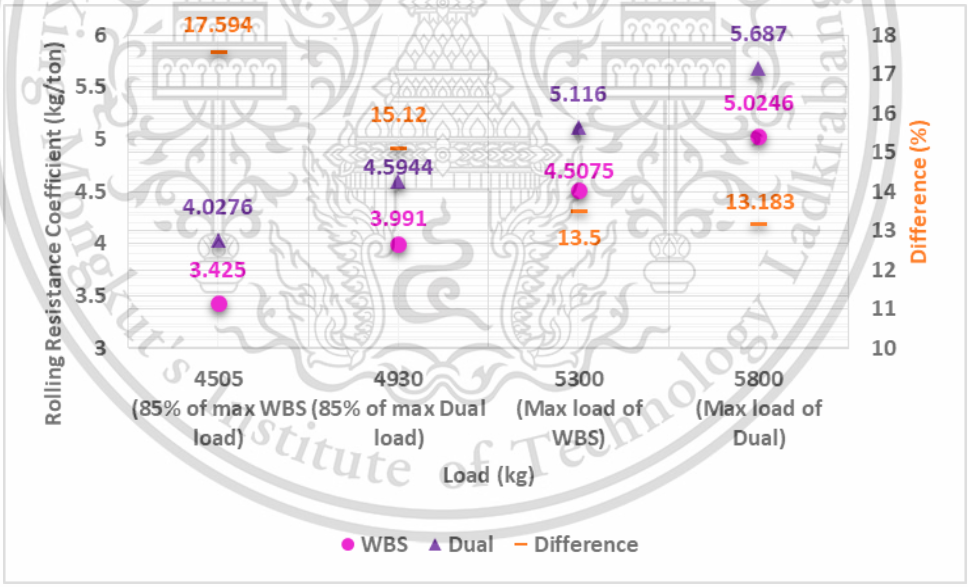

Figure 5.11 The comparison of WBS tire and Dual tires (Rolling Resistance Coefficient-Load).

The first comparison is the load variation. From the results the WBS tire has less RR and RRC than Dual tires approximately 13 - 18% in the same load.

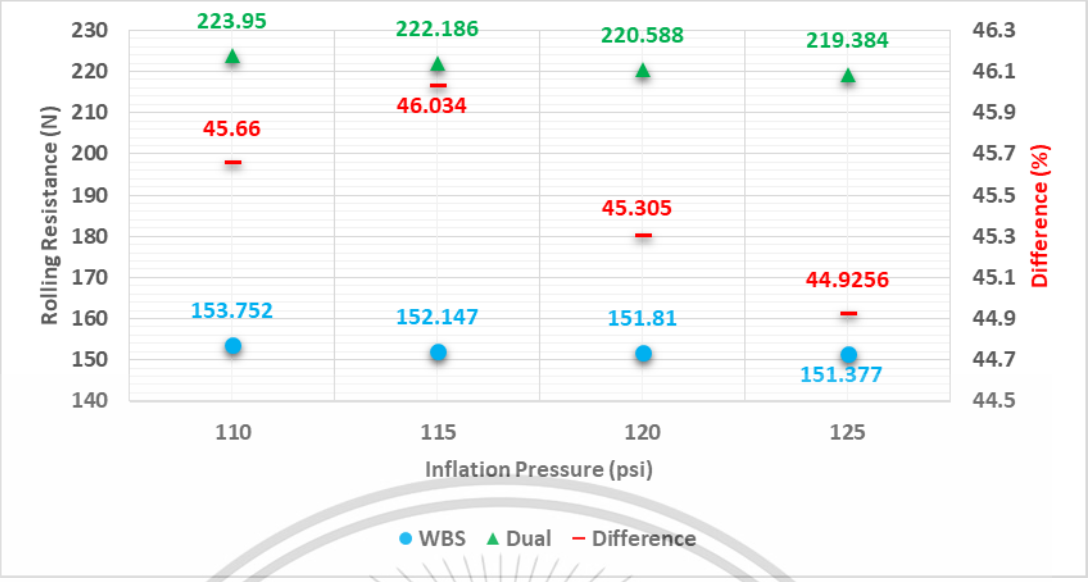

Figure 5.12 The comparison of WBS tire and Dual tires (Rolling Resistance-Inflation Pressure).

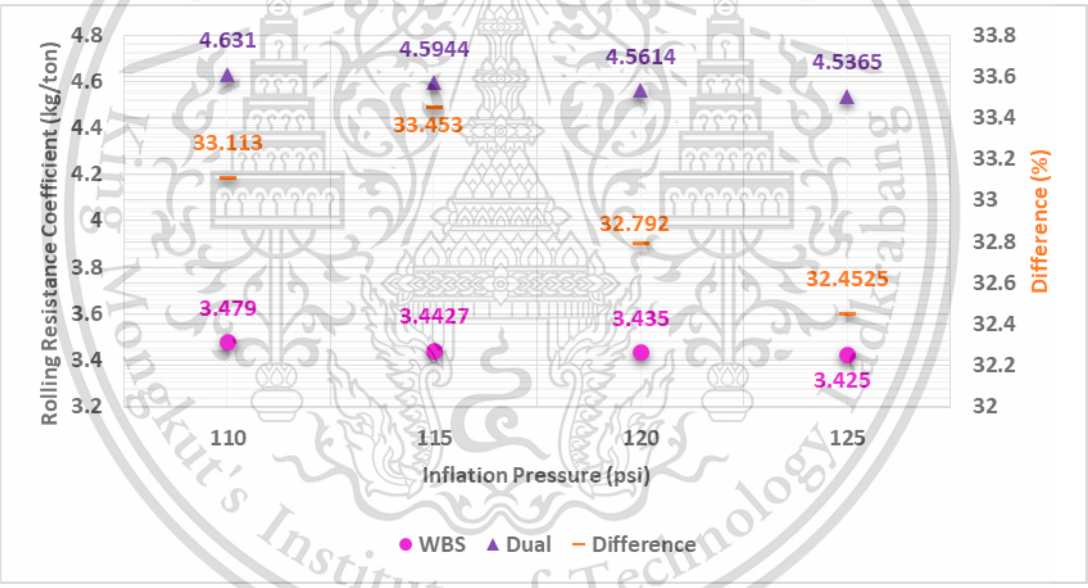

Figure 5.13 The comparison of WBS tire and Dual tires (Rolling Resistance Coefficient-Inflation Pressure).

From the results of inflation pressure variation, the WBS tire has less RR than Dual tire approximately 44 - 46% and 32 - 33.5% in RRC.

This comparison represents the WBS tire RR less than Dual tires too much, because of the load difference from UN-ECE R117 standard. The maximum load of

WBS tire and Dual tire are difference, WBS tire has less maximum received load than Dual tires.

The RR and RRC have difference on percent because the different maximum load of the WBS tire and Dual tires too.

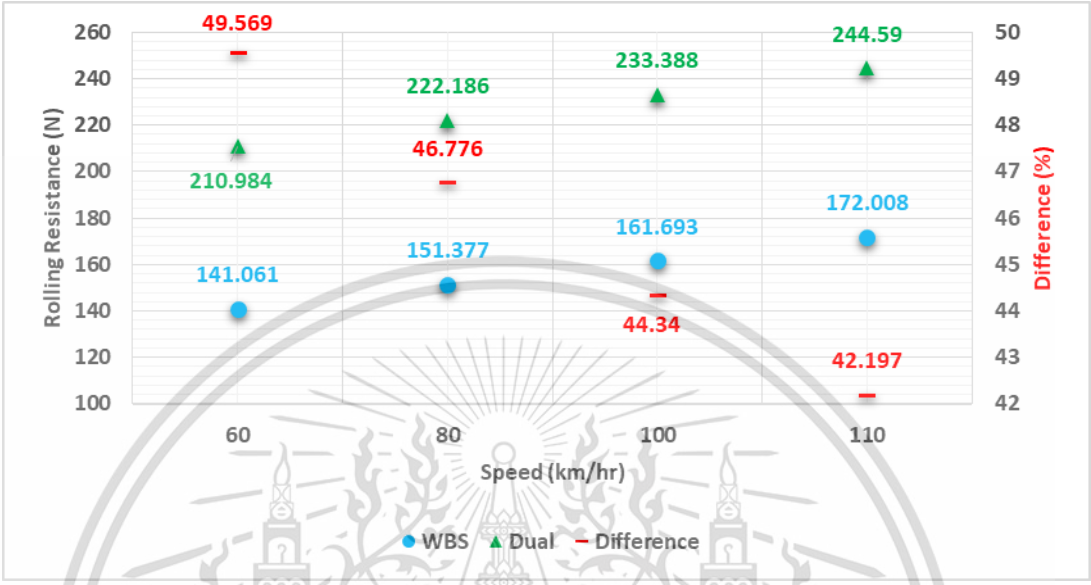

Figure 5.14 The comparison of WBS tire and Dual tires (Rolling Resistance-Speed).

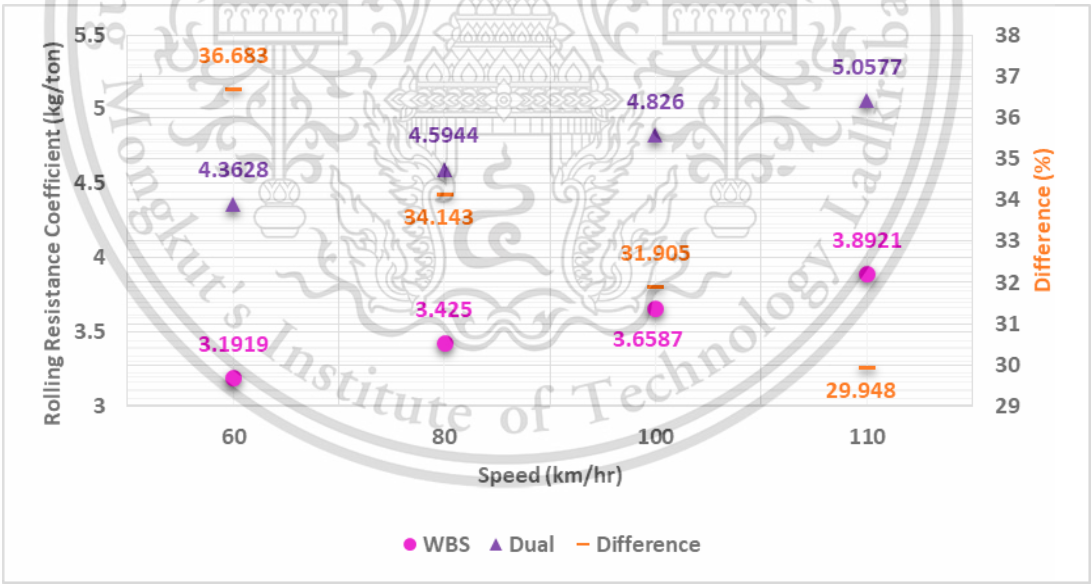

Figure 5.15 The comparison of WBS tire and Dual tires (Rolling Resistance Coefficient-Speed).

From the results of speed various comparison, the WBS tire has less RR than Dual tires approximately 42 - 50% and 30 - 37% in RRC, because of the difference of loading inputs same with inflation pressure variation.

If according to UN-ECE R117 standard in 85% of maximum loading on each tires, maximum inflation pressure on each tires and speed at 80 km/hr. The result will present as Figure 5.16.

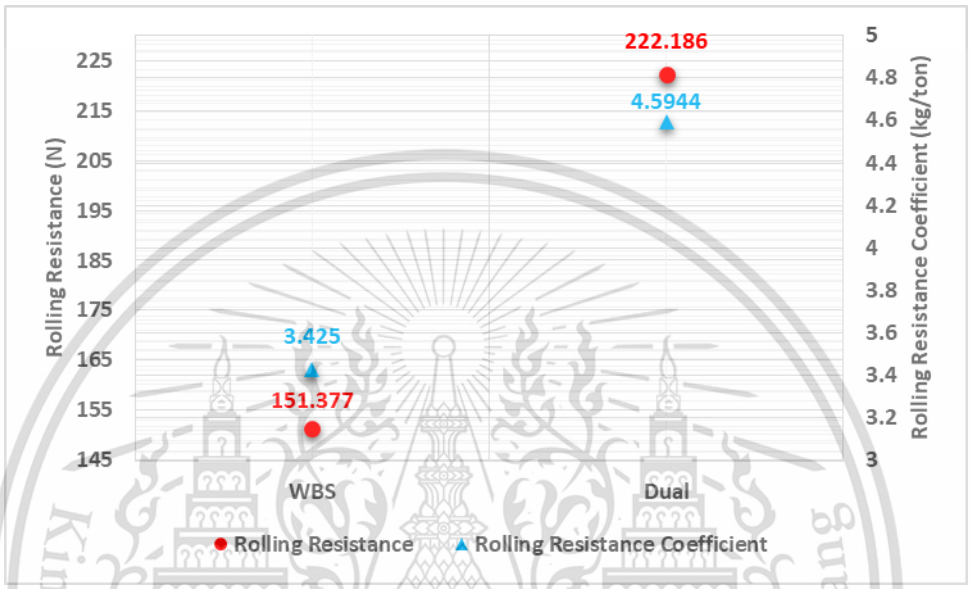

Figure 5.16 The comparison of WBS tire and Dual tires (Rolling Resistance and Rolling Resistance Coefficient-Standard).

From the result according to UN-ECE R117 standard, the RR of WBS tire less than Dual tires approximately 46.77% and 34.14% in RRC.

From these results, there could indicated to uses the WBS tire instead of Dual tires could reduce the RR and could save the fuel consumption too.

CHAPTER 6

CONCLUSIONS AND RECOMMENDATIONS

6.1 Result Conclusion

From the research, the deformation leads to energy dissipation and energy dissipation leads to cause of Rolling Resistance (RR) and Rolling Resistance Coefficient (RRC). The Wide-Base-Single (WBS) tire can decreases the RR, RRC and fuel consumption when WBS tire using instead of Dual tire using. Because the WBS tire can decreases the contact length and deformation when the tire loaded.

From the comparative results of WBS tire and Dual tires simulations by this research, the WBS tire could saving the fuel consumption and led to saving the fuel cost. The WBS tire could reduce the RR and RRC approximately 14.85% in the same load as Figure 5.10 and 5.11. But in other conditions of inflation pressure, speed variation and according to UN-ECE R117 standard, the RR and RRC had the percent of difference than load variation too much from the different maximum load of WBS tire and Dual tires when simulating the tire according to UN-ECE R117 standard, the RR and RRC of each results would difference in percent too, because of WBS tire and Dual tires had the different loading inputs and from this reason when RR of each results divided by vertical load of them, they had difference of RR and RRC in percent too. The WBS had RR lower than Dual tires in inflation pressure variation approximately 45.48% and 32.95% in RRC as Figure 5.12 and 5.13. The difference in speed various results of WBS tire had less than Dual tires approximately 45.72% in RR and 33.17% in RRC as Figure 5.14 and 5.15. According to UN-ECE R117 standard when replaced the WBS tire instated of Dual tires the RR difference would be approximately 46.77% and 34.14% in RRC as Figure 5.16. These are indicates the WBS tire using instead of Dual tires using can reduces the RR, RRC as well as fuel consumption and fuel cost.

6.2 Recommendation

Testing results of truck tires were presented the parameters relative with RR and RRC. Results represent the majority of RR was the deformation. When the tire has more

load, the deformation will rising and when has more inflation pressure, the tire will decreases the deformation, there is well known from other literatures but when the speed increasing, it causes to high energy dissipation by slippage and deformation in the tire. While the tire is rolling, the speed is increasing. The revolution of tire will depend on the speed of tire and because of this, the energy dissipation of tire per revolution is increasing. The energy dissipation will leads to the increasing of RR and RRC too.

The simulation results validate with testing results, the effective radius results are less error but RR results have more error approximately 10-20%. From the research objective, it is enough for acceptable. The error occurred from material properties. Because in the loading step from testing, there is less energy dissipation as heat but in the rolling step from testing, the tire has energy loss as heat too much. And in the simulation the author hadn't input the heat properties, Viscoelasticity and Mullins effect of material properties to the simulation model. The heat properties and Viscoelasticity weren't testing, because of the limitation of equipment and the time. The Mullins effect material property would be divergence from computation by ABAQUS program when the author inputs the property to the Finite Element Analysis (FEA) model.

The RR and RRC of simulation results less than the testing results and the relative error will be minus value. Because from the Mullins effect testing as Chapter 4 subtitle 4.2.2, the stress or loading input from testing would decreasing when the specimen reloaded again and there was steady state when had unloaded-reloaded enough to broke the crosslink of rubber bond. The testing results of subtitle 4.2.2 would represented when the specimen unloaded-reloaded in the loop 4 to 5, the loading input would began to steady state. From the testing, there could demonstrate why the RR and RRC results from simulation would less than testing results.

From the comparative results of WBS tire and Dual tires, the WBS tire can save the fuel consumption and leads to save the fuel cost. The WBS tire can reduces the RR of 14.85% in the same load and 46.77% in according to UN-ECE R117 standard when replaces instead of Dual tires. But in the reality, The WBS tire using instead of Dual tires using must be the same load with Dual tires in usability from carry the load at the same position. Because of this, the load various results is suitable for usability in reality.

From NACFE & Driving Innovation [2] and Goodyear commercial tire systems [6] literatures, they presented the RR reducing approximately 10% could contributed to fuel saving approximately 3%, it mean when reduces the RR 14.85% from Dual tires position replaces with WBS tire can saving fuel consumption approximately 4.46%. There can calculates in the result of fuel cost saving per year per truck approximately 5,890 $ dollar as presented by NACFE & Driving Innovation [2], they reported when could save fuel consumption approximately 10% per year per truck, it could save the fuel cost approximately 3,962 $ dollar, the graph will shows as Figure 6.1. And in Thailand has trucks approximately 1,200,000 units [3], it can save the fuel cost approximately 7,000,000,000 $ dollar per year in Thailand if all truck used the WBS tire instead of Dual tires in the same position as Figure 6.2.

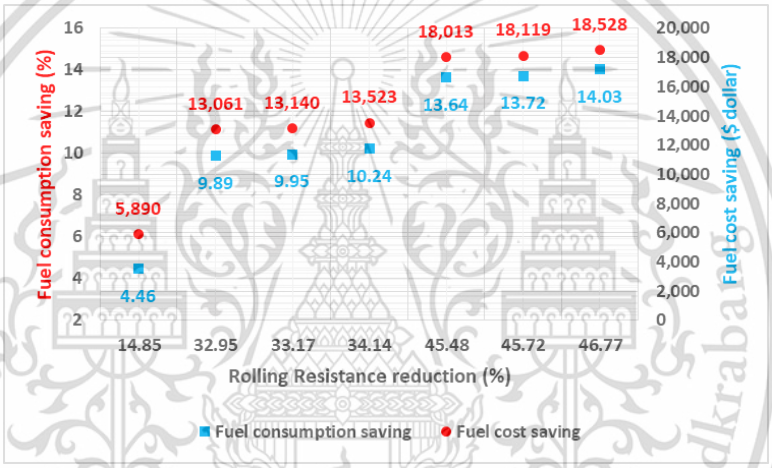

Figure 6.1 The relation of RR reduction with fuel consumption and fuel cost saving.

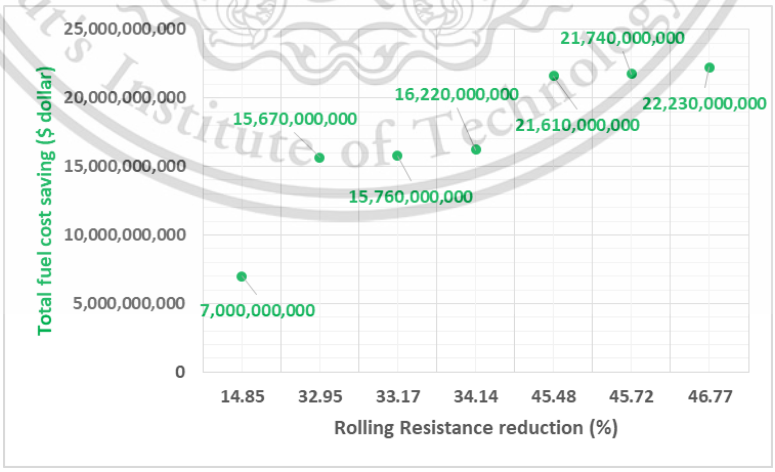

Figure 6.2 The relation of RR reduction with total fuel cost saving.

REFERENCES

[1] RAPIER, R. (2017, November 07). Renewable Gains Offset Coal's Decline In 2016. Retrieved from Financial Sense: https://www.financialsense.com/robert-rapier/renewable-gains-offset-coals-decline-in-2016

[2] American Association of State Highway and Transportation Officials (AASHTO). 444 N Capitol St. NW - Suite 249 - Washington, DC 20001."New technologies –tires-", URL: http://highwaytransport.transportation.org/Documents/Johnston.ppt, access on 26/06/2012.

[3] NACFE, D. I. (2010). Executive Report – Wide Base Tires. North America: The North American Council for Freight Efficiency and Driving Innovation.

[4] Department of Land Transport, Number of Vehicle Registered in Thailand as of 29 February 2016, URL: https://data.go.th/DatasetDetail.aspx?id=21372366-e78b-4d4a-b040-8a702ecedd5f&AspxAutoDetectCookieSupport=1

[5] EPPO. (2017). ENERGY STATISTICS OF THAILAND. Bangkok: EPPO.

[6] Goodyear commercial tire systems (2008). Factors Affecting Truck Fuel Economy. Goodyear.

[7] Oscar FranZese, e. a. (2009). Effect of Tires on Class-8 Heavy Truck Fuel Efficiency. Tennessee: Oak Ridge National Laboratory.

[8] Hamid Taghavifar., e. a. (2013). Investigating the effect of velocity, inflation pressure, and vertical load on rolling resistance of a radial ply tire. Journal of Terramechanics.

[9] Dr. Pairote Jittham., e. a. (2013). Engineering Design of Tyres for Energy Saving Tyres. Bangkok: NRCT, TRF.

[10] Jittham, P. (2009). Mechanical Testing of Rubber for Structural Finite Element Analysis. Nakhon Nayok: MTEC.

[11] Guolin Wang., e. a. (2011). Finite element analysis of Tire Thermomechanical Coupling Rolling Resistance. Electric Information and Control Engineering (ICEICE), 2011 International Conference on. Wuhan, China: IEEE.

[12] J.R. Cho, e. a. (2013). Numerical estimation of rolling resistance and temperature distribution of 3-D. International Journal of Solids and Structures, 86-96.

[13] Yang, X. (2011). Finite Element Analysis and Experimental Investigation of Tyre Characteristic for Developing Strain - Based Intelligent Tyre System. Burmingham: The University of Burmingham.

[14] Biswanath Nandi., e. a. (2014). Importance of Capturing Non-linear Viscoelastic Material Behavior in Tire Rolling Simulations. THE THIRTY-THIRD ANNUAL MEETING AND CONFERENCE ON TIRE SCIENCE AND TECHNOLOGY. Akron, Ohio: The Tire Society.

[15] Michelin. (2003). The tyre Rolling resistance and fuel saving, 2003. Clermont-Ferrand: Société de Technologie Michelin 23, rue Breschet, 63000.

[16] Durrant, C. (2017). Burning Rubber! The Surprising Cost of Rolling Resistance,. Dynamon Ltd.

[17] Tire Rolling Resistance. (2006). Retrieved from Roues Artisanales: http://www.rouesartisanales.com/article-1503651.html

[18] E/ECE/324/Rev.2/Add.116/Rev.2−E/ECE/TRANS/505/Rev.2/Add.116/Rev.2

[19] Smith, L. P. (1993). The Language of Rubber: An Introduction to the Specification and Testing of Elastomers. Butterworth-Heinemann.

[20] Ghosh P., S. A. (2006). Material property characterization for finite element analysis of tires.

[21] Bolarinwa, E. O. (2004). Investigation of the Dynamic Characteristics of Radial Tyre Using the Finite Element Method. University of Birmingham.

[22] Ogden, R. W. (1999). A Pseudo-Elastic Model for the Mullins Effect in Filled Rubber. Proceedings of the Royal Society of London, Series A, vol. 455 (pp. 2861–2877). The Royal Society.

[23] Wipoo Piwat, C. D. (2004). Hyperelastic Material Testing for Finite Element Modeling. The Conference of Mechanical Engineering Network of Thailand. Khonkaen: Khon Kaen University.

[24] (n.d.). Rolling Resistance and Industrial Wheels. America: Hamilton.

[25] Michelin North America, I. (2016). MICHELIN® XZY® 3 TIRE. North America: Michelin North America, Inc.

[26] Michelin North America, I. (2013). MICHELIN® X ONE® XZY3®3 TIRE . North America: Michelin North America, Inc.

APPENDIX A

ROLLING RESISTANCE TESTING DATA (UN-ECE R117) OF XZY3 11R22.5

MAHIDOL RUBBER SERVICE
RUBBER TECHNOLOGY RESEARCH CENTRE

Report No : 2-0018-2561
Page 1 of 8

TEST REPORT

ISSUED TO	: Asst. Prof. Dr. Chinda Charoenphonphanich 3 Chalongkrung Road, Lat Krabang, Bangkok 10520
SAMPLE RECEIVE DATE	: February 28, 2018
SAMPLE DESCRIPTION	: Truck tyre, MICHELIN, XZY3, tyre size 11R22.5 148/145K 16PR., maximum speed 110 km/h, maximum load 3,150 kg, maximum pressure 115 psi, manufacturing date 2817.
SAMPLE NAME	: MICHELIN, XZY3, tyre size 11R22.5 148/145K 16PR.
TEST DATE	: March 2 – 14, 2018
TEST METHOD	: Rolling resistance test

ใบรายงานผล (REPORT)
FM 5.10-02 REV.1/2553

RESULTS : 1st sample

Sample Name	MICHELIN, XZY3
Tyre Size	11R22.5 148/145K 16PR.
Type	Radial, Tubeless

Rolling Resistance Test

Test condition

: The tyre was assembled to testing rim and inflated to 115 psi, and then conditioned at testing temperature for 6 hours. The inflation pressure was re-adjusted prior to testing. The following test conditions were used.

- Test speed : 60, 80, 100, and 110 km/h
- Test inflation pressure : 110, 115, 120 and 125 psi
- Test load : 2,465 (24.18), 2,677.5 (26.27), 2,900 (28.45) and 3,150 (30.90) kg (kN)
- Test time per step : 210 minutes
- Test temperature : 25±5 °C

Rolling Resistance

Warm up the tyre for 180 minutes with the speed and load at surrounding temperature of 25±5 °C. After 180 minutes warming, start measuring Rolling Resistance and recording data. All necessary data for Rolling Resistance calculation are shown in Tables 1 – 3.

Table 1 Data for rolling resistance test with the load of 26.27 kN and inflated of 115 psi

Measurement	Speed (km/h)			
	60	80	100	110
Rim size test (in)	22.5 X 8.25			
Speed (km/h)	60.1	80.3	100.4	110.2
Load (kN)	26.28	26.28	26.28	26.28
Interval (minutes)	210	210	210	210
Ambient temperature (°C)	28.0	28.3	28.2	28.9
Static radius (mm)	501.7	501.8	504.1	506.1
Dynamic radius (mm)	518.5	518.5	520.6	523.2
Test drum Radius (mm)	853.8			
Tyre Spindle Force (N)	157	165	174	190

Table 2 Data for rolling resistance test with the load of 26.27 kN and speed of 80 km/h

Measurement	Inflation pressure (psi)			
	110	115	120	125
Rim size test (in)	22.5 X 8.25			
Speed (km/h)	80.3	80.3	80.4	80.4
Load (kN)	26.28	26.28	26.28	26.28
Interval (minutes)	210	210	210	210
Ambient temperature (°C)	28.1	28.3	28.6	28.2
Static radius (mm)	500.7	501.8	504.9	505.6
Dynamic radius (mm)	517.7	518.5	521.0	521.9
Test drum Radius (mm)	853.8			
Tyre Spindle Force (N)	166	165	163	162

Table 3 Data for rolling resistance test with the speed 80 km/h and inflated of 115 kPa

Measurement	Load kg (kN)			
	2,465 (24.18)	2,677.5 (26.27)	2,900 (28.45)	3,150 (30.90)
Rim size test (in)	22.5 X 8.25			
Speed (km/h)	80.4	80.3	80.4	80.3
Load (kN)	24.19	26.28	28.46	30.91
Interval (minutes)	210	210	210	210
Ambient temperature (°C)	28.3	28.3	28.5	28.6
Static radius (mm)	503.8	501.8	500.6	498.9
Dynamic radius (mm)	518.5	518.5	518.5	518.5
Test drum Radius (mm)	853.8			
Tyre Spindle Force (N)	148	165	178	200

Parasitic Losses

Warm up the tyre for 180 minutes with the speed and loading of 100 N at surrounding temperature of 25 ± 5 °C. After 180 minutes warming, start measuring parasitic losses and recording data. All necessary data for parasitic losses calculation are shown in Tables 4 – 5.

Kitwanglert Phungphlai

Table 4 Data for parasitic losses with the inflated of 115 kPa

Measurement	Speed (km/h)			
	60	80	100	110
Rim size test (in)	22.5 X 8.25			
Speed (km/h)	60.3	80.3	100.2	110.2
Load (N)	500			
Interval (minutes)	180	180	180	180
Ambient temperature (°C)	28.1	28.0	28.0	28.3
Static radius (mm)	525.6	527.5	530.0	532.4
Dynamic radius (mm)	530.2	531.8	534.5	536.1
Test drum Radius (mm)	853.8			
Tyre Spindle Force (N)	60	64	69	73

Table 5 Data for parasitic losses with the speed of 80 km/h

Measurement	Inflation pressure (psi)			
	110	115	120	125
Rim size test (in)	22.5 X 8.25			
Speed (km/h)	80.3	80.3	80.4	80.4
Load (N)	500			
Interval (minutes)	180	180	180	180
Ambient temperature (°C)	28.0	28.0	28.2	28.0
Static radius (mm)	527.3	527.5	530.4	531.2
Dynamic radius (mm)	530.3	531.8	535.4	535.4
Test drum Radius (mm)	853.8			
Tyre Spindle Force (N)	65	64	64	63

Rolling Resistance Calculation

Parasitic Losses Calculation

Example: Calculate at speed 60 km/h for Force Method of drum.

$$F_{pl} = F_t\left[1+\left(\frac{rl}{R}\right)\right]$$

$$F_{pl} = 60\left[1+\left(\frac{525.6}{853.8}\right)\right]$$

$$F_{pl} = 96.94\text{N}$$

Rolling Resistance Calculation

Example: Calculate at speed 60 km/h for Rolling Resistance for Force Method

$$F_r = F_t\left[1+\left(\frac{rl}{R}\right)\right] - F_{pl}$$

$$F_r = 157\left[1+\left(\frac{501.7}{853.8}\right)\right] - 96.94$$

$$F_r = 152.32\text{N}$$

Temperature Correction :

F_{r25} = the rolling resistance at 25 °C, in Newton (N)

$$F_{r25} = F_r\left[1+K\left(t_{amb}-25\right)\right]$$

$K = 0.006$ for Class C3 types

$$F_{r25} = 152.32\left[1+0.006\left(28.0-25\right)\right]$$

$$F_{r25} = 155.06\text{N}$$

Calculate for Outer Diameter :

$$D = d + 2H$$

$$D = 572 + 2(239)$$

$$D = 1050mm$$

Drum Diameter Correction :

$$F_{r02} \cong KF_{r01}$$

$$K = \sqrt{\frac{(R_1/R_2)(R_2 + r_T)}{(R_1 + r_T)}}$$

$$K = \sqrt{\frac{(0.8538/1)(1 + (1.050/2))}{(0.8538 + (1.050/2))}}$$

$$K = 0.97$$

$$F_{r02} \cong 0.97 \times 155.06$$

$$F_{r02} \cong 150.68 \text{ N}$$

Rolling Resistance Coefficient :

$$C_r = \frac{F_r}{L_m}$$

$$C_r = \frac{150.68}{26.28}$$

$$C_r = 5.73 \text{ kg/ton}$$

CONCLUSION : Rolling Resistance test results for Truck tyre, MICHELIN, XZY3, 11R22.5 148/145K 16PR., Manufacturing date of 2817 are shown in the Table 6 – 7.

Table 7 Results for rolling resistance with the load of 26.27 kN and inflated of 115 psi

Results	Speed (km/h)			
	60	80	100	110
Parasitic Losses (F_{pl}) (N)	96.94	103.54	111.83	118.52
Tyre Spindle Force (F_t) (N)	157	165	174	190
Rolling resistance for force method (F_r) (N)	152.32	158.43	164.29	184.10
Rolling resistance at 25 °C (F_{r25}) (N)	155.06	161.57	167.44	188.41
Rolling resistance for drum correction (F_{r02}) (N)	150.68	157.01	162.72	183.09
Rolling resistance coefficient at 25 °C (C_r) (kg/ton)	5.73	5.97	6.19	6.97

Table 8 Results for rolling resistance with the load of 26.27 kN and speed of 80 km/h

Results	Inflation pressure (psi)			
	110	115	120	125
Parasitic Losses (F_{pl}) (N)	105.14	103.54	103.76	102.20
Tyre Spindle Force (F_t) (N)	166	165	163	162
Rolling resistance for force method (F_r) (N)	158.21	158.43	155.63	155.74
Rolling resistance at 25 °C (F_{r25}) (N)	161.15	161.57	158.99	158.73
Rolling resistance for drum correction (F_{r02}) (N)	156.60	157.01	154.51	154.25
Rolling resistance coefficient at 25 °C (C_r) (kg/ton)	5.96	5.97	5.88	5.87

Table 9 Results for rolling resistance with the speed 80 km/h and inflated of 115 kPa

Results	Load kg (kN)			
	2,465 (24.18)	2,677.5 (26.27)	2,900 (28.45)	3,150 (30.90)
Parasitic Losses (F_{pl}) (N)	103.54	103.54	103.54	103.54
Tyre Spindle Force (F_t) (N)	148	165	178	200
Rolling resistance for force method (F_r) (N)	131.79	158.43	178.82	213.32
Rolling resistance at 25 °C (F_{r25}) (N)	134.40	161.57	182.58	217.93
Rolling resistance for drum correction (F_{r02}) (N)	130.60	157.01	177.42	211.78
Rolling resistance coefficient at 25 °C (C_r) (kg/ton)	5.40	5.97	6.23	6.85

TESTED BY Kitmongkol Phaopongklai
(Mr.Kitmongkol Phaopongklai)

REPORTED BY Kitmongkol Phaopongklai
(Mr.Kitmongkol Phaopongklai)

APPROVED BY
(Mr.Tasanai Boonkerdratanasakul)

APPROVED BY
(Dr. Chakrit Sirisinha)

ISSUED DATE : March 23, 2018

Remark
1. RTEC does not allow any alternation or modification of this report, or any part of this report, without prior formal written permission from RTEC.
2. RTEC will not accept liability for any damage whatsoever, resulting directly or indirectly, from using data, results, conclusions or recommendations in this report for the purpose of designing, manufacturing or for other purposes.
3. Experimental results are only valid for the specimens tested

APPENDIX B

TENSILE TESTING RAW DATA

Test: Rate 1	500.00000 mm/min
Dimension: Length	50.00000 mm
Dimension: Width	6.20000 mm
Text Inputs: Sample name	APEX
Text Inputs: Custom text input 3	APEX

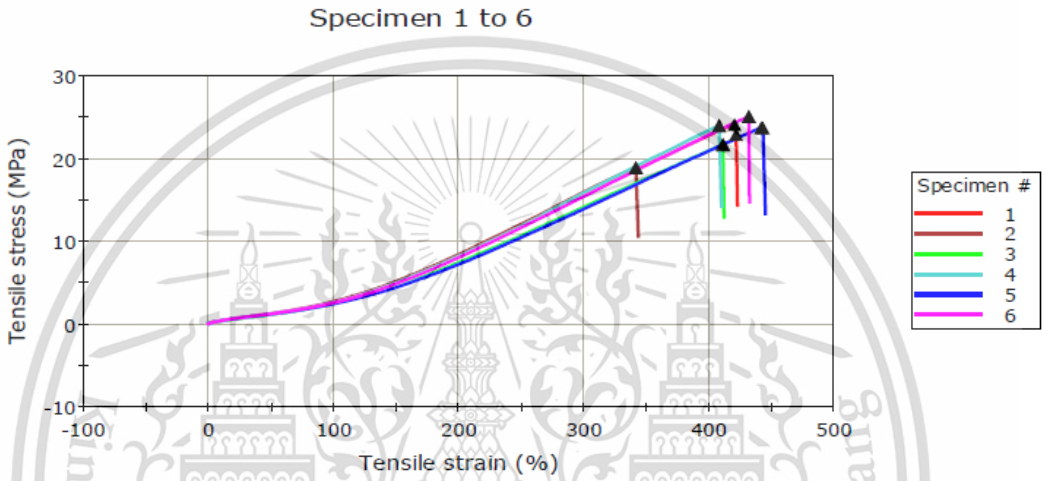

	Load at Maximum (N)	Thickness (mm)	Tensile stress at Maximum (MPa)	Tensile strain at Maximum (%)	Tensile stress at Break (MPa)	Tensile strain at Break (%)	Extension at Maximum (mm)
1	305.55	2.01	24.13	420.2	22.95	421.5	312.5
X 2	238.45	2.00	18.92	341.5	18.92	341.5	250.8
3	371.24	2.71	21.74	411.1	21.74	411.1	315.8
4	270.94	1.79	24.03	408.0	24.03	408.0	301.7
5	309.85	2.07	23.76	441.4	23.75	442.8	306.7
6	324.48	2.05	25.12	431.5	25.12	431.5	308.3
Mean	316.41	2.13	23.76	422.4	23.52	423.0	309.0
Standard Deviation	36.40	0.35	1.24	14.0	1.26	14.45	5.45

	Tensile stress at 10% Modulus (MPa)	Tensile stress at 20 % Modulus (MPa)	Tensile stress at 50% Modulus (MPa)	Tensile stress at 100% Modulus (MPa)	Tensile stress at 200% Modulus (MPa)	Tensile stress at 300% Modulus (MPa)
1	0.43	0.65	1.25	2.64	8.35	15.61
X 2	0.49	0.73	1.33	2.78	8.48	15.98
3	0.41	0.63	1.19	2.51	7.49	14.19
4	0.45	0.68	1.25	2.63	8.26	15.86
5	0.45	0.68	1.26	2.49	7.29	13.95
6	0.45	0.70	1.30	2.64	8.12	15.46
Mean	0.44	0.67	1.25	2.58	7.90	15.02
Standard Deviation	0.02	0.03	0.04	0.08	0.48	0.88

	Tensile stress at 400% Modulus (MPa)	Tensile stress at 500% Modulus (MPa)
1	22.85	-----
X 2	-----	-----
3	21.03	-----
4	23.48	-----
5	20.98	-----
6	22.93	-----
Mean	22.25	-----
Standard Deviation	1.17	-----

Test: Rate 1	500.00000 mm/min
Dimension: Length	50.00000 mm
Dimension: Width	6.20000 mm
Text Inputs: Sample name	INNER-LINER
Text Inputs: Custom text input 3	INNER-LINER

Specimen 1 to 8

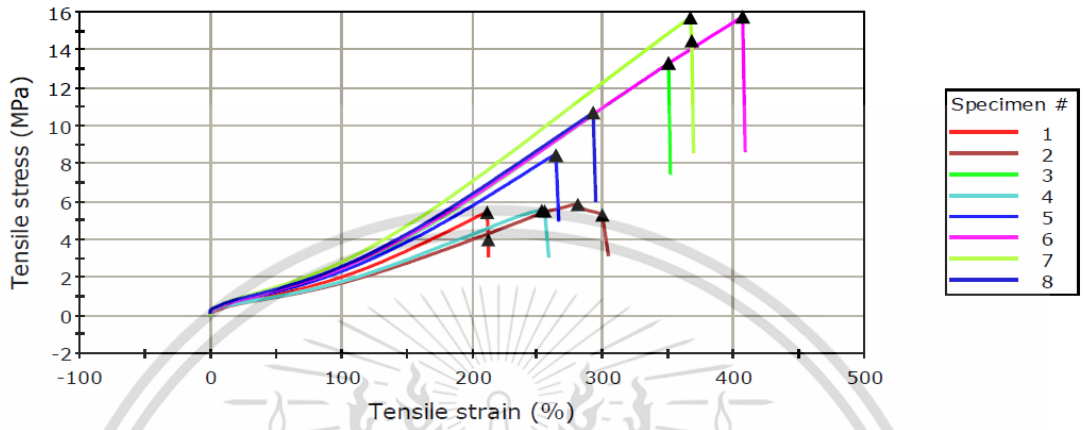

	Load at Maximum (N)	Thickness (mm)	Tensile stress at Maximum (MPa)	Tensile strain at Maximum (%)	Tensile stress at Break (MPa)	Tensile strain at Break (%)	Extension at Maximum (mm)
X 1	66.44	1.93	5.46	211.1	4.03	212.1	145.8
X 2	73.06	1.97	5.89	280.4	5.34	299.2	163.3
3	161.83	1.93	13.31	349.6	13.31	349.6	251.7
X 4	70.91	2.02	5.57	252.8	5.53	255.1	165.0
X 5	102.42	1.92	8.47	263.7	8.47	263.7	196.7
6	186.49	1.88	15.75	406.1	15.75	406.1	280.0
7	182.03	1.84	15.70	366.2	14.49	367.3	268.3
X 8	125.39	1.86	10.70	292.1	10.70	292.1	223.3
Mean	176.79	1.88	14.92	374.0	14.52	374.3	266.7
Standard Deviation	13.14	0.05	1.39	29.1	1.22	28.93	14.24

	Tensile stress at 10% Modulus (MPa)	Tensile stress at 20 % Modulus (MPa)	Tensile stress at 50% Modulus (MPa)	Tensile stress at 100% Modulus (MPa)	Tensile stress at 200% Modulus (MPa)	Tensile stress at 300% Modulus (MPa)
X 1	0.46	0.67	1.12	2.06	5.12	-----
X 2	0.45	0.63	1.00	1.74	4.03	4.95
3	0.55	0.79	1.35	2.48	6.23	10.96
X 4	0.51	0.66	1.03	1.82	4.31	-----
X 5	0.59	0.80	1.29	2.35	5.82	-----
6	0.58	0.82	1.38	2.53	6.28	10.98
7	0.65	0.91	1.54	2.85	7.11	12.31
X 8	0.66	0.88	1.43	2.61	6.44	-----
Mean	0.59	0.84	1.42	2.62	6.54	11.42
Standard Deviation	0.05	0.06	0.10	0.20	0.49	0.77

	Tensile stress at 400% Modulus (MPa)	Tensile stress at 500% Modulus (MPa)
X 1	-----	-----
X 2	-----	-----
3	-----	-----
X 4	-----	-----
X 5	-----	-----
6	15.49	-----
7	-----	-----
X 8	-----	-----
Mean	15.49	-----
Standard Deviation	-----	-----

Test: Rate 1	500.00000 mm/min
Dimension: Length	50.00000 mm
Dimension: Width	6.20000 mm
Text Inputs: Sample name	SIDEWALL
Text Inputs: Custom text input 3	SIDEWALL

Specimen 1 to 5

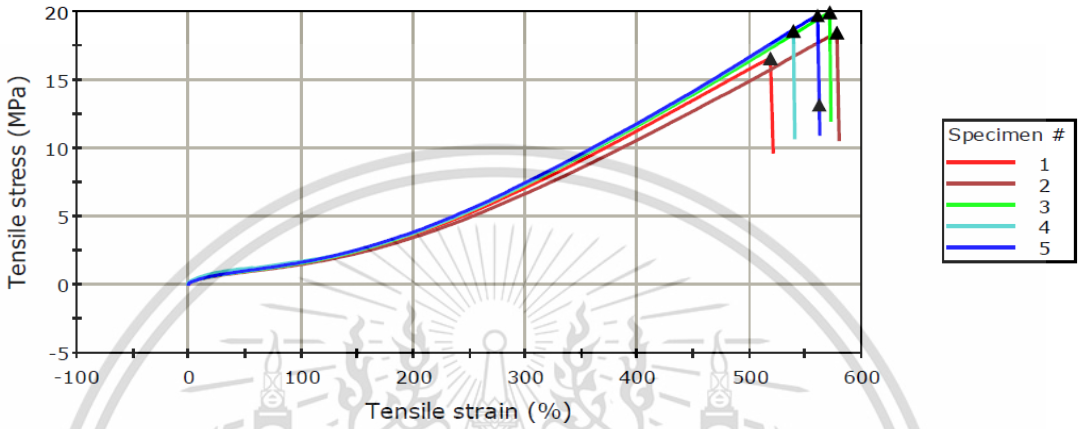

	Load at Maximum (N)	Thickness (mm)	Tensile stress at Maximum (MPa)	Tensile strain at Maximum (%)	Tensile stress at Break (MPa)	Tensile strain at Break (%)	Extension at Maximum (mm)
X 1	186.79	1.79	16.56	517.8	16.56	517.8	369.2
2	272.97	2.35	18.44	577.2	18.44	577.2	415.8
3	272.49	2.17	19.93	570.7	19.93	570.7	430.8
4	263.18	2.25	18.57	538.1	18.57	538.1	400.8
5	217.22	1.75	19.70	559.8	13.18	561.5	399.2
Mean	256.46	2.13	19.16	561.4	17.53	561.9	411.7
Standard Deviation	26.55	0.26	0.77	17.1	2.98	17.10	14.81

	Tensile stress at 10% Modulus (MPa)	Tensile stress at 20 % Modulus (MPa)	Tensile stress at 50% Modulus (MPa)	Tensile stress at 100% Modulus (MPa)	Tensile stress at 200% Modulus (MPa)	Tensile stress at 300% Modulus (MPa)
X 1	0.46	0.66	1.05	1.64	3.71	7.13
2	0.44	0.62	0.97	1.52	3.49	6.71
3	0.47	0.66	1.03	1.63	3.81	7.37
4	0.61	0.84	1.21	1.74	3.84	7.42
5	0.46	0.67	1.05	1.67	3.90	7.51
Mean	0.50	0.70	1.07	1.64	3.76	7.25
Standard Deviation	0.07	0.10	0.10	0.09	0.18	0.37

	Tensile stress at 400% Modulus (MPa)	Tensile stress at 500% Modulus (MPa)
X 1	11.31	15.83
2	10.63	14.94
3	11.65	16.41
4	11.80	16.64
5	11.84	16.71
Mean	11.48	16.18
Standard Deviation	0.57	0.83

Test: Rate 1	500.00000 mm/min
Dimension: Length	50.00000 mm
Dimension: Width	6.20000 mm
Text Inputs: Sample name	TOEGUARD
Text Inputs: Custom text input 3	TOEGUARD

Specimen 1 to 6

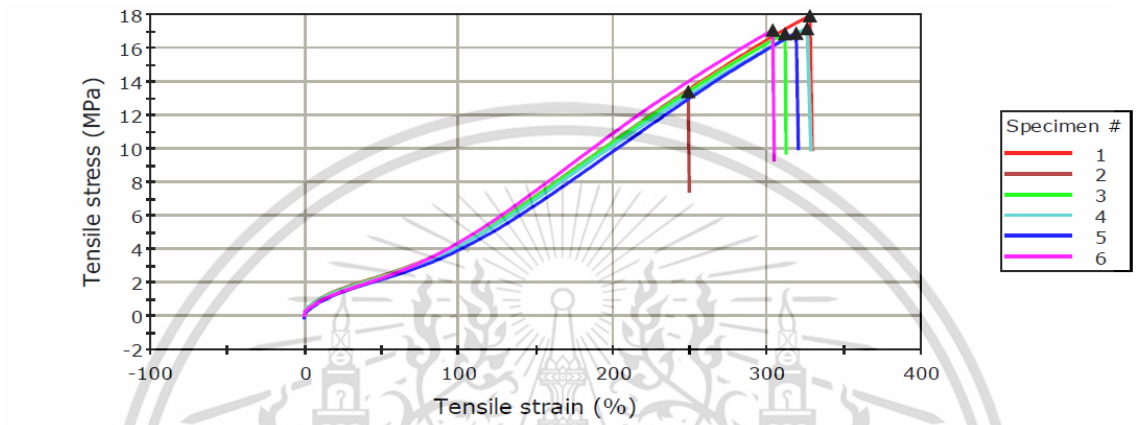

	Load at Maximum (N)	Thickness (mm)	Tensile stress at Maximum (MPa)	Tensile strain at Maximum (%)	Tensile stress at Break (MPa)	Tensile strain at Break (%)	Extension at Maximum (mm)
1	142.21	1.26	17.91	327.3	17.91	327.3	211.7
X 2	141.01	1.67	13.40	248.5	13.40	248.5	167.5
3	144.38	1.36	16.85	311.1	16.85	311.1	207.5
4	145.83	1.35	17.15	325.5	17.15	325.5	217.5
5	141.47	1.33	16.88	318.4	16.88	318.4	213.3
6	167.62	1.56	17.06	303.2	17.06	303.2	213.3
Mean	148.30	1.37	17.17	317.1	17.17	317.1	212.7
Standard Deviation	10.94	0.11	0.43	10.1	0.43	10.06	3.60

	Tensile stress at 10% Modulus (MPa)	Tensile stress at 20 % Modulus (MPa)	Tensile stress at 50% Modulus (MPa)	Tensile stress at 100% Modulus (MPa)	Tensile stress at 200% Modulus (MPa)	Tensile stress at 300% Modulus (MPa)
1	1.03	1.50	2.42	4.27	10.42	16.51
X 2	1.08	1.54	2.45	4.35	10.45	-----
3	1.05	1.48	2.38	4.29	10.39	16.30
4	1.02	1.44	2.33	4.20	10.20	15.98
5	0.88	1.32	2.22	3.97	9.86	15.94
6	0.96	1.38	2.32	4.42	10.94	16.89
Mean	0.99	1.42	2.33	4.23	10.36	16.32
Standard Deviation	0.07	0.07	0.08	0.17	0.39	0.40

	Tensile stress at 400% Modulus (MPa)	Tensile stress at 500% Modulus (MPa)
1	-----	-----
X 2	-----	-----
3	-----	-----
4	-----	-----
5	-----	-----
6	-----	-----
Mean	-----	-----
Standard Deviation	-----	-----

Test: Rate 1	500.00000 mm/min
Dimension: Length	50.00000 mm
Dimension: Width	6.20000 mm
Text Inputs: Sample name	TREAD
Text Inputs: Custom text input 3	TREAD

Specimen 1 to 5

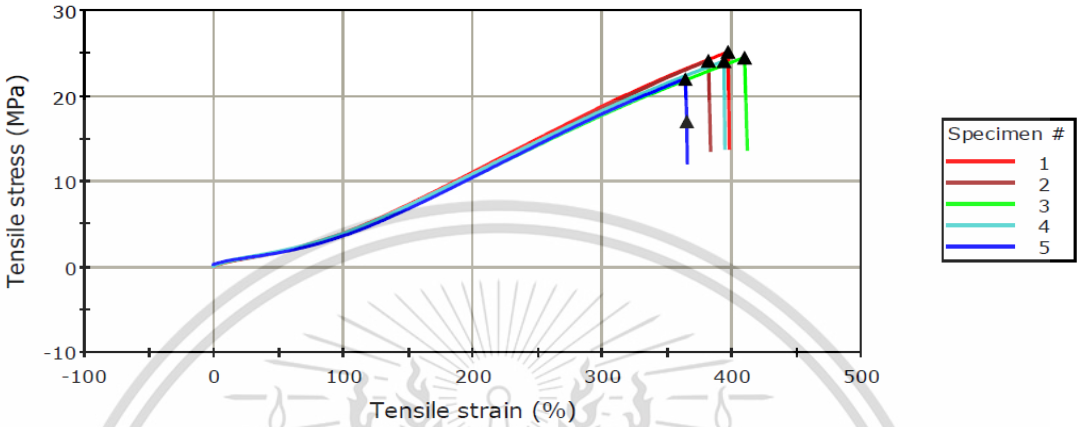

	Load at Maximum (N)	Thickness (mm)	Tensile stress at Maximum (MPa)	Tensile strain at Maximum (%)	Tensile stress at Break (MPa)	Tensile strain at Break (%)	Extension at Maximum (mm)
1	330.99	2.09	25.14	396.6	25.14	396.6	272.5
2	299.23	1.97	24.11	381.4	24.11	381.4	265.0
3	314.66	2.04	24.48	409.3	24.48	409.3	285.8
4	298.57	1.97	24.06	393.6	24.06	393.6	275.0
5	271.60	1.96	22.00	363.6	17.04	364.7	259.2
Mean	303.01	2.01	23.96	388.9	22.97	389.1	271.5
Standard Deviation	22.02	0.06	1.18	17.3	3.34	16.87	10.16

	Tensile stress at 10% Modulus (MPa)	Tensile stress at 20 % Modulus (MPa)	Tensile stress at 50% Modulus (MPa)	Tensile stress at 100% Modulus (MPa)	Tensile stress at 200% Modulus (MPa)	Tensile stress at 300% Modulus (MPa)
1	0.61	0.93	1.79	4.02	11.16	18.83
2	0.60	0.89	1.71	3.77	10.78	18.53
3	0.67	0.98	1.78	3.83	10.57	17.76
4	0.72	1.04	1.88	3.98	10.92	18.29
5	0.75	1.00	1.72	3.69	10.53	17.94
Mean	0.67	0.97	1.78	3.86	10.79	18.27
Standard Deviation	0.06	0.06	0.07	0.14	0.26	0.43

	Tensile stress at 400% Modulus (MPa)	Tensile stress at 500% Modulus (MPa)
1	-----	-----
2	-----	-----
3	23.98	-----
4	-----	-----
5	-----	-----
Mean	23.98	-----
Standard Deviation	-----	-----

APPENDIX C

MULLINS EFFECT TESTING (HYSTERESIS TESTING) RAW DATA

Text Inputs: Sample name	Apex-20 mm

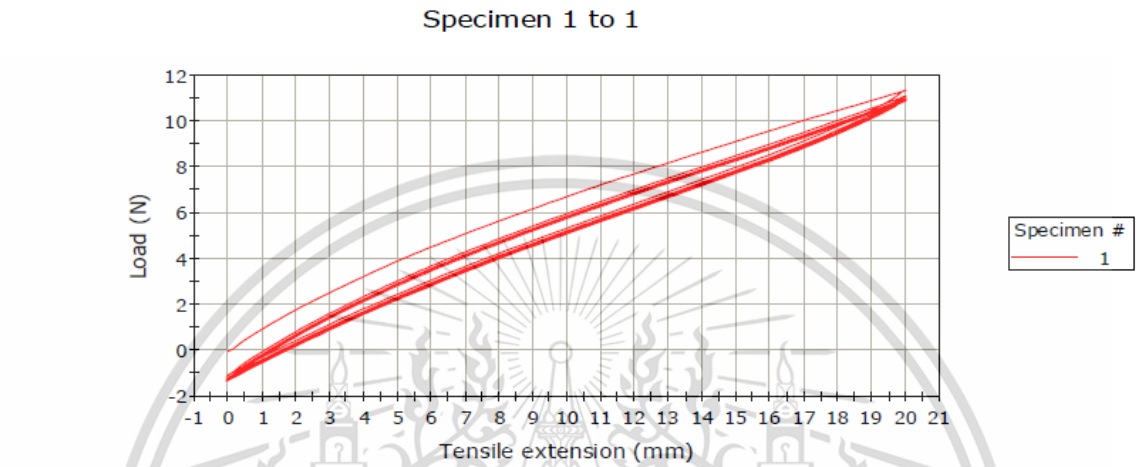

	Maximum Load (Loading1) (N)	Extension at Maximum Load (Loading1) (mm)
1	11.36	20.01

Text Inputs: Sample name	Apex-40 mm

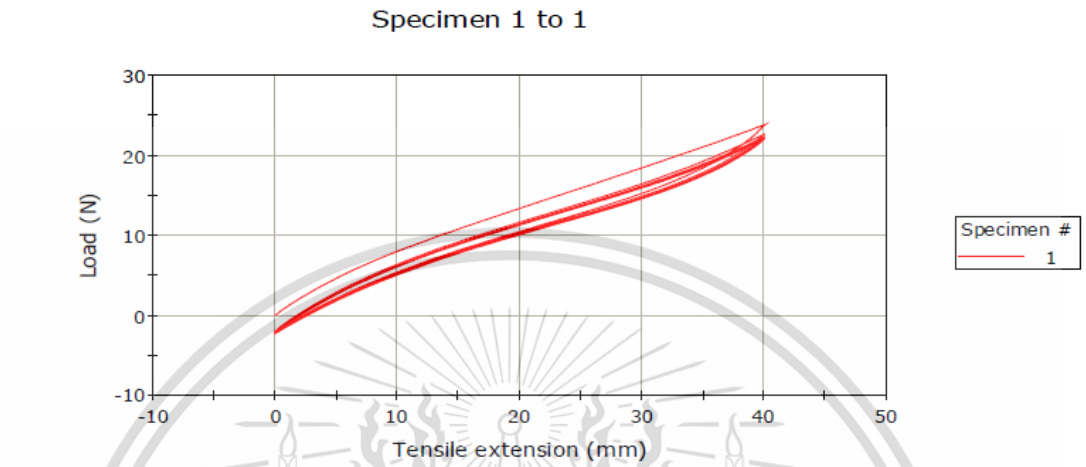

	Maximum Load (Loading1) (N)	Extension at Maximum Load (Loading1) (mm)
1	23.77	40.01

Text Inputs: Sample name	Apex-60 mm

Specimen 1 to 1

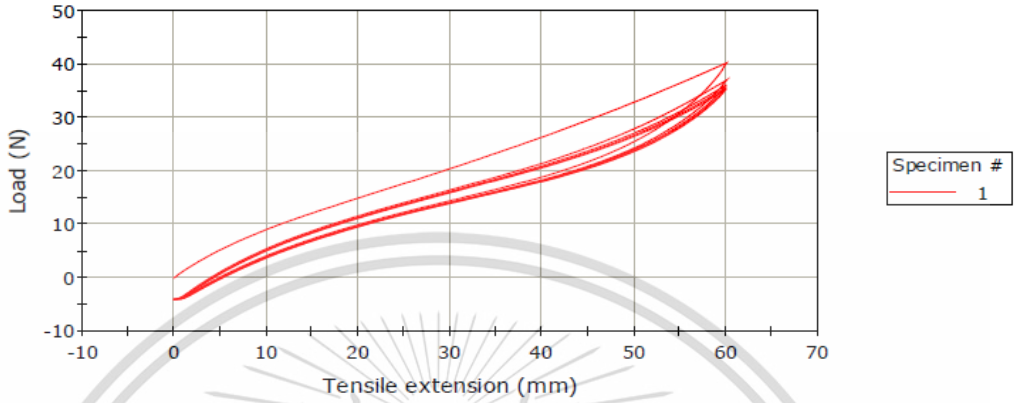

	Maximum Load (Loading1) (N)	Extension at Maximum Load (Loading1) (mm)
1	40.14	60.01

Text Inputs: Sample name	Apex-80 mm

Specimen 1 to 1

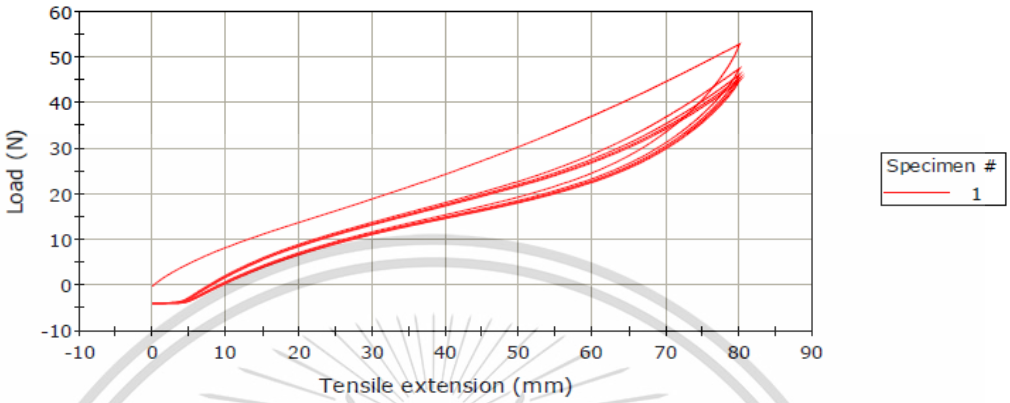

	Maximum Load (Loading1) (N)	Extension at Maximum Load (Loading1) (mm)
1	52.89	80.01

Text Inputs: Sample name	Apex-100 mm

Specimen 1 to 1

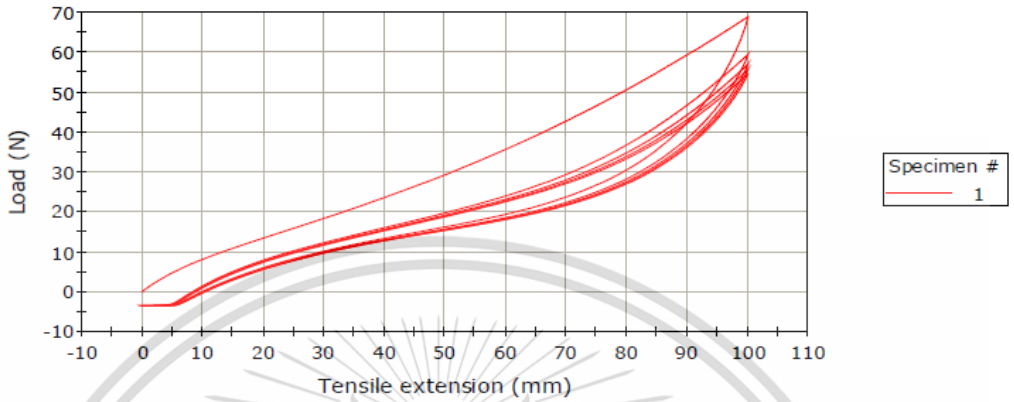

	Maximum Load (Loading1) (N)	Extension at Maximum Load (Loading1) (mm)
1	68.82	100.01

Text Inputs: Sample name	Inner-liner-20 mm

Specimen 1 to 1

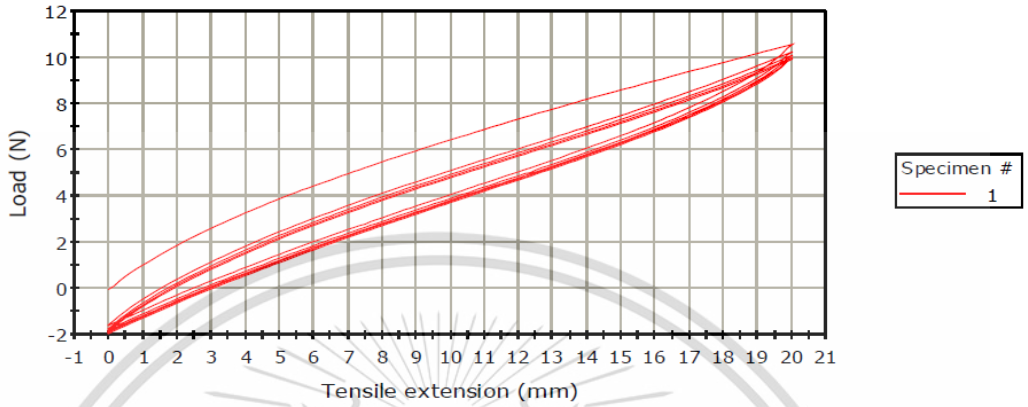

	Maximum Load (Loading1) (N)	Extension at Maximum Load (Loading1) (mm)
1	10.56	20.01

Text Inputs: Sample name	Inner-liner-40 mm

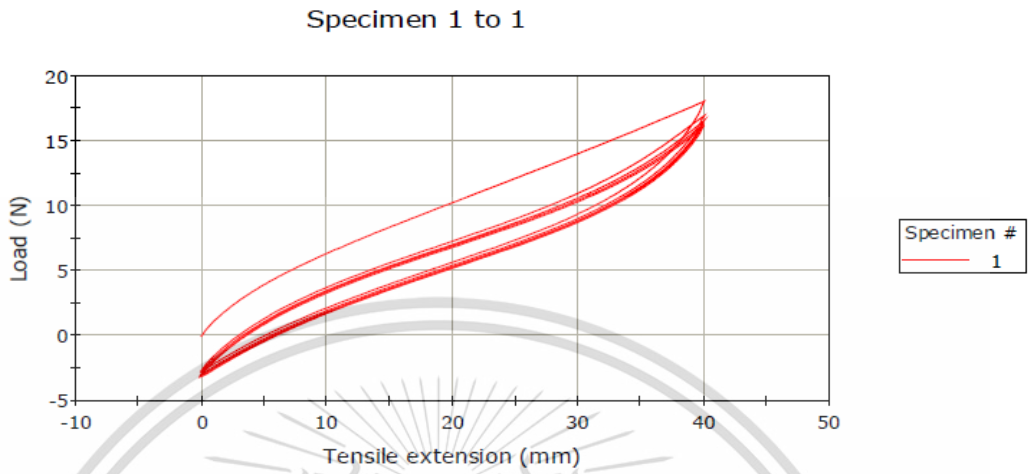

	Maximum Load (Loading1) (N)	Extension at Maximum Load (Loading1) (mm)
1	18.05	40.00

Text Inputs: Sample name	Inner-liner-60 mm

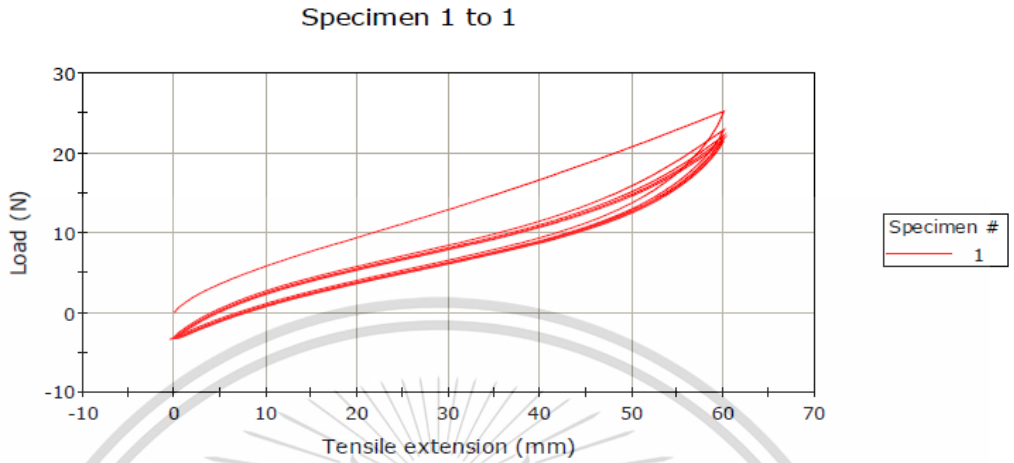

	Maximum Load (Loading1) (N)	Extension at Maximum Load (Loading1) (mm)
1	25.17	60.01

Text Inputs: Sample name	Inner-liner-80 mm

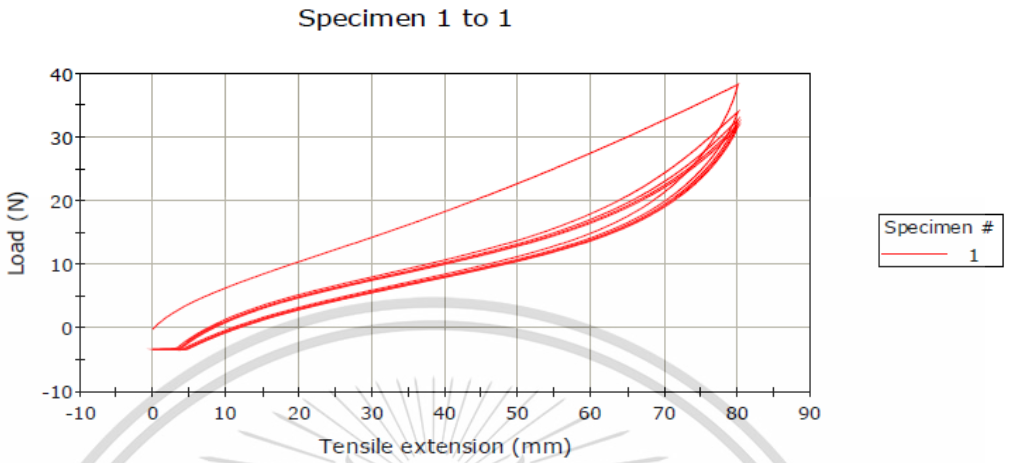

	Maximum Load (Loading1) (N)	Extension at Maximum Load (Loading1) (mm)
1	38.28	80.01

Text Inputs: Sample name	Inner-liner-100 mm

Specimen 1 to 1

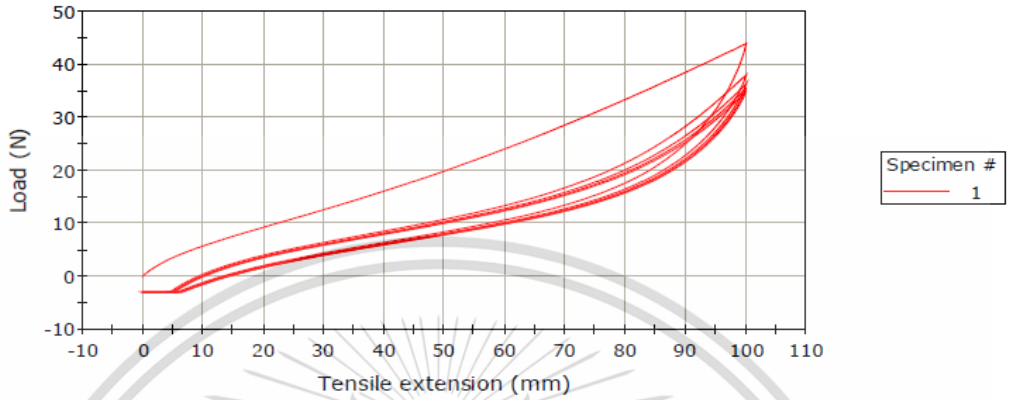

	Maximum Load (Loading1) (N)	Extension at Maximum Load (Loading1) (mm)
1	43.90	100.01

Text Inputs: Sample name	Sidewall-20 mm

Specimen 1 to 1

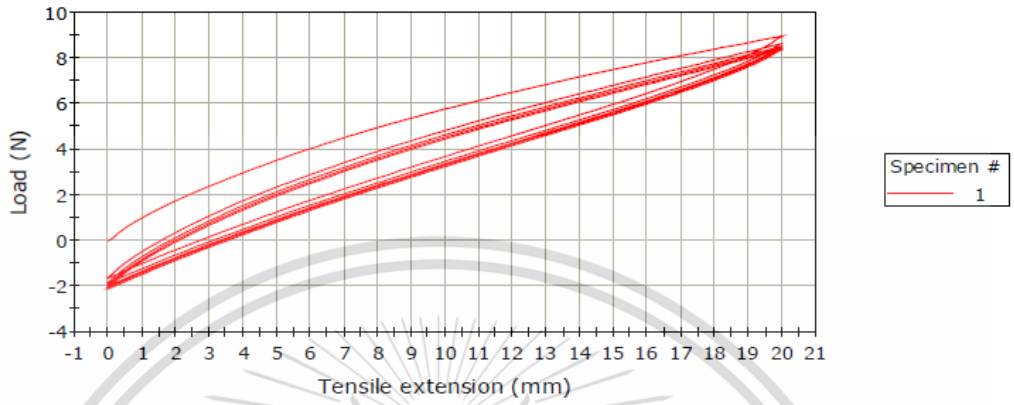

	Maximum Load (Loading1) (N)	Extension at Maximum Load (Loading1) (mm)
1	8.96	20.01

Text Inputs: Sample name	Sidewall-40 mm

Specimen 1 to 1

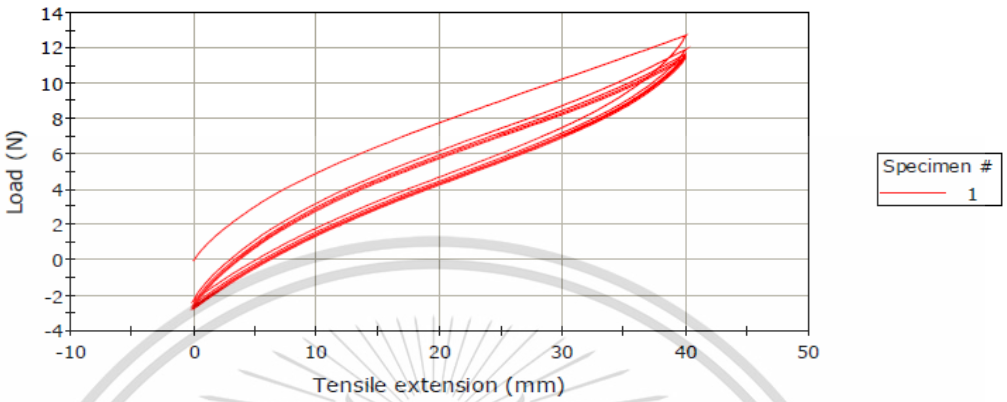

	Maximum Load (Loading1) (N)	Extension at Maximum Load (Loading1) (mm)
1	12.72	40.01

Text Inputs: Sample name	Sidewall-60 mm

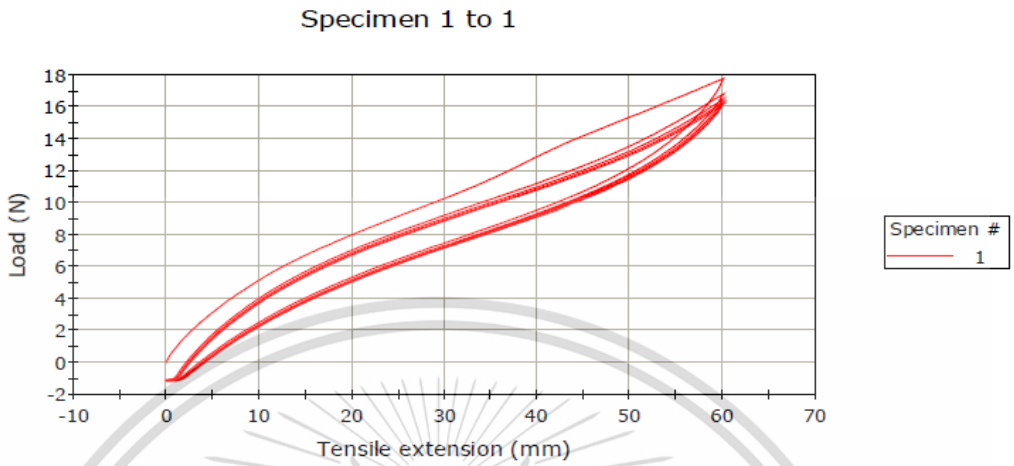

	Maximum Load (Loading1) (N)	Extension at Maximum Load (Loading1) (mm)
1	17.75	60.01

Text Inputs: Sample name	Sidewall-80 mm

Specimen 1 to 1

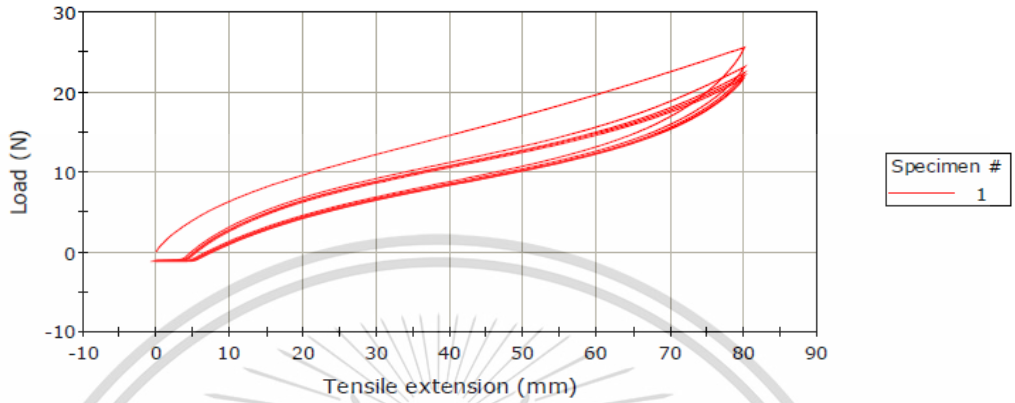

	Maximum Load (Loading1) (N)	Extension at Maximum Load (Loading1) (mm)
1	25.55	80.00

Text Inputs: Sample name	Sidewall-100 mm

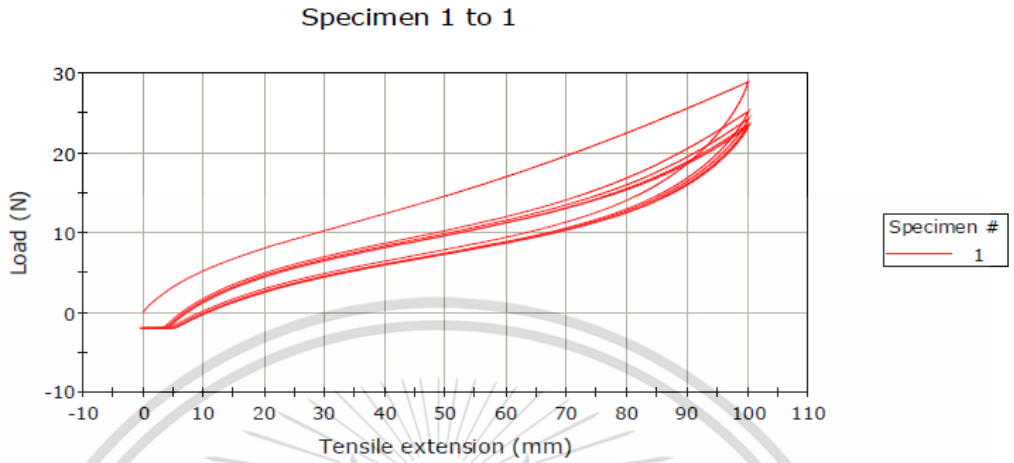

	Maximum Load (Loading1) (N)	Extension at Maximum Load (Loading1) (mm)
1	28.91	100.01

Text Inputs: Sample name	Toeguard-20 mm

Specimen 1 to 1

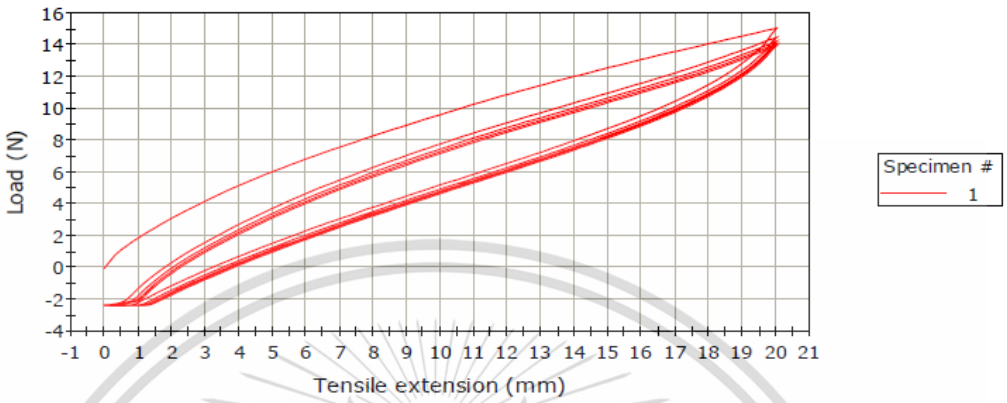

	Maximum Load (Loading1) (N)	Extension at Maximum Load (Loading1) (mm)
1	15.03	20.01

Text Inputs: Sample name	Toeguard-40 mm-

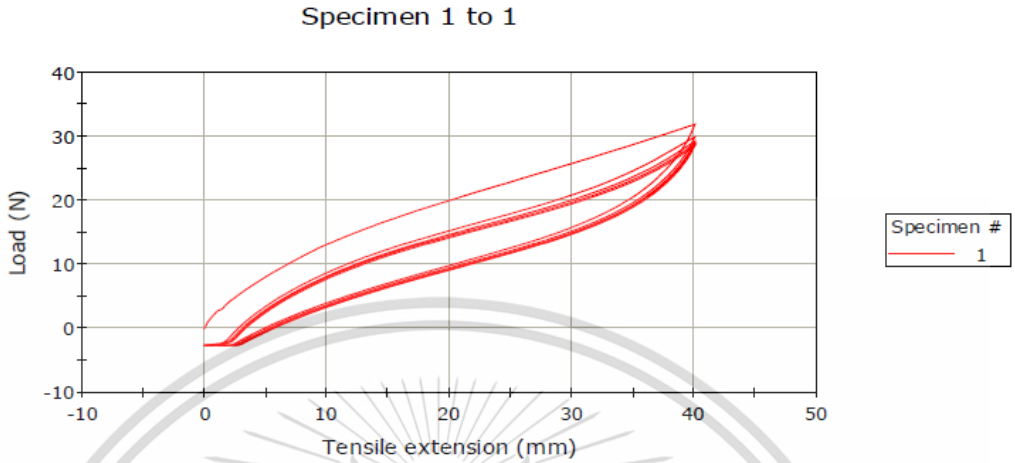

	Maximum Load (Loading1) (N)	Extension at Maximum Load (Loading1) (mm)
1	31.84	40.01

Text Inputs: Sample name	Toeguard-60 mm

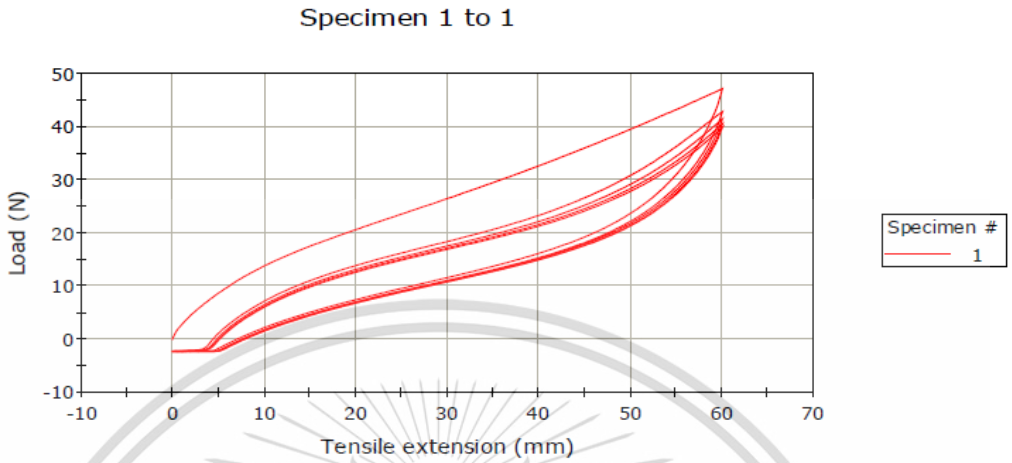

	Maximum Load (Loading1) (N)	Extension at Maximum Load (Loading1) (mm)
1	47.11	60.01

Text Inputs: Sample name	Toeguard-80 mm

Specimen 1 to 1

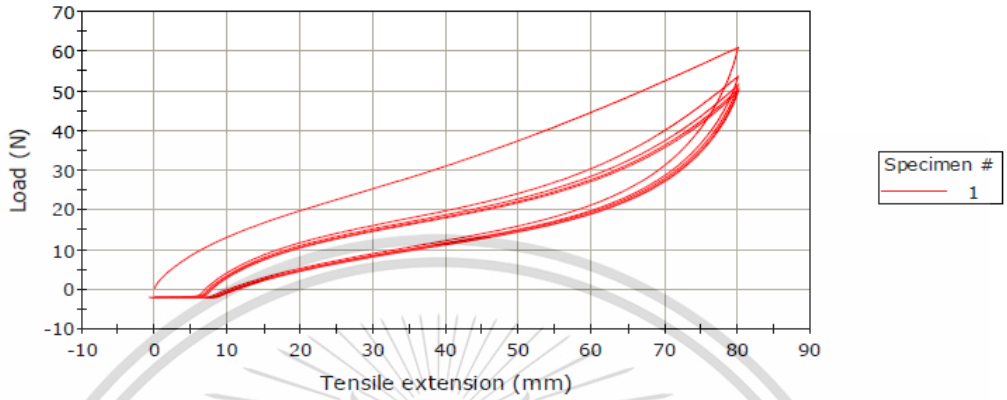

	Maximum Load (Loading1) (N)	Extension at Maximum Load (Loading1) (mm)
1	60.90	80.01

Text Inputs: Sample name	Toeguard-100 mm

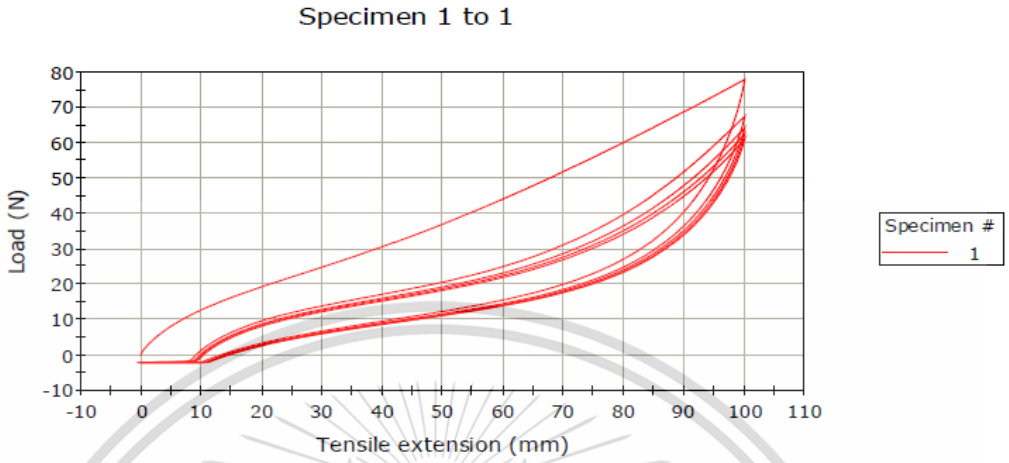

	Maximum Load (Loading1) (N)	Extension at Maximum Load (Loading1) (mm)
1	77.87	100.01

Text Inputs: Sample name	Tread-20 mm

Specimen 1 to 1

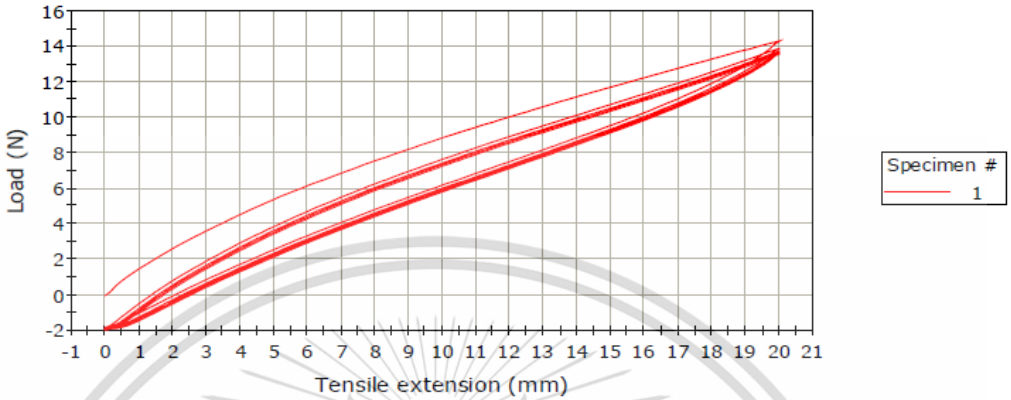

	Maximum Load (Loading1) (N)	Extension at Maximum Load (Loading1) (mm)
1	14.31	20.01

Text Inputs: Sample name	Tread-40 mm

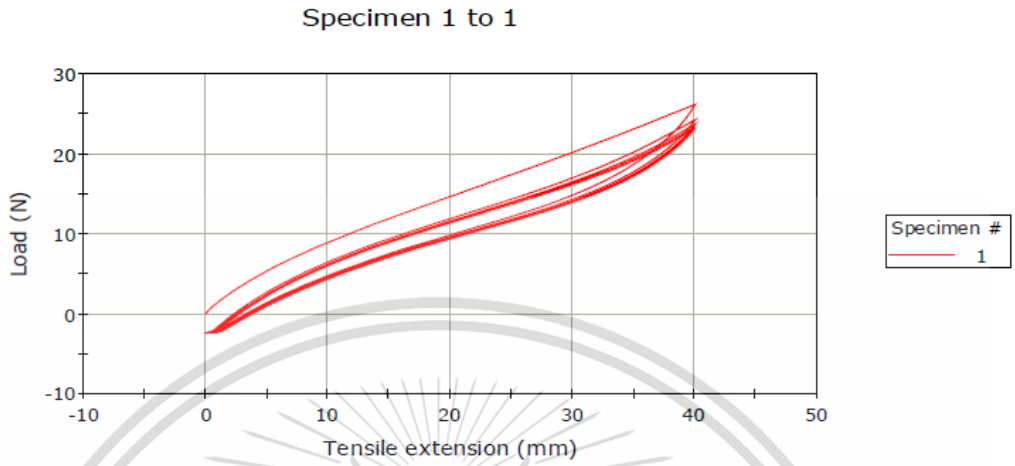

	Maximum Load (Loading1) (N)	Extension at Maximum Load (Loading1) (mm)
1	26.16	40.01

Text Inputs: Sample name	Tread-60 mm

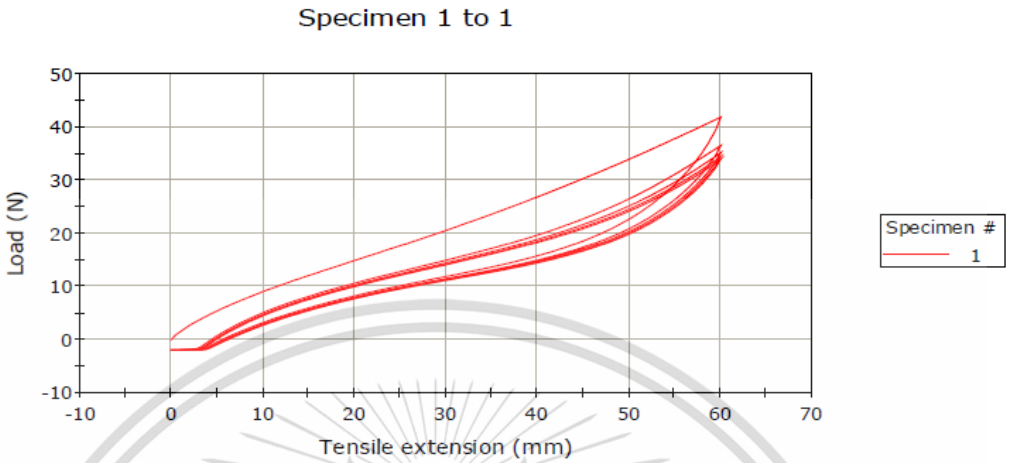

	Maximum Load (Loading1) (N)	Extension at Maximum Load (Loading1) (mm)
1	41.77	60.01

Text Inputs: Sample name	Tread-80 mm

Specimen 1 to 1

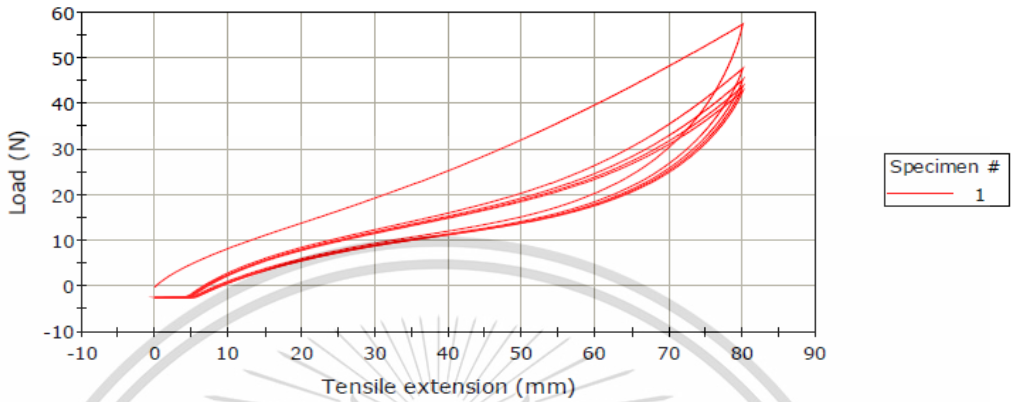

	Maximum Load (Loading1) (N)	Extension at Maximum Load (Loading1) (mm)
1	57.39	80.01

Text Inputs: Sample name	Tread-100 mm

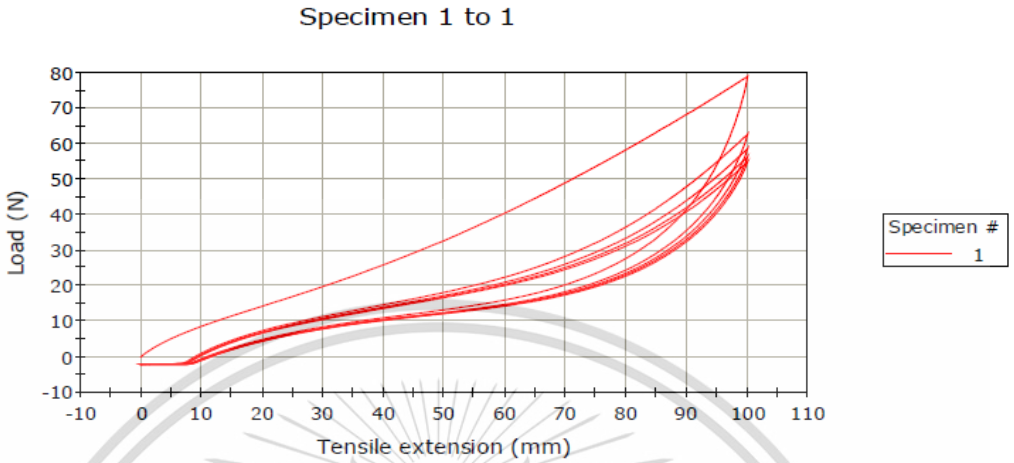

	Maximum Load (Loading1) (N)	Extension at Maximum Load (Loading1) (mm)
1	78.88	100.01

AUTHOR BIOGRAPHY

Author: Mr. Teerapan Uttaranagara

Degree: Master of Engineering

Date of Graduation: 26th June 2018

Date of Birth: 12th December 1990

Place of Birth: Bangkok,Thailand

Undergraduate and Graduate Education:

Master of Engineering in Automotive Engineering, International College
King Mongkut's Institute of Technology Ladkrabang, Bangkok, 2017

Bachelor degree in Automotive Engineering, Faculty of Engineering
Thai-Nichi Institute of Technology, Bangkok, 2012

Major: Automotive Engineering

Presentations and Publications:

[1] T. Uttaranagara, C. Charoenphonphanich, M. Okuma, S. Lapapong, "Comparison of Truck's Wide-Base-Single and Dual Tires Rolling Resistance", Technical Paper, 2018 JSAE Annual Congress (Spring), 23-25 May 2018, Yokohama, Japan.